中国科学院生态环境研究中心
Research Center for Eco-Environmental Science
Chinese Academy of Sciences (CAS)
北京市海淀区双清路 18 号　邮编：100085　　Website: www.rcees.ac.cn
#18 Shuangqing Road, Haidian District, Beijing 100085, P. R. China
Tel:　0086-10-62911239　　Email: gygao@rcees.ac.cn

August 19, 2019

Memorandum

To: Prof. Lixin Wang, Editor of *Hydrology and Earth System Science*

Subject: **Revised manuscript of hess-2019-254**

Dear Prof. Wang,

We have substantially revised our manuscript entitled as "*Temporal-dependent effects of rainfall characteristics on inter-/intra-event branch-scaled stemflow variability in two xerophytic shrubs*" after considering all the comments of Prof. David Dunkerley and another two anonymous reviewers, which are of great help to improve this manuscript.

The following are the point-to-point response to all these comments, including (1) Response to the anonymous Reviewer #1, (2) Response to Reviewer #2 (Prof. David Dunkerley), (3) Response to the anonymous Reviewer #3, (4) The revised manuscript, and (5) The revised manuscript with marks in comparation with the previous version, respectively.

中国科学院生态环境研究中心
Research Center for Eco-Environmental Science
Chinese Academy of Sciences (CAS)
北京市海淀区双清路 18 号　邮编：100085　Website: www.rcees.ac.cn
#18 Shuangqing Road, Haidian District, Beijing 100085, P. R. China
Tel: 0086-10-62911239　Email: gygao@rcees.ac.cn

Response to Reviewer #1

General Comments: The paper by Yuan et al mainly aimed to characterize the inter-/intra-event stemflow dynamics of two xerophytic shrubs and to quantify their relationships with the corresponding inter-/intra-event rainfall characteristics. They concluded that rainfall characteristics had temporal-dependent influences on corresponding stemflow variables.
From my point of view, the study has potential to make a contribution to a better understanding of, in particular, the intra-storm stemflow processes and the underlying mechanisms governing its dynamics. The experimental design and data analysis are generally acceptable, while clarity is needed in presenting the design. The figures adequately summarize the results. I recommend this paper for publication in HESS after some moderate revisions had been addressed by the authors.

Reply:

We appreciated the anonymous reviewer for the comments and suggestions, which were of great help to improve the overall quality of this manuscript. The manuscript had been carefully revised, and we tried best to submit a qualified manuscript as required.

R1C2: L 69: Change "initialed" to "initiated".

Reply: Done (Line 73, Page 4).

R1C3: L 72: I would use "leafed period" instead of "leaf period".

Reply: Done (Line 77, Page 4).

R1C4: Section 2.2: What is the time interval for recording rainfall and the stemflow in subsequent section? This needs to be clearly stated.

Reply:

Sensors were installed at the meteorological station to record wind speed (Model 03002, R. M. Young Company, USA), air temperature and relative humidity (Model HMP 155, Vaisala, Finland). They were logged at 10-min intervals by a datalogger (Model CR1000, Campbell Scientific Inc., USA) (Lines 142–146, Page 7). We recorded stemflow and rainfall via the Onset® (Onset Computer Corp., USA) RG3-M tipping-bucket rain gauges (hereinafter referred to as TBRG). When the bucket (with resolution of 0.2 mm and the equivalent volume of 3.73 mL) was filled and tipped, data of stemflow or rainfall was stored at the dynamic time interval. It depended on rainfall and stemflow intensities. In general, we recorded meteorological features of WS, T and H at 10-min intervals. However, the rainfall and stemflow was recorded at dynamics intervals between neighboring tips with the fixed 0.2-mm resolution (Lines 221–222, Page 10).

北京市海淀区双清路 18 号　邮编：100085　Website: www.rcees.ac.cn
#18 Shuangqing Road, Haidian District, Beijing 100085, P. R. China
Tel:　0086-10-62911239　Email: gygao@rcees.ac.cn

R1C5: L 184-186: According to Table 1, stemflow data of S. psammophila are not available for branches with a BD of 15-18 mm rather than 18-25 mm. Please verify this.
Reply: The typo here of "18-25 mm" had been revised to "15-18 mm" at Line 213, Page 10.

R1C6: Section 2.4: I miss the information about how many rain gauges the authors used in recording stemflow. Did each branch connect to a rain gauge? It seems to be the case from my view of Fig. 1, which makes a total of 14 rain gauges. Please explicitly state to avoid guessing.
Reply:

TBRGs had been applied in this study to automatically record stemflow volume and timing. Each TBRG connected to one experimental branches of *C. korshinskii* and *S. psammophila*. Seven branches were selected at different BD categories for each species. Therefore, we had installed 14 TBRGs for stemflow measuring in this study. It had been clearly described at the revised manuscript (Lines 220, Page 10).

R1C7: L 203: I would change "base area" to "orifice area", which is a more accurate terminology for rain gauge.
Reply: Done (Line 234, Page 11).

R1C8: L 200-210: As for mL of SFV, it should be calculated as: SFV = [mm (branch stem-flow recorded by tipping-bucket rain gauges) / 10] cm2 (orifice area of a rain gauge). I think the authors missed a 10. Therefore, for the calculation of stemflow volume and stemflow intensity, I suggest that authors provide the corresponding mathematical equations; it would be concise and easier for readers to follow.
Reply:

Thank you for commenting on the poorly explained data processing at this manuscript. At the previous version of this manuscript, we just gave the factors for calculating stemflow volume (SFV, mL), i.e., stemflow depth recorded by TBRG (SF_{RG}, mm) and orifice area (186.3 cm^2). The equation for SFV computation had been described at the revised manuscript (Equation 10) (Lines 235, Page 11). Besides, the definitions and calculations of stemflow intensity (Equation 11–13, Lines 246–248, Page 12), time lags to rains (Lines 252–257, Page 12) and other meteorological features (Equation 1–9, Lines 158–160, Line 164, Lines 184–188, Pages 8–9) had also been clearly described at section *2.2 Meteorological measurements and calculations* and *Section 2.4 Stemflow measurements and calculations*.

R1C9: L 211-215: According to the calculation of TLG, TLM, and TLE, these variables can have either negative or positive values. I encourage the authors to clarify here their respective meanings, i.e., what positive values are suggesting and what negative values are suggesting. Again, it would be easier for readers to better understand their following results.
Reply:

北京市海淀区双清路 18 号　邮编：100085　Website: www.rcees.ac.cn
#18 Shuangqing Road, Haidian District, Beijing 100085, P. R. China
Tel: 0086-10-62911239　Email: gygao@rcees.ac.cn

Thank you for this comment. Associated with the results in this study, the meanings of positive and negative values of TLG, TLE and TLM had been described at the *Section 3.2 Stemflow volume, intensity, funnelling ratio and temporal dynamics* at the revised manuscript. During the 54 events, no negative values were observed for TLG and TLM but TLE. It indicated that stemflow generally initiated and maximized after rains started for both species. However, stemflow might be ended before (negative TLE) and after (positive TLE) rains ceased. (Lines 326–329, Page 15).

R1C10: L 258-259: It would be more straightforward to add a row in Table 2 showing how many rainfall events occurred for each category (Event A to C, and others).

Reply: Done (Line 808, Page 40).

R1C11: L 291-298: If it is possible, I would also expect to see some results about the differences of stemflow variables varied among BD categories.

Reply:

Thank you for this comment. As suggested, we compared SFI and FR at different BD categories of *C. korshinskii* and *S. psammophila*. Shown at Table 4, FR of *C. korshinskii* decreased from 163.7 at the 5–10-mm branches to 97.7 at the 18–25-mm branches. The decreasing trend of FR were also noted for *S. psammophila* in the range of 44.2–212.0, as branch size increased. The results were in consistence with the findings for trees and babassu palms in an open tropical rainforest in Brazil (Germer et al., 2010), in the coastal British Columbia forest with mixed species (Spencer and Meerveld, 2016), for trees (*Pinus tabuliformis* and *Armeniaca vulgaris*) and shrubs (*C. korshinskii* and *S. psammophila*) at Loess Plateau of China (Yang et al., 2019). Because funnelling ratio was calculated as the ratio between stemflow and rainfall intensities, SFI was also compared at different BD categories. It was negatively related with branch size for both species. As indicated at Equation 14–15 (Lines 264–265, Page 12), the decreasing stemflow intensity with branch size might partly explained the negative relations between funnelling ratio and BD.

However, we did not compare all the stemflow variables at different BD categories. Because of the high expense of TBRGs (Turner et al., 2019), no more than two branches were selected for stemflow recording at each BD category. The results were much more convincing to analyze the average stemflow variables among BD categories, and compared them at different rainfall amount categories with enough events for meeting the statistical significance.

R1C12: Section 4.1: I would like to discuss with the authors about the use and importance of stemflow intensity and RSFI. I admit that stemflow intensity would be a good variable to show the dynamics of intra-event stemflow, while I am not convinced by authors about the importance of comparing the absolute values of stemflow intensity versus rainfall intensity (also demonstrated in L26-30 of Abstract). Their study is based on monitoring branch stemflow, and branch stemflow intensity was a bit higher than rainfall intensity in their study. However, in terms of stemflow‘s ecological and hydrological importance such as in providing additional soil water and sustaining vegetation growth, we pay more attention to the whole tree/shrub (rather than a single branch). From my understanding this variable is highly dependent on the size of a shrub/tree, because a lager shrub/tree (normally has larger basal diameter or canopy area) would generate substantially higher volume of stemflow, therefore stemflow intensity calculated based on collecting from individual trees/shrubs would be far greater than rainfall intensity, as examples please see Fig. 3 in cayuela et al. (2018, Journal of Hydrology) or Fig. 7 in Germer et al. (2010, Journal of Hydrology). Stemflow and rainfall differs in their paths entering into rain gauges; the orifice area makes sense for rainfall because this area is precisely where rainfall falling into and rainfall depth is then normalized, while stemflow is part of intercepted rainfall by the canopy and then comes down stems, which indicates that infiltrating soil area of stemflow is quite different than that of a rain gauge (i.e., orifice area). Therefore this variable may be prone to underestimate stemflow‘s eco-hydrological role for small shrubs, as such, in terms of ecological importance this variable seems to be less appropriate to be used for inter-specific comparison or even intra-specific comparison of varying sizes. Moreover, the authors were also recommending a future combination use of funnelling ratio and RSFI in stemflow studies. While I agree with the authors that RSFI is helpful in better understanding of the intra-event convergence effects, funnelling ratio assumes trunk/stem basal area is the true area that stemflow is delivered to the soil, whereas RSFI here is based on stemflow intensity which I have discussed above. RSFI may also be prone to underestimate stemflow‘s eco-hydrological role for small trees/shrubs while overestimate that of big trees/shrubs. I encourage authors to discuss both the advantages and limitations of stemflow intensity and

RSFI as well as their application.

Reply:

Thank you for commenting on the calculation and importance of stemflow intensity and RSFI at this manuscript. It indeed underestimated the eco-hydrological significance of stemflow by ignoring its receiving area of branch base as suggested. Therefore, we had revised the calculation of stemflow intensity on basis of basal area, and introduced funnelling ratio to assess the convergence effect of stemflow at the revised manuscript.

Please see the detailed explanations as below.

(1) Stemflow intensity had been re-computed on basis of branch basal area, and quantitatively connected to funneling ratio.

The RG3-M TBRGs had been applied to record stemflow in this study. Stemflow depth (SF_{RG}, mm) could be directly computed with tip amounts and tip resolution of 0.2 mm. Similar with the interpretation for rainfall recording, the 0.2-mm per tip represented 200 mL water deposing on the 1-m^2 ground surface. Based at the same receiving areas, we calculated stemflow intensity as the ratio between SF_{RG} and rainfall duration at the previous manuscript. However, it underestimated the eco-hydrological significance of stemflow by ignoring the limited area of trunk/branch base, over which stemflow was received. As suggested at this comment, stemflow intensity should associate with the area over which the equivalent stemflow depth is evaluated. Therefore, we re-calculated stemflow intensity and followed the definition of stemflow volume per basal area per unit time (Herwitz, 1986; Spencer and Meerveld, 2016). In this study, we calculated stemflow intensity at different time intervals, including the event base (SFI), the 10-min (SFI_{10}) and the dynamic intervals between neighboring tips of TBRG (SFI_i) (Equation 11–13) (Line 246–248, Page 12). Furthermore, we established the quantitative connections of stemflow intensity with funnelling ratio for the first time as indicated at Equation 14–15 (Lines 264–265, Page 12). RSFI had been deleted at the revised manuscript. By replacing the event-based volume of rainfall and stemflow with their intensities at the traditional expression (Herwitz, 1986), the new method enabled funnelling ratio to be computed at high temporal resolutions within event.

(2) Stemflow variables and the meteorological influences were analyzed at branch scale.

C. korshinskii and *S. psammophila* are modular organisms with multiple branches. Each

北京市海淀区双清路 18 号 邮编：100085 Website: www.rcees.ac.cn
#18 Shuangqing Road, Haidian District, Beijing 100085, P. R. China
Tel: 0086-10-62911239 Email: gygao@rcees.ac.cn

branch of them lives as independent individual which seeks its own survival goals and compete with each other for light and water (Firn, 2004; Allaby, 2010). They provide ideal experimental objects to measure the branch stemflow volume and production processes. By introducing branch basal diameter (BD, mm) as intermediate variable, stemflow volume, intensity and funnelling ratio could be upscaled from branches to shrubs (Yuan et al., 2016; 2017). Therefore, the study on branch stemflow variables was conducive to explain the meteorological influences on stemflow at shrub scale particularly for the modular organisms. To guarantee the representativeness of experimental shrubs and branches, the thorough plot investigation had been carried out. Please see Point (3) at Reply to R2C3 for describing the determination of standard shrubs at the plots of *C. korshinskii* and *S. psammophila*, and see Point (4) at Reply to R2C2 for explaining the determination of standard branches of the two shrubs. To address the branch scaled measurements of stemflow, the title had been revised as "Temporal-dependent effects of rainfall characteristics on inter-/intra-event branch-scaled stemflow variability in two xerophytic shrubs" as suggested by Reviewers 2 and 3.

R1C13: L 433-437: These sentences are somewhat redundant (have been mentioned in above sections) and can be simplified or simply deleted.

Reply: Done.

R1C14: Figure 3: Data points are average values for 7 branches for each event? Since the authors selected 7 branches of varying BD for each species to measure stemflow, a relative larger difference in stemflow would be expected among branches. It would be an option to adding error bars if they won't make the figure blurring too much.

Reply:

Stemflow variables were averaged at seven branches of *C. korshinskii* and *S. psammophila*, respectively. Inter-event variations of the average stemflow variables during the experimental period had been shown at Figure 3. The relatively high expense of TBRGs limited the number of experimental branches that could be measured (Turner et al., 2019). However, each experimental branch was carefully selected following the strict criteria. Please see Point (4) at Reply to R2C2 for explaining the representativeness of the selected seven branches. A total of

北京市海淀区双清路 18 号　邮编：100085　　Website: www.rcees.ac.cn
#18 Shuangqing Road, Haidian District, Beijing 100085, P. R. China
Tel:　0086-10-62911239　　Email: gygao@rcees.ac.cn

seven branches were selected for automatic recording via TBRGs at different BD categories of each species. That was the comprehensive results by balancing the statistical significance and TBRG expenses.

To better meeting the statistical significance, we took the average value of stemflow variables at the seven branches at each species, and focused on the comparison of them among different rainfall amount categories. We just discussed the influence of rainfall characteristics in this study, and no analysises were performed to explore the influence of branch traits affecting stemflow volume and process. The variation of stemflow variables had been described as the average±standard error (Iida et al., 2017) at Table 3 (Lines 817–824, Page 41). However, since eight stemflow variables with 54 recording points each were shown at the same figure, the error bars were not drawn at Fig.3 just to keep the intra-event variation of stemflow variables clean and tidy (Lines 835–837, Page 45).

R1C15: Figure 4:The unit of rainfall stemflow intensity should be mm h^{-1} rather than m h^{-1}. Also changes should be made in the legend, since both lines and points are included in this figure, it would be misleading by labelling “Lines in blue” or “Lines in red” without mentioning points. Moreover, since 7 branches for each species were selected for monitoring stemflow intra-event dynamics, I am wondering which branches for two species were demonstrated in this figure.

Reply:

Done. The typo unit (m h^{-1}) had been corrected to mm h^{-1}, and the misleading legends had been revised, and the branch size of *C. korshinskii* and *S. psammophila* had been added at Fig.4 (Line 837–840, Page 46).

Reference:

Allaby, M.: A Dictionary of Ecology, 4th Edn., Oxford University Press, Oxford, 2010.
Firn, R.: Plant Intelligence: an Alternative Point of View, Ann. Bot., 93, 345–351, 2004.
Germer, S., Werther, L. and Elsenbeer, H.: Have we underestimated stemflow? Lessons from an open tropical rainforest, J. Hydrol., 395, 169–179, https://doi.org/10.1016/j.jhydrol.2010.10.022, 2010.
Herwitz, S.R.: Infiltration-excess caused by Stemflow in a cyclone-prone tropical rainforest, Earth Surf. Proc. Land, 11, 401–412, https://doi.org/10.1002/esp.3290110406, 1986.

中国科学院生态环境研究中心
Research Center for Eco-Environmental Science
Chinese Academy of Sciences (CAS)
北京市海淀区双清路 18 号 邮编：100085 Website: www.rcees.ac.cn
#18 Shuangqing Road, Haidian District, Beijing 100085, P. R. China
Tel: 0086-10-62911239 Email: gygao@rcees.ac.cn

Iida, S., Levia, D.F., Shimizu, A., Shimizu, T., Tamai, K., Nobuhiro, T., Kabeya, N., Noguchi, S., Sawano, S. and Araki, M.: Intrastorm scale rainfall interception dynamics in a mature coniferous forest stand, J. Hydrol., 548, 770–783, https://doi.org/10.1016/j.jhydrol.2017.03.009, 2017.

Spencer, S. A. and van Meerveld, H. J.: Double funnelling in a mature coastal British Columbia forest: spatial patterns of stemflow after infiltration, Hydrol. Process., 30, 4185–4201, https://doi.org/ 10.1002/hyp.10936, 2016.

Turner, B., Hill, D.J., Carlyle-Moses, D.E. and Rahman, M.: Low-cost, high-resolution stemflow sensing, J. Hydrol., 570, 62–68, https://doi.org/10.1016/j.jhydrol.2018.12.072, 2019.

Yang, X.L., Shao, M.A. and Wei, X.H.: Stemflow production differ significantly among tree and shrub species on the Chinese Loess Plateau, J. Hydrol., 568, 427–436, https://doi.org/10.1016/j.jhydrol.2018.11.008, 2019.

Yuan, C., Gao, G.Y. and Fu, B.J.: Stemflow of a xerophytic shrub (*Salix psammophila*) in northern China: Implication for beneficial branch architecture to produce stemflow, J. Hydrol., 539, 577–588, https://doi.org/10.1016/j.jhydrol.2016.05.055, 2016.

Yuan, C., Gao, G.Y. and Fu, B.J.: Comparisons of stemflow and its bio-/abiotic influential factors between two xerophytic shrub species, Hydrol. Earth Syst. Sci., 21, 1421–1438, https://doi.org/10.5194/hess-21-1421-2017, 2017.

中国科学院生态环境研究中心
Research Center for Eco-Environmental Science
Chinese Academy of Sciences (CAS)
北京市海淀区双清路 18 号　邮编：100085　Website: www.rcees.ac.cn
#18 Shuangqing Road, Haidian District, Beijing 100085, P. R. China
Tel: 0086-10-62911239　Email: gygao@rcees.ac.cn

Response to Reviewer #2: Prof. Dunkerley

General Comments: The authors report on a detailed study of stemflow in two dryland shrub species, and its relationship with rainfall properties. The data come from field observations of selected branches that were equipped with stemflow collecting collars, and exposed to a number of natural rainfall events. Seven branches were instrumented for each of the two shrub species. The stemflow was recorded by directing the flow into tipping-bucket rain gauges having a 0.2 mm sensitivity.
Although the work appears to be generally thorough, there are some significant issues with it that I consider require clarification before the work could be accepted for publication.

Reply:

We would like to extend our sincere gratitude to Prof. Dunkerley for these constructive comments and suggestions. They were of great help to improve this manuscript. We have carefully revised this manuscript as required.

R2C1: The authors are concerned with the relative timing of rainfall and of the resulting stemflow. The difficulty here is that the relative timing is affected by the size of the collecting areas that contribute either rainfall or stemflow to the measuring gauges. The canopy of S. psammophila for instance is reported as 21.4 m2 (line 170), whilst the collecting area of the pluviography TBRG in the open is just 0.018 m2. Thus the canopy area of the shrub is more than 1,000 times larger. Therefore, the tiny tipping bucket (capacity about 3.65 mL, by my estimation) can potentially be filled more rapidly by stemflow than by rainfall in the open. In this way, the time until first tip (regarded by the authors as the onset of stemflow) probably occurs closer to the onset of rainfall as a function of canopy area and its effect in reducing the bucket filling time.
Therefore, among the seven instrumented branches, the timing of stemflow initiation should vary, and it might be possible to relate this to the plant morphology. However, the authors do not report the canopy collecting area for the 7 branches that they monitored for each of the two shrub species. Therefore, calculations of the kind just sketched cannot be made nor the results evaluated properly. This imposes uncertainty in the interpretation of the stemflow timing data. The ideal, of course, would be for the collecting area of foliage and branch to be as close as possible to the collecting area of the open-field rain gauge.
Indeed, the manuscript lacks any detail of the foliar area on the branches that were monitored for stemflow. For instance, leaf area and leaf wettability are not mentioned or reported. Likewise, there are no data on the shrub canopies as a whole, such as leaf area index (LAI) or canopy gap fraction. The lack of such information again makes the results somewhat difficult to interpret or to compare with results from other taxa and environments.

Reply:

Thank you for this comment. As suggested by Prof. Dunkerley, the initiation of rainfall and stemflow, and the time intervals between them were indeed strongly affected by the corresponding areas to collect them. Therefore, we had carefully discussed the influence of interception area affecting stemflow volume, depth, fraction and funnelling ratio at 53 branches of *C. korshinskii* and 98 branches of *S. psammophila* at Yuan et al. (2016; 2017), including the leaf area of individual branches, branch size, the specific surface area of canopy representing by leaves and stems at both the leafed and leafless states, respectively. By installing TBRGs at 7 branches of each species, this study mainly concentrated the branch-scaled inter-/intra-event stemflow variabilities and the influence of rainfall characteristics affecting them. The influence of leaf area index (LAI) and crown area were not discussed at the shrub scale.

The reasons were detailedly explained as below.

(1) Stemflow variables and meteorological influences were analyzed at branch scale.

C. korshinskii and *S. psammophila* are modular organisms with multiple branches. Each branch of them lives as independent individual which seeks its own survival goals and compete with each other for light and water (Firn, 2004; Allaby, 2010). They provide ideal experimental objects to measure the branch stemflow volume and production processes, which could be upscaled to stemflow variables of individual shrubs (Yuan et al., 2016; 2017). The branch-scaled study of stemflow process was conducive to better understand stemflow production at shrub scale particularly for the modular organisms. Therefore, this study focused on the branch-scaled stemflow volume, intensity, temporal dynamics and funnelling ratio of the two species, and analyzed the influences of rainfall characteristics affecting them.

(2) Stemflow variables were averaged at seven different-sized branches of each species.

Seven branches were selected to automatically record stemflow via TBRGs at different BD categories of *C. korshinskii* and *S. psammophila*, respectively. The relatively high expense of TBRGs limited the number of experimental branches that could be measured (Turner et al., 2019). However, each experimental branch was carefully selected following the strict criteria as stated at Point (3) of Reply to R2C3 and Point (4) of Reply to R2C2. Thus, we tried best to guarantee the selected experimental branches to represent the experimental shrubs, and the selected shrubs to represent the *C. korshinskii* and *S. psammophila* plots in this study. That was the comprehensive results by balancing the statistical significance and TBRG expenses.

Average stemflow variables were took at these seven branches to present the branch stemflow variables of the representative shrubs at *C. korshinskii* and *S. psammophila* plots. We mainly compared them at different rainfall amount (RA) categories, and discussed the influence of rainfall characteristics affecting them. Therefore, the variances of branch morphologies within species were not relevant to the average branch-scaled stemflow variables. However, they had been described as important background information at Table 1. The canopy traits were also stated at *Section 2.3* (Lines 197–199, Page 9).

(3) Recording stemflow process with the tipping bucket rain gauges had been justified.

Tipping bucket rain gauges (TBRGs) provided the intra-event monitoring of stemflow and had been widely applied (Iida et al., 2012), although they underestimated the inflow water with systematic mechanical errors (Turner et al., 2019). The bigger bucket volume might bring the larger underestimation (Iida et al., 2012). Therefore, RG3-M rain gauges were used in this study with the relatively smaller bucket volume of 0.2 mm (the equivalent volume of 3.73 mL, email-confirmed by the Onset company). Besides, we corrected the TBRG recording via the regressions with manual measurements as per Equation 4 to further mitigate its underestimation (Line 164, Page 8).

TBRGs offered the ability to collect the volume and timing of inflow water throughout an event (Turner et al., 2019). When the bucket was filled by rains and tipped, it was recorded as the beginning of incident rains. Comparatively, stemflow started in a much more complicated manner. Because it could not be initiated until the canopy was saturated. The larger branch leaf area could help to initiate stemflow earlier for trapping more rains, but might also result in a later generation by consuming more rains to wet canopy. Furthermore, stemflow generation also affected by the traveling time from canopy down to branch base, which was strongly affected by the bark roughness. Therefore, compared with the simply positive relation between TBRG orifice area and rains initiation in the clearings, the larger leaf area to intercept rains could not guarantee a quick start of stemflow. Our results indicated *C. korshinskii* and *S. psammophila* averagely initiated stemflow 66.2 and 54.8 min later than rains began during the 2014–2015 rainy seasons. Time lags of stemflow generation to rains was also supported by Germer (2010) and Cayuela et al. (2018). In general, TBRG was not perfect to precisely record stemflow timing, but might be the plausible devices to record stemflow process by far.

R2C2: Data processing is poorly explained. Stemflow intensity, given in mm h-1, requires that the volume of water delivered to the TBRG used to record stemflow (recorded in mL per bucket tip) must be associated with the area over which the equivalent stemflow depth is evaluated. I could not see this explained anywhere in the manuscript, and it needs to be made clear. If it was the cross-sectional area of the branch being monitored (typically about 3 cm2 by my rough estimation) then this needs to be set out in the manuscript. If the authors did use basal branch cross-sectional area, then of course the stemflow intensity can easily exceed the rainfall intensity, as a function of the very small area over which the stemflow is recorded as arriving - far smaller than the collecting area of the rainfall pluviograph. If this area were to be doubled, then the stemflow intensity would be halved (and so on). Therefore, the area used by the authors in their calculation needs to be stated (and justified by some relationship to plant water availability).

Data processing is also poorly explained in terms of the data on stemflow volume presented by the authors (e.g. in Table 3). Are the stemflow volumes reported there, and discussed at many places in the paper, the sum of the stemflow on the 7 monitored branches, or the arithmetic mean of the stemflow from the 7 branches, or are the figures scaled-up to estimate the stemflow delivered by the entire test shrub? (The test shrubs had a total of 180 and 261 branches (line 173) only 7 of which were monitored for each shrub species (amounting to a sample of 4% and

北京市海淀区双清路 18 号　邮编：100085　Website: www.rcees.ac.cn
#18 Shuangqing Road, Haidian District, Beijing 100085, P. R. China
Tel: 0086-10-62911239　Email: gygao@rcees.ac.cn

2.6% of the branches, the adequacy of which is not discussed by the authors). Whatever the authors did, it is not made clear and this needs to be corrected. Especially in relation to stemflow, all relevant parameters used in data processing must be set out clearly and systematically. Without knowing the details of the calculation procedure, the relative intensity of the stemflow and the open-field rainfalls are difficult to interpret. No formulae are presented by the authors that would allow this to be checked. My own feeling is that the stemflow flux would be a more useful figure - that is, the flow rate delivered to the base of the branch, expressed for instance in mL/minute or L/hour. If this is accompanied by a clearly-stated area over which the flow is tallied, then a stemflow intensity can be calculated.

Reply:

Thank you for this comment. The poorly-explained data processing has been carefully revised. We have detailedly described the definitions and calculations of stemflow volume, intensity, time lag to rains and other meteorological features at the revised manuscript. The representativeness of the selected was stated as below.

(1) Stemflow intensity has been computed following the definition as the stemflow volume per basal area per unit of time.

The RG3-M TBRGs had been applied to record stemflow in this study. Stemflow depth (SF_{RG}, mm) was computed with tip amounts within event by multiplying tip resolution of 0.2 mm. Similar with the interpretation for rainfall recording, the 0.2-mm per tip represented 200 mL water deposing on the 1-m^2 ground surface. Based at the same receiving areas, we calculated stemflow intensity as the ratio between SF_{RG} and rainfall duration at the previous manuscript. However, it underestimated the eco-hydrological significance of stemflow by ignoring the limited area of trunk/branch base, over which stemflow was truly received. Therefore, following the definition of stemflow volume per basal area per unit time (Herwitz, 1986; Spencer and Meerveld, 2016), we re-computed stemflow intensity with the branch base area at different temporal scales, including the event (SFI), the 10-min (SFI_{10}) and the intervals between neighboring tips of TBRG (SFI_i) (Equation 11–13 at Lines 246–248, Page 12). Furthermore, we established the quantitative connections of stemflow intensity with funnelling ratio for the first time (Equation 14 at Line 264, Page 12). By replacing the event-based volume of rainfall and stemflow with their intensities at the traditional expression, this new method enabled to calculate funnelling ratio at both inter-/intra-event scales (Lines 554–555, Page26).

(2) The detailed definition and calculation had been described for stemflow variables and rainfall characteristics.

The definitions and calculations had been described for stemflow volume (SFV, mL) (Equation 10 at Lines 235, Page 11), stemflow duration (SFD, h), time lags stemflow generation (TLG, min), maximization (TLM, min) and ending (TLE, min) at Lines 249–257, Page 12, the regression for rectifying the TBRG recordings with manual measurements (Equation 4) at Lines 164, Page 8, evaporation coefficient (E, unitless) (Equation 1–3) at Lines 158–160, Page 8, the allometric equations for estimating leaf area of branches at *C. korshinskii* and *S. psammophila* at Lines 215–218, Page 10.

北京市海淀区双清路 18 号　邮编：100085　　Website: www.rcees.ac.cn
#18 Shuangqing Road, Haidian District, Beijing 100085, P. R. China
Tel:　0086-10-62911239　　Email: gygao@rcees.ac.cn

(3) Stemflow variables had been averaged at different BD categories to analyze the most influential rainfall characteristics affecting them.

Stemflow variables were averaged at different-sized branches to present the branch-scaled stemflow variables of the representative shrubs at *C. korshinskii* and *S. psammophila* plots. We carefully checked the results of stemflow variables, and listed the average values of seven branches during rainfall events with different intensity peak amounts at Table 3 (Lines 817–824, Page 41). Please see the detailed description at Point (2) of Reply to R2C1.

(4) Seven representative branches were selected for stemflow recording at each species.

This study selected 4 shrubs for measuring stemflow and 1 shrub for establishing allometric equations of biomass and leaf areas at each species (Yuan et al., 2016; 2017). Please see Point (3) at Reply to R2C3 for a detailed description of the representativeness of selected experimental shrubs. The morphological features had been measured for all the 180 and 261 branches at these 5 shrubs of *C. korshinskii* and *S. psammophila*, respectively, thus to determining the standard branches for stemflow recording in this study. BD categories were grouped to guarantee the minimum branch amount at each category for meeting the statistical significance. The ≤5-mm branches were not included in stemflow measurements, because they were too weak to bear the fossil collars for trapping stemflow. Considering the high meteorological sensitivity of stemflow temporal dynamics, we tried best to select the experimental branches at the same shrub, which were most likely exposed to the similar rainfall characteristics. Moreover, the qualified branches should have the outlayer-of-canopy positions, no intercrossing with neighboring ones and no turning point in height from branch tip to base (Lines 209–210, Page 10). Therefore, apart from the ≤5-mm branches at both species, the >25-mm branches at *C. korshinskii* for not enough qualified individuals, and 15–18-mm branches at *S. psammophila* for TBRG malfunctioning, there are averagely 28 and 41 branches available for stemflow recording per shrub of *C. korshinskii* and *S. psammophila*, respectively (Table R2-1 as below). Finally, 7 branches were selected at each species, which took 25.0% and 17.1% of the available ones per shrub at *C. korshinskii* and *S. psammophila*, respectively. Additionally, the high expense of TBRG was an important reason to limit the amount of experimental shrub and branch for automatic recording of stemflow (Turner et al., 2019).

Table R2-1. Branch morphological features of the experimental shrubs of *C. korshinskii* and *S. psammophila*.

BD categories	*C. korshinskii*				*S. psammophila*			
	BD (mm)	BL (cm)	BA (°)	BN	BD (mm)	BL (cm)	BA (°)	BN
≤5	4.1	90.4	64.1	40	4.8	166	66	2
5–10	7.3	124.9	61.8	82	8.0	204	64	53
10–15	12.5	161.1	51.7	36	12.9	253	58	82
15–18	16.3	170.6	48.7	13	16.5	280	52	56
18–25	19.3	192.3	51.3	9	20.3	302	50	59
>25	NA	NA	NA	NA	28.7	366	50	9

中国科学院生态环境研究中心
Research Center for Eco-Environmental Science
Chinese Academy of Sciences (CAS)
北京市海淀区双清路 18 号　邮编：100085　　Website: www.rcees.ac.cn
#18 Shuangqing Road, Haidian District, Beijing 100085, P. R. China
Tel:　0086-10-62911239　　Email: gygao@rcees.ac.cn

Note: BD, BL, BA and BN are the basal diameter, length, angle and number of branches.

R2C3: In summary, what I find to be missing from the manuscript includes
-some discussion of why 7 stems were studied and whether this is a sufficient sample
-some consideration of the filling time of the buckets in the tipping-bucket gauges used for rainfall and stemflow measurement, and the effect of this on the lag time before the start of stemflow (and the cessation of stemflow after rain ends)
-more detail on the shrubs - including the variability of canopy size etc across the population from which the two sample shrubs were drawn, and some information on leaf area and wettability, if available
-a proper accounting of how stemflow flux was calculated and how the area over which the intensity was scaled was selected.

Reply:

(1) Please see Point (4) at Reply to R2C2 and Point (3) at Reply to R2C3 for explaining the representativeness of selected 7 branches and 4 shrubs for stemflow recording, respectively.

(2) Although TBRGs offered the ability to collect stemflow production at high temporal resolution and time lags to rain, they suffered from systematic errors owing to the rate of water delivery to tip buckets (Turner et al., 2019). The TBRGs missed the records of inflow water during tipping intervals, and they consumed water to wet buckets at the beginning (Groisman and Legates, 1994). The calibration was needed to rectify the volume recordings via regressions with the manual measurement results. However, it was difficult for rectifying the temporal data currently. Therefore, applying the TBRG with relative high accuracy was necessary. Iida et al. (2012) reported that the tipping time increased with the bucket volume by comparing different models of TBRG, including the RG3-M (3.73±0.01 mL), OW-34 (15.7±0.3 mL), UIZ-TB20 (198.3±3.3 mL), TXQ-200 (188.7±10.3 mL) and TXQ-400 (403.9±6.9 mL). We chose RG3-M with the small bucket volume of 3.73 mL to mitigate the underestimation in this study. Please see Point (3) at Reply to R2C1 to justify the feasibility of applying TBRGs.

(3) The plot investigations had been carried out at April of 2014 for the 20-year-old *C. korshinskii* and *S. psammophila*. For *C. korshinskii*, three subplots with the size of 5 m×5 m had been selected along the plot diagonal, including subplot A (5 shrubs) and C (6 shrubs) at the ends and subplot B (6 shrubs) at the middle. As indicated at Table R2-2 as below, the average canopy height and area were 1.9±0.1 m and 4.8±0.6 m^2, respectively. Because the runoff and sediment plots had already been constructed at the center of *S. psammophila* plot (Fig. R2-1 as below), we selected the subplot (13 shrubs) at northeastern part with the size of 20 m×20 m. The average canopy height and area were 3.5±0.2 m and 19.1±2.2 m^2, respectively (Table R2-3 as below). Thus, standard shrub could be determined to represent the two plots. Finally, five experimental shrubs of each species had been selected for stemflow measurements and allometric equation establishments of *C. korshinskii* (2.1±0.2 m and 5.1±0.3 m^2) and *S. psammophila* (3.5±0.2 m and 21.4±5.2 m^2), respectively.

中国科学院生态环境研究中心
Research Center for Eco-Environmental Science
Chinese Academy of Sciences (CAS)
北京市海淀区双清路 18 号　邮编：100085　Website: www.rcees.ac.cn
#18 Shuangqing Road, Haidian District, Beijing 100085, P. R. China
Tel: 0086-10-62911239　Email: gygao@rcees.ac.cn

As stated at Point (4) of Reply to R2C2, the standard branches could be determined and seven branches were finally selected for stemflow recording. According to the allometric equations established for estimating leaf area of individual branches (LA, cm^2) (Yuan et al., 2016; 2017), LA of experimental shrubs were estimated in the range of 837.7–6394.7 cm^2 and 626.3–7513.7 cm^2 at different BD categories for *C. korshinskii* and *S. psammophila*, respectively (Table 1 at Lines 805–807, Page 39). Rainfall intervals, the time intervals between neighboring rains (RI, h), was applied to indirectly represent the branch wettability. The drier barks could be estimated when RI was larger. The results of MCA and stepwise regression indicated that RI tightly corresponded to time lags of stemflow ending, but there was no significant quantitative relationship between them for for *C. korshinskii* (R^2=0.005, p=0.28) or *S. psammophila* (R^2=0.002, p=0.78) (Fig.7) (Lines 846–847, Page 49).

Table R2-2. Investigation of canopy morphology at *C. korshinskii* plot.

Plots	Shrubs	Canopy heights (m)	Canopy area (m^2)
A	1	1.7	4.6
	2	1.2	2.1
	3	1.9	3.7
	4	1.4	2.5
	5	2.0	5.7
B	6	1.7	5.5
	7	1.8	4.3
	8	1.8	3.8
	9	2.1	6.8
	10	2.5	11.6
	11	2.3	6.7
C	12	1.3	3.4
	13	1.9	5.9
	14	1.9	2.7
	15	1.8	2.8
	16	2.0	4.0
	17	2.2	5.5
Average		1.9±0.1	4.8±0.6

Table R2-3. Investigation of canopy morphology at *S. psammophila* plot.

Shrubs	Canopy heights (m)	Canopy area (m^2)
1	3.8	24.0
2	3.8	18.5
3	3.6	21.8
4	3.7	24.0

中国科学院生态环境研究中心
Research Center for Eco-Environmental Science
Chinese Academy of Sciences (CAS)
北京市海淀区双清路 18 号　邮编：100085　Website: www.rcees.ac.cn
#18 Shuangqing Road, Haidian District, Beijing 100085, P. R. China
Tel: 0086-10-62911239　Email: gygao@rcees.ac.cn

5	3.2	20.6
6	2.6	13.2
7	2.9	5.8
8	3.3	25.9
9	3.2	8.3
10	4.4	22.5
11	4.4	29.7
12	2.9	7.4
13	3.8	25.7
Average	3.5±0.2	19.1±2.2

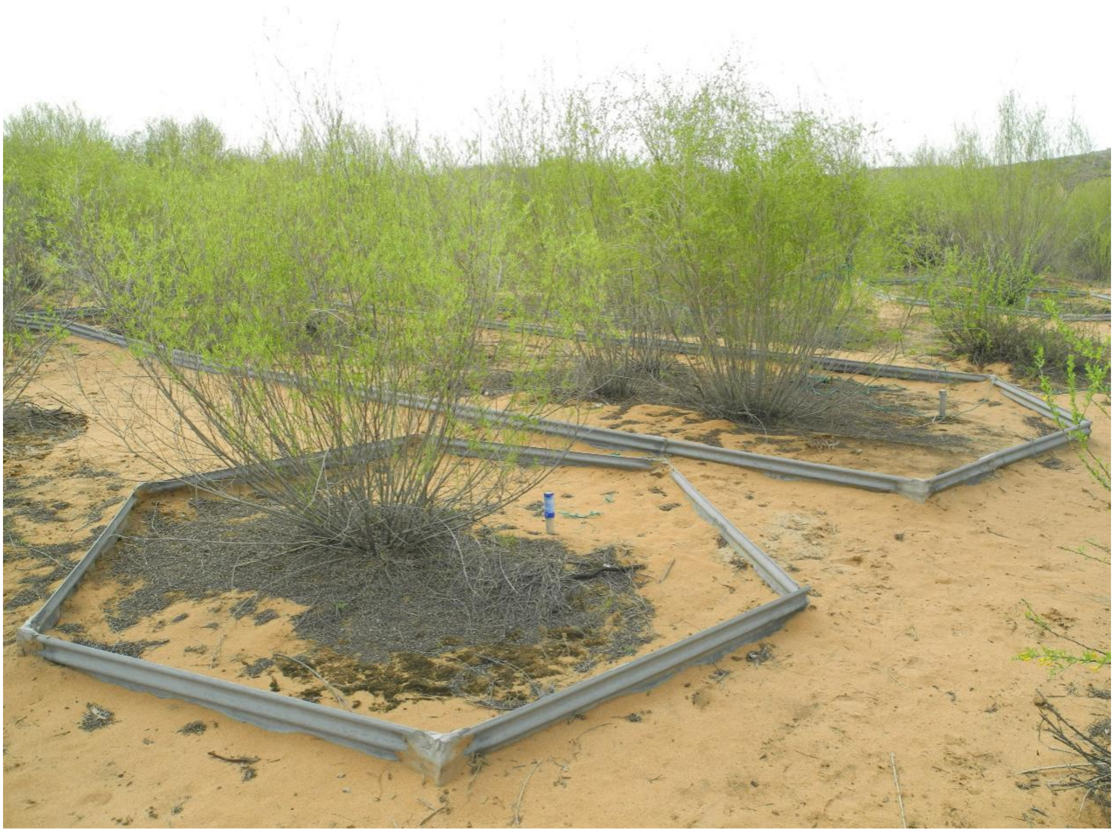

Fig. R2-1. The established runoff and sediment plots at the *S. psammophila* plot.

(4) Stemflow intensity had been re-calculated on the basis of branch basal area. Please see the detailed description at Point (1) of Reply to R2C2.

R2C4: More detailed comments:
lines 49-50: it is difficult to generalise from these few data to all "water stressed regions" (and need to define what a water-stressed region is)

Reply: Done. We have revised the “water-stressed regions” into “dryland ecosystems with

北京市海淀区双清路 18 号 邮编：100085 Website: www.rcees.ac.cn
#18 Shuangqing Road, Haidian District, Beijing 100085, P. R. China
Tel: 0086-10-62911239 Email: gygao@rcees.ac.cn

annual mean rainfall ranging in 154–900 mm" (Line 53, Page 3), which was cited from the reporting of Magliano et al. (2019).

R2C5: line 57: mL/g of what? biomass?

Reply: It was the unit of stemflow productivity (Yuan et al., 2016; 2017), which represented the stemflow volume of unit biomass. The description has been added at Line 57, Page 3.

R2C6: line 61: a flow in units of mL/min is a flux, not a speed

Reply: Done. We change the "speed" into "flux" at Line 61, Page 3.

R2C7: line 69: should presumably say 'not until AFTER canopies became saturated'

Reply: Done (Line 73, Page 4).

R2C8: line 70: need to define RA when this contraction is first used. It is used again in line 138 before being defined.

Reply: RA has been firstly used and explained at Line 52, Page 3.

R2C9: line 76: missing a space before 0.4

Reply: Done.

R2C10: lines 77-78: need to include branch surfaces also line 83: need to state which measure is maximized

Reply: Done. "branch surfaces" has been included at Line 79, and the "stemflow flux" has been stated at Line 84 of Page 4 at the revised manuscript.

R2C11: line 85: explain why time lags are important: presumably the last stemflow would occur as a very small (negligible) flux, so why is the timing of the last stemflow important? More generally, the authors could say something about why the time variation of stemflow during rainfall is important. Do peaks of stemflow flux exceed soil infiltration capacity, perhaps? Otherwise, why is this important?

Reply: Thank you for this comment. Stemflow might take a minor part of rainfall amount, but it greatly contributes to the survival of xerophytic plant species (Návar, 2011), the maintenance of patch structures in arid areas (Kéfi et al., 2007), and the normal functioning of rainfed dryland ecosystems (Wang et al., 2011) (Lines 52–57, Page 3). Previous studies failed to depict stemflow processes and quantify their relations with rainfall characteristics within events, particularly for xerophytic shrubs (Lines 20–23, Page 1). Time lags of stemflow generation, maximization and ending to rains depicted dynamic stemflow process, and were conducive to better understand the hydrological process occurred at the interface between the intercepted rains and soil moisture (Sprenger et al., 2019). It was important to discuss the temporal persistence in spatial patterns of soil moisture particularly at the intra-event scale (Gao et al.,

2019) (Lines 86–92, Pages 4–5).

R2C12: line 100: no need to repeat the number of rainfall events here, and again in line 222 and again in line 248. Once is sufficient.
Reply: Done.

R2C13: line 106: please define 'stemflow intensity' and provide a formula somewhere in the paper
Reply: Done. The definition and formula had been detailedly described at Lines 236–248, Pages 11–12.

R2C14: line 139: please explain what 'analogue' means here
Reply: Done. The "analogue period of time to dry canopies from antecedent rains" had been revise to "same period of time to dry canopies from antecedent rains as that reported by Giacomin and Trucchi (1992), Zhang et al. (2015), Zhang et al., (2017) and Yang et al. (2019)" at Lines 168–170, Page 8.

R2C15: lines 147-148: all these timing data are a function of the tipping-bucket filling time (see discussion earlier in this report). When using a TBRG, it is difficult to tell precisely when rain begins or ends, owing to the time that might be required to fill the first tipping- bucket.
Reply: The better understanding of stemflow temporal variables was conducive to address the eco-hydrological importance of stemflow as stated at Reply to R2C11. TBRG was not perfect to precisely record stemflow timing, but might be the plausible devices to record stemflow process by far. Please see Point (3) at Reply to R2C1 for justifying the usage of TBRGs to record stemflow process.

R2C16: line 153: how is raindrop morphology reflected in this? please explain
Reply: The raindrop momentum was calculated with raindrop size and velocity as indicated at Equation 5–9 (Line 184–188, Page 9), which represent the comprehensive effects of raindrop morphology (size) and kinetic energy (velocity).

R2C17: line 160: why is mean intensity used here?
Reply: The average rainfall intensity was used here to compute the average raindrop diameter and finally raindrop momentum on event base. The 10-min maximum raindrop momentum (F_{10}, mg·m·s^{-1}) and the average raindrop momentum at the first and last 10 min (F_{b10} and F_{e10}, respectively, mg·m·s^{-1}) could be calculated with I_{10}, I_{b10} and I_{e10} as indicated at Equation 5–9 (Line 184–188, Page 9), respectively.

R2C18: line 168: since this paper reports a study of branch stemflow only, the title of the paper should be amended to indicate this clearly (i.e., not a study of stemflow on an entire plant)

Reply: Done. We have revised the title to “Temporal-dependent effects of rainfall characteristics on inter-/intra-event branch-scaled stemflow variability in two xerophytic shrubs” as suggested as Reviewer 3.

R2C19: line 171: to what extent were the studied shrubs representative of the wider population? please present some data.

Reply: *C. korshinskii* and *S. psammophila* were the dominant shrub species at the arid and semi-arid regions of northwestern China, including Inner Mongolia Autonomous Region, Ningxia Hui Autonomous Region, Xinjiang Uygur Autonomous Region, Qinghai province, Gansu province, Shaanxi province, Shanxi province (Chao and Gong, 1999). Since both species had good drought tolerance, they were commonly planted for soil and water conservation, sand fixation and wind barrier (Li, 2012; Hu et al., 2016; Liu et al., 2016; Zhang et al., 2018). As the typical xerophytic shrub species at this region, they had extensive distributions particularly in arid and desert steppes (Li et al., 2016) at Lines 129–132, Page 6. Besides, please see Point (3) at Reply to R2C3 for explaining the representativeness of the selected 4 experimental shrubs for the *C. korshinskii* and *S. psammophila* plots.

R2C20: lie 181: please explain what is meant by ’canopy skirt locations’. The photos suggest that there were many overhanging leaves and branches. Some of the stemflow collars were placed quite high off the ground (as far as can be judged from the photos, as no quantitative information on this is included in the paper). How do the authors know that the stemflow at these heights would actually reach the ground, and not drip off the branches?

Reply: The “canopy-skirt locations” has been revised to “the outlayer-of-canopy” at Lines 210，Page 10. The photo shot the lower part of branches to show foil collar and TBRG for stemflow trapping and recording, which might not provide a very clear view of leaves on the upper branches. In contrast to the centered branches, stemflow of branches at the outlayer got less influences from the neighboring ones. We automatically recorded stemflow volume and timing via the RG3-M TBRG with height of 25.7 cm. Therefore, the foil collars were installed at branches nearly 40 cm off the ground (Lines 223–224, Page 11). It might be the minimum height for foil collars so as to keep the hose straight, which channelled stemflow down to TBRGs. The lost by dripping off was believed to be acceptable, compared with the commonly-used method to trap stemflow at breast height (1.2 or 1.3 m off ground) at tress particularly at rainforest, where the stemflow volume was much larger.

R2C21: line 189-190: what was the external diameter? this should be included as the dimensions of the stemflow collars are critical - it does not seem sufficient simply to assert that they caught no rainfall or released drips of throughfall from above.

Reply: The “external diameter” has been revised to “orifice diameter” at Line 234. The limited orifice diameter of foil collars minimized the accessing of throughfall and rains into them (Yuan et al., 2017) (Lines 225–227, Page 11).

中国科学院生态环境研究中心
Research Center for Eco-Environmental Science
Chinese Academy of Sciences (CAS)
北京市海淀区双清路 18 号　邮编：100085　　Website: www.rcees.ac.cn
#18 Shuangqing Road, Haidian District, Beijing 100085, P. R. China
Tel: 0086-10-62911239　　Email: gygao@rcees.ac.cn

R2C22: line 270: how were rainfall intensity peaks identified? What makes one peak an intensity peak?

Reply: SFI_i, the instantaneous stemflow intensity, was computed in terms of the tip volume (3.73 mL), branch basal area (mm^2) and time intervals between neighboring tips recorded by TBRGs as indicated Equation 13 (Line 248, Page 12). The largest SFI_i was defined as the peak intensity at the incident rains.

R2C23: line 292: is the reference to the volume from a single branch or the total from the 7 branches?

Reply: We focused on the average stemflow variables of 7 experimental branches, and analyzed the most influential rainfall characteristics affecting them. Please see the detailed explanation at Point 2 of Reply to R2C1 and Point 3 of Reply to R2C2.

R2C24: lines 300-310: this is difficult to read, owing to the need to recall the meaning of the very many contractions. Some reminders of what these mean would be useful here.

Reply: As indicated at the suggestion commenting at Line 70 of R2C5, the contraction was only explained when it was first used. For an easy reading, the list of symbols had been prepared as appendix at the revised manuscript (Lines 592–593, Pages 27–29).

R2C25: line 342: a stemflow intensity of 1232 mm h-1 is large. What was the flux? I presume that in the case of the authors own work in the present study, the flux was within the capacity of the tipping-bucket gauges (typically a few hundred mm h-1 at maximum) since the rainfall was not very intense. Some comment on this would be worthwhile.

Reply: As indicated at the manual of RG3-M TBRG (https://www.onsetcomp.com/products/data-loggers/rg3-m), data could be automatically recorded at rains with the maximum intensity of 127 $mm \cdot h^{-1}$. The unit depth (mm) of inflow water recorded by TBRG was interpreted to the equivalent 1000 cm^3 water on the 1-m^2 ground surface. However, stemflow intensity was computed with branch basal areas. It approximately ranged in 34–770 mm^2 for *C. korshinskii* and *S. psammophila* in this study, which took less than 0.8‰ of 1 m^2. Therefore, it could be estimated that the RG3-M TBRG offers the ability to record stemflow with the maximum intensity greater than 15000 $mm \cdot h^{-1}$.

R2C26: lines 383-384: but these fluxes would surely depend on the antecedent leaf and branch wetness, and on meteorological conditions such as wind speed and vapour deficit (the latter is not reported, incidentally).

Reply: Thank you for this comment. The evaporation coefficient (E, unitless) had been included at the revised manuscript. E was computed with air temperature, relative humidity and wind speed as indicated at Equation 1–3 (Lines 158–160, Page 8). It represented the comprehensive influences of these meteorological characteristics. By performing the multiple correspondence analysis (MCA), E and rainfall duration (RD) were tested to closely relate with stemflow duration (Lines 360–362, Page 17). However, the stepwise regression analysis finally confirmed the dominant influence of RD affecting SFD (Lines 381–382, Page 18). Rainfall intervals, the time intervals between neighboring rains (RI, h), was applied to indirectly represent the branch wettability. Please see the detailed description at Point (3) at Reply to R2C3.

R2C27: Table 2: why are only 3 rainfall events listed here? More than 40 more are simply lumped under "others" and no details are provided. Why?

Reply: Event A, B and C represented three categories of events with the single, double and multiple intensity peak amounts. It had been described at the note of Table 2 (Lines 808–816, Page 40) and *Section 3.1* (Lines 301–303, Pages 14). There were 17, 11 and 15 events at Event A, B and C, respectively. Because the remaining 11 events had the average RA of 0.6 mm, no more than three recordings had been observed within event which was limited by 0.2-mm resolution of TBRGs. Therefore, they could not be categorized and grouped as Event others (Lines 303– 06, Page 14).

R2C28: Figure 4 shows units of m/h which I presume should be mm/h

Reply: Done.

Reference:

Allaby, M.: A Dictionary of Ecology, 4th Edition., Oxford University Press, Oxford, 2010.

Cayuela, C., Llorens, P., Sánchez-Costa, E., Levia, D.F. and Latron, J.: Effect of biotic and abiotic factors on inter- and intra-event variability in stemflow rates in oak and pine stands in a Mediterranean mountain area, J. Hydrol., 560, 396–406, https://doi.org/10.1016/j.jhydrol.2018.03.050, 2018.

Chao, P. N. and Gong, G. T.: *Salix (Salicaceae)*, in: Flora of China, edited by: Wu, Z. Y., Raven, P. H., and Hong, D. Y., Science Press, Beijing and Missouri Botanical Garden Press, St. Louis, 162–274, 1999.

Dunkerley, D.: Stemflow on the woody parts of plants: dependence on rainfall intensity and event profile from laboratory simulations, Hydrol. Process., 28, 5469–5482, http://dx.doi.org/10.1002/hyp.10050, 2014a.

Dunkerley, D.: Stemflow production and intrastorm rainfall intensity variation: an experimental analysis using laboratory rainfall simulation, Earth Surf. Proc. Land., 39, 1741–1752, http://dx.doi.org/10.1002/esp.3555, 2014b.

Firn, R.: Plant Intelligence: an Alternative Point of View, Ann. Bot., 93, 345–351, 2004.

Gao, X.D., Zhao, X.N., Pan, D.L., Yu, L.Y. and Wu, P.T.: Intra-storm time stability analysis of surface soil water content, Geoderma, 352, 33–37, https://doi.org/10.1016/j.geoderma.2019.06.001, 2019.

Germer, S., Werther, L. and Elsenbeer, H.: Have we underestimated stemflow? Lessons from an open tropical rainforest, J. Hydrol., 395, 169–179, https://doi.org/10.1016/j.jhydrol.2010.10.022, 2010.

Groisman, P. Y. and Legates, D. R.: The accuracy of United States precipitation data, B. Am. Meteorol. Soc., 75, 215–227, 1994.

Giacomin, A. and Trucchi, P.: Rainfall interception in a beech coppice (*Acquerino, Italy*). J. Hydrol., 137, 141–147, https://doi.org/10.1016/0022-1694(92)90052-W, 1992.

Herwitz, S.R.: Infiltration-excess caused by Stemflow in a cyclone-prone tropical rainforest, Earth Surf. Proc. Land, 11, 401–412, https://doi.org/10.1002/esp.3290110406, 1986.

Hu, R., Wang, X.P., Zhang, Y.F., Shi, W., Jin, Y.X. and Chen, N.: Insight into the influence of sand-stabilizing shrubs on soil enzyme activity in a temperate desert, Catena, 137, 526–535, http://dx.doi.org/10.1016/j.catena.2015.10.022, 2016.

Iida, S., Shimizu, T., Kabeya, N., Nobuhiro, T., Tamai, K., Shimizu, A., Ito, E., Ohnuki, Y., Abe, T., Tsuboyama, Y., Chann, S. and Keth, N.: Calibration of tipping-bucket flow meters and rain gauges to measure gross rainfall, throughfall, and stemflow applied to data from a Japanese temperate coniferous forest and a Cambodian tropical deciduous forest, Hydrol. Process., 26, 2445–2454, https://doi.org/10.1002/hyp.9462, 2012.

Kéfi, S., Rietkerk, M., Alados, C.L., Pueyo, Y., Papanastasis, V.P., ElAich, A. and De Ruiter, P.C.: Spatial vegetation patterns and imminent desertification in Mediterranean arid ecosystems, Nature, 449, 213–217, https://doi.org/10.1038/nature06111, 2007.

Li, X.R., 2012. Eco-Hydrology of Biological Soil Crusts in Desert Regions of China. Higher Education Press, Beijing (In Chinese).

Li, Y.Y., Chen, W.Y., Chen, J.C. and Shi, H.: Contrasting hydraulic strategies in *Salix psammophila* and *Caragana korshinskii* in the southern Mu Us Desert, China, Ecol. Res., 31, 869–880, https://doi.org/10.1007/s11284-016-1396-1, 2016.

Liu, Y.X., Zhao, W.W., Wang, L.X., Zhang, X., Daryanto, S. and Fang, X.N.: Spatial variations of soil moisture under *Caragana korshinskii* kom. from different precipitation zones: field based analysis in the Loess Plateau, China, Forests, 7, https://doi.org/10.3390/f7020031, 2016.

Magliano, P.N., Whitworth-Hulse, J.I. and Baldi, G.: Interception, throughfall and stemflow partition in drylands: Global synthesis and meta-analysis, J. Hydrol., 568, 638–645, https://doi.org/10.1016/j.jhydrol.2018.10.042, 2019.

Návar, J.: Stemflow variation in Mexico's northeastern forest communities: Its contribution to soil moisture content and aquifer recharge, J. Hydrol., 408, 35–42, https://doi.org/10.1016/j.jhydrol.2011.07.006, 2011.

Spencer, S. A. and van Meerveld, H. J.: Double funnelling in a mature coastal British Columbia forest: spatial patterns of stemflow after infiltration, Hydrol. Process., 30, 4185–4201, https://doi.org/ 10.1002/hyp.10936, 2016.

Sprenger, M., Stumpp, C., Weiler, M., Aeschbach, W., Allen, S.T., Benettin, P., Dubbert, M., Hartmann, A., Hrachowitz, M., Kirchner, J.W., McDonnell, J.J., Orlowski, N., Penna, D.,

北京市海淀区双清路 18 号　邮编：100085　　Website: www.rcees.ac.cn
#18 Shuangqing Road, Haidian District, Beijing 100085, P. R. China
Tel:　0086-10-62911239　　Email: gygao@rcees.ac.cn

Pfahl, S., Rinderer, M., Rodriguez, N., Schmidt, M. and Werner, C.: The Demographics of Water: A Review of Water Ages in the Critical Zone, Rev. Geophys., 57, 1–35, https://doi.org/10.1029/2018RG000633, 2019.

Turner, B., Hill, D.J., Carlyle-Moses, D.E. and Rahman, M.: Low-cost, high-resolution stemflow sensing, J. Hydrol., 570, 62–68, https://doi.org/10.1016/j.jhydrol.2018.12.072, 2019.

Wang, X.P., Wang, Z.N., Berndtsson, R., Zhang, Y.F. and Pan, Y.X.: Desert shrub stemflow and its significance in soil moisture replenishment, Hydrol. Earth Syst. Sci., 15, 561–567, https://doi.org/10.5194/hess-15-561-2011, 2011.

Yuan, C., Gao, G.Y. and Fu, B.J.: Stemflow of a xerophytic shrub (*Salix psammophila*) in northern China: Implication for beneficial branch architecture to produce stemflow, J. Hydrol., 539, 577–588, https://doi.org/10.1016/j.jhydrol.2016.05.055, 2016.

Yuan, C., Gao, G.Y. and Fu, B.J.: Comparisons of stemflow and its bio-/abiotic influential factors between two xerophytic shrub species, Hydrol. Earth Syst. Sci., 21, 1421–1438, https://doi.org/10.5194/hess-21-1421-2017, 2017.

Zhang, Y.F., Wang X.P., Hu, R., Pan Y.X. and Paradeloc, M.: Rainfall partitioning into throughfall, stemflow and interception loss by two xerophytic shrubs within a rain-fed re-vegetated desert ecosystem, northwestern China, J. Hydrol., 527, 1084–1095, https://doi.org/10.1016/j.jhydrol.2015.05.060, 2015.

Yang, X.L., Shao, M.A. and Wei, X.H.: Stemflow production differ significantly among tree and shrub species on the Chinese Loess Plateau, J. Hydrol., 568, 427–436, https://doi.org/10.1016/j.jhydrol.2018.11.008, 2019.

Zhang, Y., Li, X.Y., Li, W., Wu, X.C., Shi, F.Z., Fang, W.W. and Pei, T.T.: Modeling rainfall interception loss by two xerophytic shrubs in the Loess Plateau, Hydrol. Process., 31, 1926–1937, https://doi.org/10.1002/hyp.11157, 2017.

Zhang, Y.F., Wang, X.P., Hu, R. and Pan, Y.X.: Meteorological influences on process-based spatial-temporal pattern of throughfall of a xerophytic shrub in arid lands of northern China, Sci. Total. Environ., 619, 1003–1013, https://doi.org/10.1016/j.scitotenv.2017.11.207, 2018.

中国科学院生态环境研究中心
Research Center for Eco-Environmental Science
Chinese Academy of Sciences (CAS)
北京市海淀区双清路 18 号 邮编：100085 Website: www.rcees.ac.cn
#18 Shuangqing Road, Haidian District, Beijing 100085, P. R. China
Tel: 0086-10-62911239 Email: gygao@rcees.ac.cn

Response to Reviewer #3

General Comments: After careful review, I think, in many ways, this is a good manuscript. The work has been well done and the manuscript is well organized. The paper has an appropriate length and the topic is of interest to the general readers of HESS…I recommend this manuscript for publication after a minor revision.

Reply:

We appreciated the anonymous reviewer for the comments and suggestions. This manuscript will be carefully revised as suggested prior to being submitted.

R3C1: My major concern is the reasonability of the stemflow variables used in this study. For instance, in Line 207, the authors said that the average (SFI) and 10-min maximum (SFI10) stemflow intensities were calculated by the branch stemflow as recorded by the tipping-bucket rain gauges (mm) and rainfall duration (h). In my opinion, stemflow intensities should be defined as the branch stemflow depth (which can be calculated from branch stemflow volume as divided by branch basal area) in a certain time. In the current form, the authors underestimated stemflow intensities. Also, in Line 216, the ratio of the intra-event stemflow intensity (RSFI, unitless) should be calculated basing on the suggested calculation of stemflow intensity.

Reply:

Thank you for commenting on the calculation of stemflow variables in this study. As suggested at this comment, it indeed underestimated the eco-hydrological significance of stemflow to compute stemflow intensity by ignoring the limited area of branch base, over which stemflow was received. Therefore, we had re-computed stemflow intensity following the definition as stemflow volume per basal area per unit of time (Herwitz, 1986; Spencer and Meerveld, 2016). It had been calculated at different time intervals, including the event (SFI, $mm \cdot h^{-1}$), 10-min (SFI_{10}, $mm \cdot h^{-1}$) and dynamic time interval between neighboring tips (SFI_i, $mm \cdot h^{-1}$). Besides, RSFI had been deleted, and funnelling ratio had been introduced to assess the convergence effect of stemflow at the revised manuscript. It had been quantitatively connected with stemflow intensity for the first time as indicated at Equations 14–15 (Lines 264–265, Page 12). Please see the detailed explanation at Point (1) of Reply to R1C12, and Point (1) of Reply to R2C2.

R3C2: I also state minor comments as follows. L1: Only seven branches were used to measure stemflow for each shrub species (The studied shrubs had a total of 180 and 261 branches), So the suggested title is: Temporal-dependent effects of rainfall characteristics on inter-/intra-event branch-scale stemflow variability in two xerophytic shrubs.

Reply: Done.

中国科学院生态环境研究中心
Research Center for Eco-Environmental Science
Chinese Academy of Sciences (CAS)
北京市海淀区双清路 18 号　邮编：100085　　Website: www.rcees.ac.cn
#18 Shuangqing Road, Haidian District, Beijing 100085, P. R. China
Tel:　0086-10-62911239　　Email: gygao@rcees.ac.cn

R3C3: L220-226: It could be better if the authors provide the formula for each stemflow variables.

Reply:

Done. The detailed descriptions and calculations of stemflow variables had been stated at the revised manuscript, including stemflow volume (SFV, mL) (Equation 10) at Line 235, Page 11, stemflow duration (SFD, h), time lags stemflow generation (TLG, min), maximization and ending (TLE, min) at Lines 249–257, Page 12, stemflow intensities at the event bases (SFI), the 10-min interval (SFI_{10}) and the dynamic intervals between neighboring tips of TBRG (SFI_i) (Equation 11–13) at Lines 246–248, Page 12, funnelling ratio at event base (FR) and the 100-s (FR_{100}) intervals (Equation 14–15) at Lines 264–265, Page 12.

R3C4: L658. Table 1: What is the standard for base diameter (BD) categorization? In the current form, the class interval (5–10, 10–15, 15–18, 18–25, >25 mm) is variable. Why not 5-10, 10-15, 15-20, 20-25, and >25 mm? Please explain it.

Reply:

Thanks for this comment. Based on the plot investigation for *C. korshinskii* and *S. psammophila*, standard shrubs canopies could be determined. Four shrubs and 1 shrub had been selected for stemflow measurements and allometric equations establishments. By measuring branch morphologies at all the branches at these five shrubs of each species, BD categories was determined to guarantee the minimum branch amount at each category for meeting the statistical significance. There was comparatively smaller amount of the 20–25-mm branches of *C. korshinskii*. Applying the categories interval of 15–18 and 18–25 was aimed to make sure the minimum branches amount between these two neighboring categories for meeting the statistical significance. Please see Point (4) at Reply to R2C2 and Point (3) at Reply to R2C3 for explaining the representativeness of selected 7 branches and 4 shrubs for stemflow recording, respectively.

R3C5: L662. Table 2: Do the rainfall indicators including RA, RD, RI, I, I10, Ib10 etc differ statically significantly among Event A, Event B, Event C and Others? Please provide the ANVOA results here. L670. Table 3: The comment is the same with the last one. Please provide the statistical results to depict the difference in the stemflow variables among Event A, Event B, Event C and Others.

Reply:

Thank you for this comment. The One-way analysis of variance (ANOVA) with LSD post hoc test had been performed to determine whether rainfall characteristics and stemflow variables differed significantly among event categories, and whether funnelling ratio and stemflow intensities differed significantly among BD categories for *C. korshinskii* and *S. psammophila*. The level of significance was set at 95% confidence interval (p=0.05) (Lines 284–289, Pages 13–14). The ANOVA results had been stated in the section *3.1 Rainfall characteristics* at Lines 307–312, Page 14–15, *Section 3.2 Stemflow volume, intensity, funnelling ratio and temporal dynamics* at Lines 337–342, Page 16, and Table 2–4 (Lines 808–829, Pages 40–42).

Reference:

Herwitz, S.R.: Infiltration-excess caused by Stemflow in a cyclone-prone tropical rainforest, Earth Surf. Proc. Land, 11, 401–412, https://doi.org/10.1002/esp.3290110406, 1986.

Spencer, S. A. and van Meerveld, H. J.: Double funnelling in a mature coastal British Columbia forest: spatial patterns of stemflow after infiltration, Hydrol. Process., 30, 4185–4201, https://doi.org/ 10.1002/hyp.10936, 2016.

Temporal-dependent effects of rainfall characteristics on inter-/intra-event branch-scaled stemflow variability in two xerophytic shrubs

Chuan Yuan[1, 2, 3], Guangyao Gao[2], Bojie Fu[2], Daming He[1, 3], Xingwu Duan[1, 3], and Xiaohua Wei[4]

[1]Institute of International Rivers and Eco–security, Yunnan University, Kunming 650091, China

[2]State Key Laboratory of Urban and Regional Ecology, Research Center for Eco-Environmental Sciences, Chinese Academy of Sciences, Beijing 100085, China

[3]Yunnan Key Laboratory of International Rivers and Trans-boundary Eco–security, Kunming 650091, China

[4]Department of Earth, Environmental and Geographic Sciences, University of British Columbia (Okanagan campus), Kelowna, British Columbia, V1V 1V7, Canada

Correspondence: Guangyao Gao (gygao@rcees.ac.cn)

Abstract

Stemflow is important for recharging root-zone soil moisture in arid regions. Previous studies have generally focused on stemflow volume, efficiency and influential factors but have failed to depict stemflow processes and quantify their relations with rainfall characteristics within events, particularly for xerophytic shrubs. Here, we measured the stemflow volume, intensity, funnelling ratio, duration, and time lags to rain at two dominant shrub species (*Caragana korshinskii* and *Salix psammophila*) and rainfall characteristics during 54 events at the semi-arid Liudaogou catchment of the Loess Plateau, China, during the 2014–2015 rainy seasons. Funnelling ratio was calculated as the ratio between stemflow and rainfall intensities at the inter-/intra-event bases for the first time. Our results indicated that the stemflow of *C. korshinskii* and *S. psammophila* were averagely started 66.2 and 54.8 min, maximized 109.4 and 120.5 min after rains began, and ended 20.0 and 13.5 min after rains ceased. They had shorter stemflow duration (3.8 and 3.4 h) and significantly larger stemflow intensities (517.5 and 367.3 mm·h^{-1}) than those of rains (4.7 h and 4.5 mm·h^{-1}). As branch size increased, both species shared the decreasing funnelling ratios (97.7–163.7 and 44.2–212.0) and stemflow intensities (333.8–716.2 mm·h^{-1} and 197.2–738.7 mm·h^{-1}). Tested by the multiple correspondence analysis and stepwise regression, rainfall amount and duration controlled stemflow volume and duration, respectively, at event scale by linear relations (p<0.01). Rainfall intensity and raindrop momentum controlled stemflow intensity and time lags to rains for both species within event by linear or power relationships (p<0.01). Rainfall intensity was the key factor affecting stemflow process of *C. korshinskii*, whereas raindrop momentum had the greatest influence on stemflow process of *S. psammophila*. Therefore, rainfall characteristics had temporal-dependent influences on corresponding stemflow variables, and the influence also depended on specific species.

1 Introduction

Stemflow directs the intercepted rains from canopy to the trunk base. The funnel-shaped canopy and underground preferential paths, i.e., roots, worm paths and soil macropores, converge rains to recharge the root-zone moisture (Johnson and Lehmann, 2006; Li et al., 2008). Stemflow is important to concentrate water (Levia and Germer, 2015), nutrients (Dawoe et al., 2018), pathogens (Garbelotto et al., 2003) and bacteria (Bittar et al., 2018) from the phyllosphere into the pedosphere (Teachey et al., 2018), even though stemflow accounts for only a minor part of rainfall amount (RA) (6.2%) in contrast to throughfall (69.8%) and interception loss (24.0%) in dryland ecosystems with annual mean rainfall ranging in 154–900 mm (Magliano et al., 2019). Stemflow greatly contributes to the survival of xerophytic plant species (Návar, 2011), the maintenance of patch structures in arid areas (Kéfi et al., 2007), and the normal functioning of rainfed dryland ecosystems (Wang et al., 2011).

To quantify the ecohydrological importance of stemflow, numerous studies have been conducted on stemflow production and efficiency from various aspects, including stemflow volume (mL), depth (mm), percentage (%), funnelling ratio (unitless), and productivity ($mL \cdot g^{-1}$, the branch stemflow volume of unit biomass) (Herwitz, 1986; Yuan et al., 2016; Zabret et al., 2018; Yang et al., 2019). By installing automatic recording devices, the stemflow process has been gradually determined at 1-h intervals (Spencer and van Meerveld, 2016), 5-min intervals (André et al., 2008; Levia et al., 2010) and 2-min intervals (Dunkerley, 2014b). This determination allowed to compute stemflow intensity ($mm \cdot h^{-1}$) (Germer et al., 2010), flux ($mL \cdot min^{-1}$) (Yang, 2010) and time lag after rain (Cayuela et al., 2018). Differing from an event-based calculation, the stemflow process provided insights into the fluctuation of stemflow production at a high temporal resolution.

It permits a better interpretation of the “hot moment” and “hot spot” effects of many ecohydrological processes (Bundt et al., 2001; McClain et al., 2003). Quantifying the short-intensity burst and temporal characteristics shed light on the dynamic process and pulse nature of stemflow (Dunkerley, 2019).

Stemflow cannot be initiated until canopies were saturated by the rains (Martinez-Meza and Whitford, 1996). The minimal RA needed to start stemflow was usually calculated by regressing stemflow volume with RA at different plant species (Levia and Germer, 2015). It also varied with canopy states, i.e., 10.9 and 2.5–3.4mm for the leafed oak and beech tress, and 6.0 mm and 1.5–1.9 mm for them in the leafless period (André et al., 2008; Staelens et al., 2008). Stemflow also frequently continued after rains ceased due to the rainwater retained on the canopy/branch surface (Iida et al., 2017). *Salix psammophila* and an open tropical forest started stemflow 5–10 min and 15 min later than the beginning of a rain event in the Mu Us desert of China (Yang, 2010) and the Amazon basin of Brazil (Germer et al., 2010), respectively. However, 1 h and 1.5 h were needed to start stemflow after the beginning of a rain event for pine and oak trees in north-eastern Spain, respectively (Cayuela et al., 2018). For *S. psammophila*, stemflow flux was maximized 20–210 min after the beginning of a rain event (Yang, 2010), and stemflow ceased 11 h after rains seaced in an open tropical forest (Germer et al., 2010). Time lags of stemflow generation, maximization and ending to rains depicted dynamic stemflow process, and were conducive to better understand the hydrological process occurred at the interface between the intercepted rains and soil moisture (Sprenger et al., 2019). It was important to discuss the temporal persistence in spatial patterns of soil moisture particularly at the intra-event scale (Gao et al., 2019). However, stemflow time lags have not been systematically studied for xerophytic shrubs.

The preferential paths at the underside of branches for delivering stemflow complicates stemflow processes within events (Dunkerley, 2014a). The influences of bark microrelief on stemflow are strongly affected by dynamic rain processes, such as rainfall intensity and raindrop striking within events (van Stan and Levia, 2010). While exceeding the holding capacity of branches, high rainfall intensity could overload and interrupt this preferential path (Carlyle-Mose and Price, 2006). Raindrops hit the canopy surface and create splashes on the surface. This process is conducive to wetting branches at the lower layers and accelerating the establishment of the preferential paths of stemflow transportation (Bassette and Bussière, 2008). Nevertheless, the interaction between the stemflow process and intra-event rainfall characteristics has not been substantially studied.

This study was designed at the event and process scales to investigate inter-/intra-event stemflow variability of two dominant xerophytic shrubs. Stemflow volume, intensity, funnelling ratio and temporal dynamics of *Caragana korshinskii* and *S. psammophila* were recorded during 54 rainfall events in the 2014–2015 rainy seasons on the Loess Plateau of China. Temporal dynamics were expressed as stemflow duration and time lags of stemflow generation, maximization and cessation to rains. Raindrop momentum was introduced to represent the comprehensive effects of raindrop size, velocity, inclination angle and kinetic energy at the stemflow process. Funnelling ratio had been calculated at the event base and the 100-s intervals to assess the convergence effects of stemflow. This study specifically aimed to (1) depict the stemflow process in terms of stemflow intensity and temporal dynamics, (2) identify the dominant rainfall characteristics influencing inter-/intra-event stemflow variables, and (3) quantify the relationships between stemflow process variables and rainfall characteristics. Achieving these objectives would advance our knowledge of the process-based stemflow production to better understand the pulse nature of stemflow and its interactions with dynamic rain processes.

2 Materials and Methods

2.1 Site description

This study was conducted in the Liudaogou catchment (110°21′–110°23′E, 38°46′–38°51′N) in Shenmu city, Shaanxi Province, China, during the 2014–2015 rainy seasons. This catchment is 6.9 km^2 and 1094–1273 m above sea level (m.a.s.l.). A semiarid continental climate prevails in this area. The mean annual precipitation (MAP) is 414 mm (1971–2013). Most MAP (77%) occurs from July to September (Jia et al., 2013). The mean annual potential evaporation is 1337 mm (Yang et al., 2019). The mean annual temperature is 9.0 °C. The dominant shrubs include *C. korshinskii*, *S. psammophila*, and *Amorpha fruticosa*. The dominant grasses are *Artemisia capillaris*, *Artemisia sacrorum*, *Medicago sativa*, *Stipa bungeana*, etc.

C. korshinskii and *S. psammophila* are dominant shrub species at the arid and semi-arid regions of northwestern China (Hu et al., 2016; Liu et al., 2016). They were commonly planted for soil and water conservation, sand fixation and wind barrier, and had extensive distributions at this region (Li et al., 2016). The both species have inverted-cone crowns and no trunks, with multiple branches running obliquely from the base. As modular organisms and multi-stemmed shrub species, their branches live as independent individuals and compete with each other for water and light (Firn, 2004). Two plots were established in the southwestern catchment for these two xerophytic shrubs planted in the 1990s (Fig. 1). *C. korshinskii* and *S. psammophila* plots share similar stand conditions with elevations of 1179 and 1207 m.a.s.l., slopes of 13° and 18°, and sizes of 3294 and 4056 m^2, respectively. The *C. korshinskii* plot has a ground surface of loess and aspect of 224°, while the *S. psammophila* plot has a ground surface of sand and an aspect of 113°.

2.2 Meteorological measurements and calculations

A meteorological station was installed at the experimental plot of *S. psammophila* to record rainfall characteristics and wind speed (WS, $m \cdot s^{-1}$) (Model 03002, R. M. Young Company, USA), air temperature (T, °C) and relative humidity (H, %) (Model HMP 155, Vaisala, Finland). They were logged at 10-min intervals by a datalogger (Model CR1000, Campbell Scientific Inc., USA). Evaporation coefficient (E, unitless) was calculated to present the evaporation intensity (Equations 1–3) via aerodynamic approaches (Carlyle-Mose and Schooling, 2015). Tipping-bucket rain gauges (hereinafter referred to as "TBRG") automatically recorded the volume and timing of rainfall and stemflow (Herwitz, 1986; Germer et al., 2010; Spencer and Meerveld, 2016; Cayuela et al., 2018). To mitigate the systematic errors for missing the records of inflow during tipping intervals (Groisman and Legates, 1994), we chose the Onset® (Onset Computer Corp., USA) RG3-M TBRG with the relatively smaller underestimation for its smaller bucket volume (3.73±0.01 mL) (Iida et al., 2012). Besides, three 20-cm-diameter standard rain gauges were placed around TBRG with a 0.5-m distance at the 120° separation (Fig. 1). The regression (R^2=0.98, p<0.01) between manual measurements and automatic recording further mitigated the understanding of inflow water by applying TBRG (Equation 4).

$$e_s = 0.611 \times \exp\left(17.27 \times T \big/ (237.7 + T)\right) \quad (1)$$

$$VPD = e_s \times (1 - H) \quad (2)$$

$$E = WS \times VPD \quad (3)$$

where e_s is the saturation vapor pressure (kPa); T is air temperature (°C); H is air relative humidity (%); VPD is the vapor pressure deficit (kPa); and E is the evaporation coefficient (unitless).

$$IW_A = IW_R \times 1.32 + 0.16 \quad (4)$$

where IW_R is the recording of Inflow water (including rainfall and stemflow) via TBRG (mm), and IW_A is the adjusted inflow water (mm).

Discrete rainfall events were defined by a measurable RA of 0.2 mm (the resolution limit of the TBRG) and the smallest 4-h gap without rains. That was the same period of time to dry canopies from antecedent rains as reported by Giacomin and Trucchi (1992), Zhang et al. (2015), Zhang et al., (2017) and Yang et al. (2019). Rainfall interval (RI, h) was calculated to indirectly represent the bark wetness. Other rainfall characteristics were also computed, including the RA (mm), rainfall duration (RD, h), the average and 10-min maximum rainfall intensity of incident rains (I and I_{10}, $mm \cdot h^{-1}$), and the 10-min average rainfall intensity after rain begins (I_{b10}, $mm \cdot h^{-1}$) and before rain ends (I_{e10}, $mm \cdot h^{-1}$). By assuming a perfect sphere of a raindrop (Uijlenhoet and Torres, 2006), raindrop momentum in the vertical direction (F, $mg \cdot m \cdot s^{-1}$) (Equation 8–9) was computed to comprehensively represent the effects of raindrop size (D, mm) (Equation 5), terminal velocity (v, $m \cdot s^{-1}$) (Equation 6), average inclination angle (θ, °) (Equation 7) affecting stemflow process

(Brandt, 1990; Kimble, 1996; van Stan et al., 2011; Carlyle-Moses and Schooling, 2015). The 10-min maximum raindrop momentum (F_{10}, mg·m·s^{-1}) and the average raindrop momentum at the first and last 10 min (F_{b10} and F_{e10}, respectively, mg·m·s^{-1}) could be calculated with I_{10}, I_{b10} and I_{e10} as indicated at Equation 5–9, respectively. For the 0.8-km distance between the two plots, the meteorological data were used at the *C. korshinskii* plot.

$$D = 2.23 \times (0.03937 \times I)^{0.102} \tag{5}$$

$$v = 3.378 \times \ln(D) + 4.213 \tag{6}$$

$$\tan\theta = {}^{WS}\!/_{v} \tag{7}$$

$$F_0 = m \times v = ({}^{1}\!/_{6} \times \rho \times \pi \times D^3) \times v \tag{8}$$

$$F = F_0 \times \cos\theta \tag{9}$$

where D is raindrop diameter (mm); I is the average rainfall intensity of incident rains (mm·h^{-1}); v is raindrop velocity (m·s^{-1}); θ is average inclination angle of raindrops (°); WS is the average wind speed of incident rains (m·s^{-1}); F_0 is the average raindrop momentum (mg·m·s^{-1}); m is the average raindrop mass (g); ρ is the density of freshwater at standard atmospheric pressure and 20°C (0.998 g·cm^{-3}).

2.3 Experimental branch selection and measurements

This study focused on the branch-scaled stemflow production of the 20-year-old *C. korshinskii* and *S. psammophila*. Based on plot investigation, the canopy traits of standard shrubs were determined. Four shrubs were selected accordingly at each species with similar crown areas and heights (5.1±0.3 m^2 and 2.1±0.2 m for *C. korshinskii* and 21.4±5.2 m^2 and 3.5±0.2 m for *S. psammophila*, respectively). The approximately 10-m gap between them guaranteed shrubs exposing to the similar meteorological conditions (Yuan et al., 2016). We measured branch morphologies of all 180 and 261 branches at experimental shrubs of *C. korshinskii* and *S. psammophila*, respectively, including BD (Basal diameter, mm) with a Vernier calliper (Model 7D-01150, Forgestar Inc., Germany), branch length (BL, cm) with a measuring tape, and branch angle (BA, °) with pocket geologic compass (Model DQL-8, Harbin Optical Instrument Factory, China), respectively. Thus, BD categories were determined at 5–10 mm, 10–15 mm, 15–18 mm, 18–25 mm and >25 mm to guarantee the appropriate branch amounts within categories for meeting the statistical significance. Two representative branches with median BDs were selected in each category for stemflow recording. The experimental branches had no intercrossing with neighbouring ones and no turning point in height from branch tip to base. The outlayer-of-canopy positions avoided over-shading by the upper layer branches and permitted convenient measurements. Since the qualified branch with the >25-mm size was not enough for *C. korshinskii* and the TBRG malfunctioned at the 15–18-mm branches of *S. psammophila*, stemflow data were not available in these BD categories. In total, 7 branches were selected for stemflow measurements at each species (Table 1). As the important interface to intercept rains at the growing season, the well-verified allometric growth equations were performed to estimate the branch leaf area (LA, cm^2) of *C korshinskii* ($LA=39.37\times BD^{1.63}$ R^2=0.98) (Yuan et al., 2017) and *S. psammophila* ($LA=18.86\times BD^{1.74}$ R^2=0.90) (Yuan et al., 2016), respectively.

2.4 Stemflow measurements and calculations

A total of 14 TBRGs had been applied to automatically record the branch stemflow production of *C. korshinskii* and *S. psammophila*. The data of stemflow volume and timing were automatically recorded at dynamic intervals between neighboring tips. We installed aluminium foil collars to trap stemflow at branches nearly 40 cm off the ground, higher than TBRG orifice with height of 25.7 cm (Fig. 1). They were fitted around the entire branch circumference and sealed by neutral silicone caulking. The limited orifice diameter of foil collars minimized the accessing of throughfall and rains into them (Yuan et al., 2017). The 0.5-cm-diameter polyvinyl chloride hoses hung vertically and channelled stemflow from the collars to TBRGs with a minimum travel time. TBRGs were covered with the polyethylene films to prevent the accessing of throughfall and splash (Fig. 1). These apparatuses were periodically checked against leakages or blockages by insects and fallen leaves. Stemflow variables were computed as follow.

(1) Stemflow volume (SFV, mL): the average stemflow volume of individual branches. Adjusted with Equation 4 firstly, SFV was computed with the TBRG recordings (SF_{RG}, mm) by multiplying its orifice area (186.3 cm^2) (Equation 10).

$$SFV = SF_{RG} \times 18.63 \tag{10}$$

(2) Stemflow intensity: the branch stemflow volume per branch basal area per unit time. SFI ($mm \cdot h^{-1}$) is the average stemflow intensity of incident rains, which is computed by the event-based SFV (mL), branch basal area (BBA, mm^2) and RD (h) (Equation 11) (Herwitz, 1986; Spencer and Meerveld, 2016). SFI_{10} ($mm \cdot h^{-1}$) is the 10-min maximum stemflow intensity, which is calculated with the 10-min maximum stemflow volume (SFV_{10}, mL) and BBA (mm^2) (Equation 12). SFI_i ($mm \cdot h^{-1}$) is the instantaneous stemflow intensity, which is calculated by the tip volume of TBRG (3.73 mL), BBA (mm^2) and time intervals between neighbouring tips (t_i, h) (Equation 13). The comparison between SFI_i and the corresponding

rainfall intensity depicted the synchronicity of stemflow with rains within event.

$$\mathrm{SFI} = 1000 \times \mathrm{SFV} / (\mathrm{BBA} \times \mathrm{RD}) \tag{11}$$

$$\mathrm{SFI}_{10} = 6000 \times \mathrm{SFV}_{10} / \mathrm{BBA} \tag{12}$$

$$\mathrm{SFI}_{\mathrm{i}} = 3730 / \left(\mathrm{BBA} \times \mathrm{t}_{\mathrm{i}}\right) \tag{13}$$

(3) Stemflow temporal dynamics: stemflow duration and time lags to rains.

SFD (h): stemflow duration. It is computed by different timings between the first- and last-tips of stemflow via TBRG.

TLG (min): time lag of stemflow generation after rain begins. It is computed by different first-tip timings between rainfall and stemflow via TBRG.

TLM (min): time lag of stemflow maximization after rain begins. It is computed by different timings between the largest-$\mathrm{SFI_i}$ and first-rainfall tips via TBRG.

TLE (min): time lag of stemflow ending after rain ceases. It is computed by different last-tip timings between rainfall and stemflow via TBRG.

(4) Funnelling ratio: the efficiency for capturing and delivering raindrops from the canopies to trunk/branch base (Siegert and Levia, 2014; Cayuela et al., 2018). By introducing RD at both numerator and denominator of the original equation (Herwitz, 1986), FR (unitless) was transformed as the ratio between stemflow and rainfall intensities at the event base (Equation 14). FR_{100} described the within-event funnelling ratio at the 100-s interval after rain began (Equation 15).

$$\mathrm{FR} = 1000 \times \frac{\mathrm{SFV}}{\mathrm{BBA} \times \mathrm{RA}} = 1000 \times \frac{\frac{\mathrm{SFV}}{\mathrm{BBA}} / \mathrm{RD}}{\mathrm{RA} / \mathrm{RD}} = \frac{\mathrm{SFI}}{\mathrm{I}} \tag{14}$$

$$\mathrm{FR}_{100_{\mathrm{i}}} = \mathrm{SFI}_{100_{\mathrm{i}}} / \mathrm{I}_{100_{\mathrm{i}}} \tag{15}$$

where SFV is branch stemflow volume (mL); RA is rainfall amount (mm); BBA is branch basal diameter (mm^2); RD is rainfall duration (h); SFI and I were stemflow and rainfall intensities ($mm \cdot h^{-1}$), respectively; FR_{100i} is funnelling ratio at the number *i* interval of 100 s after rain begins.

2.5 Data analysis

Stemflow variables were averaged at different BD categories to analyse the most influential rainfall characteristics affecting them. Pearson correlation analyses were firstly performed to test the relationships between rainfall characteristics (RA, RD, RI, I, I_{10}, I_{b10}, I_{e10}, F, F_{10}, F_{b10}, F_{e10} and E) and stemflow variables (SFV, SFI, SFI_{10}, FR, TLG, TLM, TLE and SFD). The significantly related factors were grouped in terms of median value, and compiled into indicator matrices. They were standardized for a cross-tabulation check as required by the multiple correspondence analysis (MCA) (Levia et al., 2010; van Stan et al., 2011, 2016). All qualified data were restructured into orthogonal dimensions (Hair et al., 1995), where distances between row and column points were maximized (Hill and Lewicki, 2007). As shown at correspondence maps, the clustering rainfall characteristics tightly related to the centred stemflow variable. Finally, stepwise regressions were operated to identify the most influential rainfall characteristics (Carlyle-Moses and Schooling, 2015). The quantitative relations were established in terms of the qualified level of significance ($p < 0.05$) and the highest coefficient of determination (R^2). One-way analysis of variance (ANOVA) with LSD post hoc test was used to determine whether rainfall characteristics, and stemflow variables significantly differed among event categories, and whether funnelling ratio and stemflow intensity significantly differed among BD categories for *C.*

korshinskii and *S. psammophila*. The level of significance was set at 95% confidence interval (p=0.05). SPSS 21.0 (IBM Corporation, USA), Origin 8.5 (OriginLab Corporation, USA) and Excel 2019 (Microsoft Corporation, USA) were used for data analysis.

3 Results

3.1 Rainfall characteristics

A total of 20, 8, 10, 8, 4 and 4 rainfall events were recorded in the RA categories of ≤2 mm, 2–5 mm, 5–10 mm, 10–15 mm, 15–20 mm and >20 mm, respectively. The total RAs at these categories were 22.1 mm, 26.1 mm, 68.8 mm, 93.3 mm, 74.8 mm and 110.0 mm, respectively. During these events, the average I, I_{10}, I_{b10} and I_{e10} were 4.5±1.0 mm·h^{-1}, 10.9±2.1 mm·h^{-1}, 5.5±1.4 mm·h^{-1} and 2.8±0.7 mm·h^{-1}, respectively. The average F, F_{10}, F_{b10} and F_{e10} were 16.1±1.2 mg·m·s^{-1}, 24.9±1.4 mg·m·s^{-1}, 18.4±1.4 mg·m·s^{-1} and 16.0±1.0 mg·m·s^{-1}, respectively. RD, RI and E averaged 4.7±0.8 h, 50.6±6.1 h, and 0.9±0.2, respectively (Table 2).

Rainfall events were further categorized in terms of rainfall-intensity peak amount, including Events A (the single-peak events), B (the double-peak events) and C (the multiple-peak events). There were 17, 11 and 15 events at Event A, B and C, respectively. Because the remaining 11 events had the average RA of 0.6 mm, no more than three recordings had been observed within event which was limited by 0.2-mm resolution of TBRGs. Therefore, they could not be categorized and grouped as Event others (Table 2). Compared with Events A and B, Event C possessed significantly different rainfall characteristics, e.g., the significantly larger RA (11.7 vs. 4.1 and 5.2 mm) and RD (10.3 vs. 2.5 and 3.6 h) but the significantly smaller I_{10} (9.5 vs. 15.5 and 12.7 mm·h^{-1}), I_{b10} (2.8 vs.

7.7 and 9.9 mm·h^{-1}), F_{b10} (15.4 vs. 19.7 and 21.7 mg·m·s^{-1}) and F_{e10} (13.4 vs. 17.3 and 16.6 mg·m·s^{-1}), the non-significantly smaller I_{e10} (2.1 vs. 4.3 and 3.6 mm·h^{-1}), F_{10} (24.2 vs. 27.8 and 26.6 mg·m·s^{-1}) and E (0.4 vs. 0.9 and 1.0), respectively (Table 2).

In general, rainfall events were skewedly distributed in terms of RA. The occurrences of events with a RA≤2 mm dominated the experimental period (40.7%), but the events with RA>20 mm were the greatest contributor to the total RA (28.0%). However, a relatively equal distribution was noted during events with single (17 events), double (11 events) and multiple (15 events) rainfall-intensity peaks. Comparatively, the multiple-peak events had significantly larger rainfall amounts, durations, intensities and raindrop momentums.

3.2 Stemflow volume, intensity, funnelling ratio and temporal dynamics

Stemflow variables of *C. korshinskii* and *S. psammophila* showed great inter-event variations during the experimental period (Fig. 3). *C. korshinskii* had larger SFV, SFI, SFI_{10}, FR, SFD, TLG and TLE (226.6±46.4 mL, 517.5±82.1 mm·h^{-1}, 2057.6±399.7 mm·h^{-1}, 130.7±8.2, 3.8±0.8 h, 66.2±10.6 min and 20.0±5.3 min, respectively) but smaller TLM (109.4±20.5 min) than those of *S. psammophila* (172.1±34.5 mL, 367.3±91.1 mm·h^{-1}, 1132.2±214.3 mm·h^{-1}, 101.6±10.4, 3.4±0.9 h, 54.8±11.7 min, 13.5±17.2 min, and 120.5±22.1 min, respectively) (Table 3). During the 54 events, no negative values were observed for TLG and TLM but TLE. It indicated that stemflow generally initiated and maximized after rains started for both species. However, stemflow might be ended before (negative TLE) and after (positive TLE) rains ceased.

Stemflow well synchronized to rains with similar intensity peak shapes, amounts and positions for both species. These results were vividly demonstrated at representative rains with different intensity peak amounts and RAs, including events on July 17, 2015 (Event A, 20.7 mm), July 29, 2015 (Event B, 7.3 mm), and September 10, 2015 (Event C, 13.3 mm) (Fig. 4). *C. korshinskii* had larger FR_{100} (91.7, 76.1 and 94.0, respectively) than those of *S. psammophila* (32.8, 26.3 and 43.7, respectively) during representative events. It indicated a comparatively greater ability of converging rains for *C. korshinskii* within event.

Stemflow variables varied between rainfall event categories. For Event C in comparison to Events A and B, *S. psammophila* had significantly larger SFV (435.2 vs. 102.6 and 145.7 mL), SFD (8.3 vs. 1.2 and 3.4 h), TLM (235.8 vs. 64.3 and 93.4 min), FR (129.1 vs. 77.1 and 91.4), non-significantly larger TLE (20.8 vs. 17.1 and 8.6 min) but significantly smaller SFI (246.6 vs. 648.1 and 421.5 $mm{\cdot}h^{-1}$) and SFI_{10} (888.4 vs. 1672.7 and 1582.8 $mm{\cdot}h^{-1}$), respectively (Table 3). SFI decreased at events with increasing intensity peak amounts as shown at Events A–C. The drop of SFI was offset by the decreasing I to some extent (Table 2), which might partly explain the increasing trend of FR from Event A to C. *C. korshinskii* shared similar changing trends of stemflow variables between event categories with those of *S. psammophila*, except for the non-significantly smaller TLE (18.5 min) at Event C in contrast to TLE at Event A and B (22.3 and18.7 min).

Funnelling ratio and stemflow intensity negatively related with branch size. *C. korshinskii* and *S. psammophila* had significantly greater FR, SFI, and SFI_{10} at the 5–10 mm branches than those at the larger branches (Table 4). For *C. korshinskii*, FR decreased from 163.7±12.2 at the 5–10-mm branches to 97.7±9.2 at the 18–25-mm branches, respectively. It was consistent with decreasing SFI (333.8–716.2 $mm{\cdot}h^{-1}$) at the corresponding BD categories (Table 4). As branch size increased, *S. psammophila* shared similar decreasing trends of FR (44.2–212.0) and SFI (197.2–738.7 mm·h^{-1}), respectively.

3.3 Relationships between stemflow variables and rainfall characteristics

C. korshinskii and *S. psammophila* had similar correspondence patterns between rainfall characteristics and stemflow variables. As shown in Fig. 5, the one-to-one correspondences were observed for SFV and TLE. The larger (or smaller) SFV and TLE corresponded to the larger (or smaller) RA and RI, respectively. This result demonstrated the dominant influences of RA and RI on SFV and TLE, respectively. The one-to-two correspondences was noted for SFD with RD and E. The larger (or smaller) SFD corresponded to the larger (or smaller) RD and smaller (or larger) E. RA had been identified as the dominant rainfall characteristic affecting FR based on the analysis for 53 branches of *C. korshinskii* and 98 branches of *S. psammophila* at the same plots during the same experimental period (Yuan et al., 2017). It seemed that event-based stemflow production (the volume, duration and efficiency) were strongly influenced by rainfall characteristics at inter-event scale (the rainfall amount and duration).

The one-to-more correspondences were observed for TLM, TLG, SFI and SFI_{10}. The larger (or smaller) TLM corresponded to the smaller (or larger) rainfall characteristics of I, I_{10}, I_{b10}, I_{e10}, F, F_{10}, F_{b10} and F_{e10}. The same correspondences were applied to the larger (or smaller) TLG, and the smaller (or larger) SFI and SFI_{10}. It seemed that the within-event stemflow processes (SFI, SFI_{10}, TLG and TLM) were strongly affected by rainfall characteristics at intra-event scale (the rainfall intensity and raindrop momentum). Therefore, these results indicated that rainfall characteristics influenced stemflow variables at the corresponding temporal scales. This influence occurred at the inter-event scale between SFV and RA, FR and RA, SFD and RD, and at the intra-event scale for stemflow time lags (TLG and TLM) and intensities (SFI and SFI_{10}) with rainfall intensity (I, I_{10}, I_{b10} and I_{e10}) and raindrop momentum (F, F_{10}, F_{b10} and F_{e10}). The only exception was noted between TLE and RI for the mismatched temporal sales.

Stepwise regression analysis identified the most influential rainfall characteristics affecting stemflow intensities and temporal dynamics. RD was the dominant rainfall characteristics affecting SFD. I_{10} significantly affected the TLM of the both species. For *C. korshinskii*, I, I_{10} and F were the most influential factors on SFI, SFI_{10} and TLG, respectively. However, for *S. psammophila*, F, F_{10} and F_{b10} significantly affected SFI, SFI_{10} and TLG, respectively. The results of multiple regression analysises indicated that there were linear relationships between SFI and I (R^2=0.74, p<0.01) and SFI_{10} and I_{10} (R^2=0.85, p<0.01) for *C. korshinskii* and between SFD and RD for *C. korshinskii* (R^2=0.95, p<0.01) and *S. psammophila* (R^2=0.92, p<0.01) (Fig. 6). Moreover, power functional relations were found between SFI and F (R^2=0.82, p<0.01), SFI_{10} and F_{10} (R^2=0.90, p<0.01) (Fig. 6), TLG and F_{b10} (R^2=0.55, p<0.01) and TLM and I_{10} (R^2=0.40, p<0.01) (Fig. 7) for *S. psammophila*, and TLG and F (R^2=0.56, p <0.01) and TLM and I_{10} (R^2=0.38, p<0.01) (Fig. 7) for *C. korshinskii*. However, there was no significant quantitative relationship between TLE and RI for *C. korshinskii* (R^2=0.005, p=0.28) or *S. psammophila* (R^2=0.002, p=0.78) (Fig. 7).

4 Discussion

4.1 Stemflow intensity and funnelling ratio

Stemflow intensity is generally greater than rainfall intensity at different plant life forms. The xerophytic shrubs of *C. korshinskii* and *S. psammophila* had larger average stemflow intensities than the average rainfall intensity (517.5 and 367.3 mm·h^{-1} vs. 4.5 mm·h^{-1}). Broadleaf and coniferous species (*Quercus pubescens* Willd. and *Pinus sylvestris* L., respectively) also have larger maximum stemflow intensities than the maximum rainfall intensity in north-eastern Spain (Cayuela et al., 2018). The gap between stemflow and rainfall intensities generally increased as the recording time intervals decreased. While recording at the 1-h intervals, approximately 20-, 17-, 13- and 2.5-fold greater peak stemflow intensities had been observed for trees of Cedar, Birch, Douglas Fir and Hemlock, respectively, at the coastal British Columbia forest (Spencer and Meerveld, 2016). For *C. korshinskii* and *S. psammophila*, in comparison to I_{10} (10.9 mm·h^{-1}) at 10-min intervals, the SFI_{10} (2057.6 and 1132.2 mm·h^{-1}, respectively) was over 103.9-fold greater. The recordings at 6-min interval indicated a 157-fold larger of stemflow intensity (18840 mm·h^{-1}) than rainfall intensity (120 mm·h^{-1}) in the cyclone-prone tropical rainforest with extremely high MAP of 6570 mm (Herwitz, 1986). While calculating the dynamic time interval between neighbouring tips of TBRG, SFI_i (10816.2 mm·h^{-1}) was 150.2-fold greater than the corresponding rainfall intensity (72 mm·h^{-1}). Therefore, stemflow recorded at a higher temporal resolution might provide more information into the dynamic nature of stemflow and real-time responses to rainfall characteristics within events.

Greater stemflow intensity than rainfall intensity is hydrologically significant at terrestrial ecosystems. This scenario indicates the convergence of the canopy-intercepted rains into the limited area around trunk or branch bases within a certain time period, i.e., 8.0% and 3.5% of rains being directed to the trunk base only accounting for 0.3% and 0.4% of plot area in the open rainforest (Germer et al., 2010) and undisturbed lowland tropical rainforest (Manfroi et al., 2004), respectively. Besides, FR, which compared SFV with RA that would have been collected at the same area as the basal area at an event scale (Herwitz, 1986), is commonly applied to assess the convergence effect via stemflow volume, rainfall amount and basal area (Carlyle-Moses et al., 2010; Siegert and Levia, 2014; Fan et al., 2015; Yang et al., 2019). If FR is greater than 1, more water is collected at the trunk or branch base than at the clearings. Both methods successfully quantified the convergence effects of stemflow. However, the former provided a possibility to assess it at high temporal resolutions within event.

This study established the quantitative connection between FR and stemflow intensity for the first time. As per Equation 14 and the average stemflow and rainfall intensities listed at Table 2 and 3, FR could be estimated to be 115.0 and 81.6 for *C. korshinskii* and *S. psammophila*, respectively. Those results approximately agreed with FR of 173.3 and 69.3 (Yuan et al., 2017) and 124.9 and 78.2 (Yang et al., 2019) for the two species by applying the traditional calculation based on SFV and RA (Herwitz, 1986). As branch size increased, FR of *C. korshinskii* decreased from 163.7 at the 5–10-mm branches to 97.7 at the 18–25-branches. The decreasing trend of FR of *S. psammophila* were also noted in the range of 44.2–212.0 with increasing BD. The negative relation between BD and FR agreed with the reports for trees and babassu palms in an open tropical rainforest in Brazil (Germer et al., 2010), the mixed-species coastal forest at British Columbia of Canada (Spencer and Meerveld, 2016), for trees (*Pinus tabuliformis* and *Armeniaca vulgaris*) and shrubs (*C. korshinskii* and *S. psammophila*) on the Loess Plateau of China (Yang et al., 2019). It might be partly explained by the decreasing stemflow intensities with increasing branch size as per Equation 14. Our results found that SFI decreased from 716.2 to 333.8 for *C. korshinskii*, and 738.7 to 197.2 for *S. psammophila* as branch size increased (Table 4). It well justified the importance of branch size on stemflow intensity. Associated with the infiltration rate, the stemflow-induced hydrological process might be strongly affected, i.e., soil moisture recharge, Hortonian overland flow (Herwitz, 1986), Saturation overland flow (Germer et al., 2010), soil erosion (Liang et al., 2011), nutrient leaching (Corti et al., 2019), etc. Therefore, more attention should be paid to tree/branch size and size-related stand age at future studies while modeling the stemflow-induced terrestrial hydrological fluxes.

The importance had been addressed to study the funnelling ratio at the stand scale (Carlyle-Moses et al., 2018); however, it had not been adequately studied at the intra-event scale. This study calculated the average funnelling ratio at the event base and the 100-s intervals after rain began. Thus, the convergence effect of stemflow could be better understood at the inter-/intra-event scales. Our results found that FR_{100} were over 1.8-fold greater than FR of *C. korshinskii* (282.7 vs. 130.7) and *S. psammophila* (203.4 vs. 101.6), respectively. It indicated that funnelling ratio fluctuated dramatically within event. Therefore, computing FR at event and ignoring it at high temporal resolutions within event might underestimate the eco-hydrological significance of stemflow.

In general, stemflow intensity highly related to funnelling ratio. For addressing its eco-hydrological importance, stemflow intensity should be precisely defined. It had been expressed as the stemflow volume per basal area of branches/trunks per unit time with the unit of $mm \cdot h^{-1}$ (Herwitz, 1986; Spencer and Meerveld, 2016) and $mm \cdot 5\ min^{-1}$ (Cayuela et al., 2018). However, stemflow intensity had also been described as stemflow volume per unit time with the unit of L·week^{-1} (Schimmack et al., 1993) and L·h^{-1} (Liang et al., 2011; Germer et al., 2013). We highly recommended the former definition. Because of its highly spatial-related (Herwitz, 1986; Liang et al., 2011; 2014), the eco-hydrological significance of stemflow would be underestimated by ignoring the basal area, over which stemflow was received. Moreover, as per this definition, stemflow intensity quantitively connected with funnelling ratio via Equation 14. Thus, funnelling ratio could be used to assess the convergence effect of stemflow at both inter- and intra-event scales.

4.2 Stemflow temporal dynamics

Stemflow well synchronized to the rains. It agreed with the report of Levia et al. (2010), who demonstrated a marked synchronicity between SFV and RA in 5-min intervals for *Fagus. grandifolia*. The duration and time lags to rains were critical to describe stemflow temporal dynamics. Our results indicated that in comparison to *S. psammophila*, *C. korshinskii* takes a longer time to initiate (66.2 vs. 54.8 min), end (20.0 vs. 13.5 min) and produce stemflow (3.8 vs. 3.4 h) but a shorter time to maximize stemflow (109.4 vs. 120.5 min, respectively). Moreover, the TLMs of both species were in the range of the TLMs for *S. psammophila* (20–210 min) in the Mu Us desert of China (Yang, 2010).

Varying TLGs were documented for different species. Approximately 15 min, 1 h and 1.5 h were needed to initiate the stemflow of palms (Germer, 2010), pine trees and oak trees (Cayuela et al., 2018), respectively. In addition, an almost instantaneous start of stemflow had also been observed as rain began for *Quercus rubra* (Durocher, 1990), *Fagus grandifolia* and *Liriodendron tulipifera* (Levia et al., 2010). Compared to the positive TLE dominating xerophytic shrubs, the TLE greatly varied with tree species. TLE was as much as 48 h for Douglas fir, oak and redwood in California, USA (Reid and Levia, 2009), and almost 11 h for palm trees in Brazil (Germer, 2010). However, for sweet chestnut and oak, almost no stemflow continued when rains ceased in Bristol, England (Durocher, 1990). These scenarios might occur due to the sponge effect of the canopy surface (Germer, 2010), which buffered stemflow generation, maximization and cessation before saturation. These conclusions were consistent with the smaller stemflow intensities of *C. korshinskii* and *S. psammophila* than the rainfall intensity when rain began, as part of the rains was used to wet canopies (Fig. 4). The hydrophobic bark traits benefited stemflow initiation with the limited time lags to rains. In contrast, the hydrophilic bark traits were conducive for continuing stemflow after rain ceased, which kept the preferential flow paths wetter for longer time periods (Levia and Germer, 2015). As a result, it took time to transfer intercepted rains from the leaf, branch and trunk to the base. This process strongly affects the stemflow volume, intensity and loss as evaporation.

The dynamics of intra-event rainfall intensity complicated the stemflow time lags to rains. A 1-h lag to begin and stop stemflow with the beginning and ending of rains had been observed for ashe juniper trees during high-intensity events, but no stemflow was generated at low-intensity storms (Owens et al., 2006). Rainfall intensity was an important dynamic rainfall characteristic affecting stemflow volume. Owens et al. (2006) found the most significant difference between various rainfall intensities located in the stemflow patterns other than throughfall and interception loss. During events with a front-positioned, single rainfall-intensity peak, *S. psammophila* maximized stemflow in a shorter time than *C. korshinskii* did in the Mu Us desert (30 and 50 min) (Yang, 2010). These results highlighted the amounts and occurrence time of rainfall-intensity peak affecting the stemflow process, which was consistent with the finding of Dunkerley (2014b).

Raindrops presented rainfall characteristics at finer temporal-spatial scales. They were usually ignored because rains were generally regarded as a continuum rather than a discrete process consisting of individual raindrops of various sizes, velocities, inclination angles and kinetic energies. Raindrops hit the canopy surface and created splashes at different canopy layers (Bassette and Bussière, 2008; Li et al., 2016). This process accelerated canopy wetting and increased water supply for stemflow production. Therefore, raindrop momentum was introduced in this study to represent the comprehensive effects of raindrop attributes. Our results indicated that raindrop momentum was sensitive to predicting the variations in stemflow intensity and temporal dynamics with significant linear or power functional relations (Figs. 6 and 7). Compared with the importance of rainfall intensity for *C. korshinskii*, raindrop momentum more significantly affected the stemflow process of *S. psammophila.* This result might be related to the larger canopy size and height of *S. psammophila* (21.4±5.2 m^2 and 3.5±0.2 m) than that of *C. korshinskii* (5.1±0.3 m^2 and 2.1±0.2 m, respectively). More layers were available within canopies of *S. psammophila* to intercept the splashes created by raindrop striking (Bassette and Bussière, 2008; Li et al., 2016), thus shortening the paths and having more water supply for stemflow production.

4.3 Temporal-dependent influence of rainfall characteristics

This study discussed stemflow variables and rainfall characteristics at inter-/intra-event scales. We found that rainfall characteristics affected stemflow variables at the corresponding temporal scales. RA and RD controlled SFV, FR and SFD, respectively, at the inter-event scale. However, stemflow intensity (e.g., SFI and SFI_{10}) and temporal dynamics (e.g., TLG and TLM) were strongly influenced by rainfall intensity (e.g., I, I_{10} and I_{b10}) and raindrop momentum (e.g., F, F_{10} and F_{b10}) at the intra-event scales. These results were verified by the well-fitting linear or power functional equations among them (Figs. 6 and 7). Furthermore, the influences of rainfall intensity and raindrop momentum on stemflow process were species-specific. In contrast to the significance of rainfall intensity on the stemflow process of *C. korshinskii*, raindrop momentum imposed a greater influence on the stemflow process of *S. psammophila*.

In general, rainfall characteristics had temporal-dependent influences on the corresponding stemflow variables. The only exception was found between TLE and RI. RI tightly corresponded to TLE for both species tested by the MCA, but there was no significant quantitative relationship between them (R^2=0.005, p=0.28 for *C. korshinskii*, and R^2=0.002, p=0.78 for *S. psammophila*). This result might be related to the mismatched temporal scales between TLE and RI. TLE represented stemflow temporal dynamics at the intra-event scale, while RI was the interval times between neighbouring rains at the inter-event scale. The mismatched temporal scales might also partly explain the long-standing debates on the controversial positive, negative and even no significant influences of rainfall intensity (depicting raining process at 5 min, 10 min, 60 min, etc.) on event-based stemflow volume (Owens et al., 2006; André et al., 2008; Zhang et al., 2015).

5 Conclusions

Stemflow intensity and temporal dynamics are important in depicting the stemflow process and its interactions with rainfall characteristics within events. We categorized stemflow variables into the volume, intensity, funnelling ratio and temporal dynamics, thus to representing the stemflow yield, efficiency and process. Funnelling ratio had been calculated as the ratio between stemflow and rainfall intensities for the first time. It enabled it to assess the convergence of stemflow at the inter-/intra-event scales. Over 1.8-fold greater FR_{100} were noted than FR at representative events for *C. korshinskii* and *S. psammophila*, respectively. The eco-hydrological significance of stemflow might be underestimated by ignoring stemflow production at high temporal resolutions within event. FR decreased with increasing branch size of both species. It could be partly explained by the decreasing trends of SFI as branch size increased. The influences of rainfall characteristics were quantified at a fine temporal scale by introducing SFI_i, FR_{100}, raindrop momentum, rainfall-intensity peak amounts and intra-event positions. The results indicated that rainfall characteristics had temporal-dependent influences on stemflow variables. RA and RD controlled SFV, FR and SFD at the inter-event scale. Rainfall intensity and raindrop momentum significantly affected stemflow intensity and time lags to rains at the intra-event scale except for TLE. Although there was tight correspondence between TLE and RI by MCA, there was no significant quantitative relationship (R^2<0.005, p>0.28) due to the mismatched temporal scale between them. These findings advance our understanding of the stemflow process and its influential mechanism and help model the critical process-based hydrological fluxes of terrestrial ecosystems.

Data availability. The data collected in this study are available upon request to the authors.

Author contributions. GYG and CY set up the research goals and designed field experiments. CY measured and analyzed the data. GYG and BJF provided the financial support for the experiments, and supervised the execution. CY created the figures and wrote the original draft. GYG, BJF, DMH, XWD and XHW reviewed and edited the draft in serval rounds of revision.

Competing interests. The authors declare that they have no conflict of interest.

Acknowledgements. This research was sponsored by the National Natural Science Foundation of China (nos. 41390462, 41822103 and 41901038), the National Key Research and Development Program of China (no. 2016YFC0501602), the Chinese Academy of Sciences (no. QYZDY-SSW-DQC025), the Youth Innovation Promotion Association CAS (no. 2016040), and the China Postdoctoral Science Foundation (no. 2018M633427). We appreciate Prof. D. F. Levia in University of Delaware for reviewing and improving this manuscript. Thanks to Liwei Zhang for the catchment GIS mapping. Special thanks are given to Shenmu Erosion and Environment Research Station for experimental support to this research.

Appendix

List of symbols

Abbreviation	Descriptions	Unit
a.s.l.	above sea level	NA
BA	Branch angle	°
BBA	Branch basal area	mm^2
BD	Branch diameter	mm

BL	Branch length	cm
D	Diameter of rain drop	mm
e_s	Saturation vapor pressure	kPa
E	Evaporation coefficient	unitless
F	Average raindrop momentum in the vertical direction of incident event	$mg \cdot m \cdot s^{-1}$
F_0	Average raindrop momentum of incident event	$mg \cdot m \cdot s^{-1}$
F_{10}	The 10-min maximum raindrop momentum	$mg \cdot m \cdot s^{-1}$
F_{b10}	Average raindrop momentum at the first 10 min	$mg \cdot m \cdot s^{-1}$
F_{e10}	Average raindrop momentum at the last 10 min	$mg \cdot m \cdot s^{-1}$
FR	Average funnelling ratio of incident event	unitless
FR_{100}	Funnelling ratio at the 100-s intervals after rain begins	unitless
H	Air relative humidity	%
I	Average rainfall intensity of incident event	$mm \cdot h^{-1}$
I_{10}	The 10-min maximum rainfall intensity	$mm \cdot h^{-1}$
I_{b10}	Average rainfall intensity at the first 10-min of incident event	$mm \cdot h^{-1}$
I_{e10}	Average rainfall intensity at the last 10-min of incident event	$mm \cdot h^{-1}$
IW_A	The adjusted inflow water at TBRG	mm
IW_R	The recorded inflow water at TBRG	mm
LA	Leaf area of individual branch	cm^2
MAP	Mean annual precipitation	mm
MCA	Multiple correspondence analysis	NA
NA	Not applicable	NA
p	Level of significance	NA
R^2	Coefficient of determination	NA
RA	Rainfall amount	mm
RD	Rainfall duration	h
RI	Rainfall interval	h
SE	Standard error	NA
SFD	Stemflow duration from its beginning to ending	h
SFI	Average stemflow intensity of incident event	$mm \cdot h^{-1}$
SFI_{10}	The 10-min maximum stemflow intensity of incident event	$mm \cdot h^{-1}$
SFI_i	Instantaneous stemflow intensity	$mm \cdot h^{-1}$
SF_{RG}	Stemflow depth recorded by TBRG	mm
SFV	Stemflow volume	mL
t_i	Time intervals between neighboring tips	h
T	Air temperature	°C
TBRG	Tipping bucket rain gauge	NA
TLE	Time lag of stemflow ending to rainfall ceasing	min
TLG	Time lag of stemflow generation to rainfall beginning	min
TLM	Time lag of stemflow maximization to rainfall beginning	min
v	Terminal velocity of rain drop	$m \cdot s^{-1}$
VPD	Vapor pressure deficit	kPa
WS	Wind speed	$m \cdot s^{-1}$
ρ	Density of freshwater at standard atmospheric pressure and 20°C	$g \cdot cm^{-3}$

θ	Inclination angle of rain drop	°

References

André, F., Jonard, M. and Ponette, Q.: Influence of species and rain event characteristics on stemflow volume in a temperate mixed oak-beech stand, Hydrol. Process., 22, 4455–4466. https://doi.org/10.1002/hyp.7048, 2008.

Bassette, C. and Bussière, F.: Partitioning of splash and storage during raindrop impacts on banana leaves, Agr., Forest Meteorol., 148, 991–1004, https://doi.org/10.1016/j.agrformet.2008.01.016, 2008.

Bittar, T.B., Pound, P., Whitetree, A., Moore, L.D. and van Stan John, T.: Estimation of throughfall and stemflow bacterial flux in a subtropical oak-cedar forest. Geophys. Res. Lett., 45, 1410–1418, https://doi.org/10.1002/2017GL075827, 2018.

Brandt, C.J.: Simulation of the size distribution and erosivity of raindrops and throughfall drops. Earth. Surf. Proc. Land., 15, 687–698, https://doi.org/10.1002/esp.3290150803, 1990.

Bundt, M., Widmer, F., Pesaro, M., Zeyer, J. and Blaser, P.: Preferential flow paths: biological 'hot spots' in soils. Soil. Biol. Biochem., 33, 729–738, https://doi.org/10.1016/S0038-0717(00)00218-2, 2001.

Carlyle-Moses, D.E., Iida, S.I., Germer, S., Llorens, P., Michalzik, B., Nanko, K., Tischer, A. and Levia, D.F.: Expressing stemflow commensurate with its ecohydrological importance, Adv. Water Resources, 121, 472–479, https://doi.org/10.1016/j.advwatres.2018.08.015, 2018.

Carlyle-Moses, D.E. and Price, A.G.: Growing-season stemflow production within a deciduous forest of southern Ontario, Hydrol. Process., 20, 3651–3663, https://doi.org/10.1002/hyp.6380, 2006.

Carlyle-Moses, D.E. and Schooling, J.: Tree traits and meteorological factors influencing the initiation and rate of stemflow from isolated deciduous trees, Hydrol. Process., 29, 4083–4099, https://doi.org/10.1002/hyp.10519, 2015.

Carlyle-Moses, D.E., Park, A.D. and Cameron, J.L.: Modelling rainfall interception loss in forest restoration trials in Panama, Ecohydrology, 3, 272–283, https://doi.org/10.1002/eco.105, 2010.

Cayuela, C., Llorens, P., Sánchez-Costa, E., Levia, D.F. and Latron, J.: Effect of biotic and abiotic factors on inter- and intra-event variability in stemflow rates in oak and pine stands in a Mediterranean mountain area, J. Hydrol., 560, 396–406, https://doi.org/10.1016/j.jhydrol.2018.03.050, 2018.

Corti, G., Agnelli, A., Cocco, S., Cardelli, V., Masse, J. and Courchesne, F.: Soil affects throughfall and stemflow under Turkey oak (*Quercus cerris* L.), Geoderma, 333, 43–56, https://doi.org/10.1016/j.geoderma.2018.07.010, 2019.

Dawoe, E.K., Barnes, V.R. and Oppong, S.K.: Spatio-temporal dynamics of gross rainfall partitioning and nutrient fluxes in shaded-cocoa (*Theobroma cocoa*) systems in a tropical semi-deciduous forest, Agroforst. Syst., 92, 397–413, https://doi.org/10.1007/s10457-017-0108-3, 2018.

Dunkerley, D.L.: Stemflow production and intrastorm rainfall intensity variation: an experimental analysis using laboratory rainfall simulation, Earth. Surf. Proc. Land., 39, 1741–1752, https://doi.org/10.1002/esp.3555, 2014.

Dunkerley, D.L.: Stemflow on the woody parts of plants: dependence on rainfall intensity and event profile from laboratory simulations, Hydrol. Process., 28, 5469–5482, https://doi.org/10.1002/hyp.10050, 2014.

Dunkerley, D.L.: Rainfall intensity bursts and the erosion of soils: an analysis highlighting the need for high temporal resolution rainfall data for research under current and future climates, Earth Surf. Dynam., 7, 345–360, https://doi.org/10.5194/esurf-7-345-2019, 2019.

Durocher, M.G.: Monitoring spatial variability of forest interception, Hydrol. Process., 4, 215–229, https://doi.org/10.1002/hyp.3360040303, 1990.

Fan, J.L., Baumgartl, T., Scheuermann, A. and Lockington, D.A.: Modeling effects of canopy and roots on soil moisture and deep drainage. Vadose. Zone. J., 14, 1–18, https://doi.org/10.2136/vzj2014.09.0131, 2015.

Firn, R.: Plant intelligence: an alternative point of view, Ann. Bot., 93, 345–351, https://doi.org/10.1093/aob/mch058, 2004.

Gao, X.D., Zhao, X.N., Pan, D.L., Yu, L.Y. and Wu, P.T.: Intra-storm time stability analysis of surface soil water content, Geoderma, 352, 33–37, https://doi.org/10.1016/j.geoderma.2019.06.001, 2019.

Garbelotto, M.M., Davidson, J.M., Ivors, K., Maloney, P.E., Hüberli, D., Koike, S.T. and Rizzo, D.M.: Non-oak native plants are main hosts for sudden oak death pathogen in California, Calif. Agric, 57, 18–23, https://doi.org/10.3733/ca.v057n01p18, 2003.

Germer, S.: Development of near-surface perched water tables during natural and artificial stemflow generation by babassu palms, J. Hydrol., 507, 262–272, http://dx.doi.org/10.1016/j.jhydrol.2013.10.026, 2013.

Germer, S., Werther, L. and Elsenbeer, H.: Have we underestimated stemflow? Lessons from an open tropical rainforest, J. Hydrol., 395, 169–179, https://doi.org/10.1016/j.jhydrol.2010.10.022, 2010.

Giacomin, A. and Trucchi, P.: Rainfall interception in a beech coppice (Acquerino, Italy). J. Hydrol., 137, 141–147, https://doi.org/10.1016/0022-1694(92)90052-W, 1992.

Groisman, P.Y. and Legates, D.R.: The accuracy of United States precipitation data, B. Am. Meteorol. Soc., 75, 215–227, https://doi.org/10.1175/1520-0477(1994)075<0215:TAOUSP>2.0.CO;2, 1994.

Hair, J.F., Anderson, R.E., Tatham, R.L. and Black, W.C.: Multivariate Data Analysis, fourth ed. Prentice Hall College Division, 745 p, 1995.

Herwitz, S.R.: Infiltration-excess caused by Stemflow in a cyclone-prone tropical rainforest, Earth Surf. Proc. Land, 11, 401–412, https://doi.org/10.1002/esp.3290110406, 1986.

Hill, T. and Lewicki, P.: Statistics: Methods and Applications. Statsoft, Tulsa, 800 p, 2007.

Hu, R., Wang, X.P., Zhang, Y.F., Shi, W., Jin, Y.X. and Chen, N.: Insight into the influence of sand-stabilizing shrubs on soil enzyme activity in a temperate desert, Catena, 137, 526–535, http://dx.doi.org/10.1016/j.catena.2015.10.022, 2016.

Iida, S., Levia, D.F., Shimizu, A., Shimizu, T., Tamai, K., Nobuhiro, T., Kabeya, N., Noguchi, S., Sawano, S. and Araki, M.: Intrastorm scale rainfall interception dynamics in a mature coniferous forest stand, J. Hydrol., 548, 770–783, https://doi.org/10.1016/j.jhydrol.2017.03.009, 2017.

Iida, S., Shimizu, T., Kabeya, N., Nobuhiro, T., Tamai, K., Shimizu, A., Ito, E., Ohnuki, Y., Abe, T., Tsuboyama, Y., Chann, S. and Keth, N.: Calibration of tipping-bucket flow meters and rain gauges to measure gross rainfall, throughfall, and stemflow applied to data from a Japanese temperate coniferous forest and a Cambodian tropical deciduous forest, Hydrol. Process., 26, 2445–2454, https://doi.org/10.1002/hyp.9462, 2012.

Jia, X.X., Shao, M.A., Wei, X.R. and Wang, Y. Q.: Hillslope scale temporal stability of soil water storage in diverse soil layers, J. Hydrol., 498, 254–264, https://doi.org/10.1016/j.jhydrol.2013.05.042, 2013.

Johnson, M.S. and Lehmann, J.: Double-funneling of trees: Stemflow and root-induced preferential flow, Ecoscience, 13, 324–333, https://doi.org/0.2980/i1195-6860-13-3-324.1, 2006.

Kéfi, S., Rietkerk, M., Alados, C.L., Pueyo, Y., Papanastasis, V.P., ElAich, A. and De Ruiter, P.C.: Spatial vegetation patterns and imminent desertification in Mediterranean arid ecosystems, Nature, 449, 213–217, https://doi.org/10.1038/nature06111, 2007.

Kimble, P.D.: Measuring the momentum of throughfall drops and raindrops. Master Thesis. Western Kentucky University, Bowling Green, 126 pp, 1996.

Levia, D.F. and Germer, S.: A review of stemflow generation dynamics and stemflow-environment interactions in forests and shrublands, Rev. Geophys., 53, 673-714, 2015, https://doi.org/10.1002/2015RG000479, 2015.

Levia, D.F., van Stan, J.T., Mage, S.M. and Kelley-Hauske, P.W.: Temporal variability of stemflow volume in a beech-yellow poplar forest in relation to tree species and size, J. Hydrol., 380, 112–120, https://doi.org/10.1016/j.jhydrol.2009.10.028, 2010.

Liang, W.L., Kosugi, K. and Mizuyama, T.: Soil water dynamics around a tree on a hillslope with or without rainwater supplied by stemflow, Water Resour. Res., https://doi.org/10.1029/2010WR009856, 2011.

Liang, W.L., Kosugi, K. and Mizuyama, T.: Soil water redistribution processes around a tree on a hillslope: the effect of stemflow on the drying process, Ecohydrology, 8, 1381–1395, https://doi.org/10.1002/eco.1589, 2014.

Li X., Xiao, Q.F., Niu, J.Z., Dymond, S., van Doorn, N.S., Yu, X.X., Xie, B.Y., Lv, X.Z., Zhang, K.B. and Li, J.: Process-based rainfall interception by small trees in Northern China: The effect of rainfall traits and crown structure characteristics, Agric. For. Meteorol., 218–219, 65–73, https://doi.org/10.1016/j.agrformet.2015.11.017, 2016.

Li, X.Y., Liu, L.Y., Gao, S.Y., Ma, Y.J. and Yang, Z.P.: Stemflow in three shrubs and its effect on soil water enhancement in semiarid loess region of China, Agric. For. Meteorol., 148, 1501–1507, https://doi.org/10.1016/j.agrformet.2008.05.003, 2008.

Li, Y.Y., Chen, W.Y., Chen, J.C. and Shi, H.: Contrasting hydraulic strategies in *Salix psammophila* and *Caragana korshinskii* in the southern Mu Us Desert, China, Ecol. Res., 31, 869–880, https://doi.org/10.1007/s11284-016-1396-1, 2016.

Liu, Y.X., Zhao, W.W., Wang, L.X., Zhang, X., Daryanto, S. and Fang, X.N.: Spatial variations of soil moisture under *Caragana korshinskii* kom. from different precipitation zones: field based analysis in the Loess Plateau, China, Forests, 7, https://doi.org/10.3390/f7020031, 2016.

Magliano, P.N., Whitworth-Hulse, J.I. and Baldi, G.: Interception, throughfall and stemflow partition in drylands: Global synthesis and meta-analysis, J. Hydrol., 568, 638–645, https://doi.org/10.1016/j.jhydrol.2018.10.042, 2019.

Manfroi, O.J., Koichiro, K., Nobuaki, T., Masakazu, S., Nakagawa, M., Nakashizuka, T. and Chong, L.: The stemflow of trees in a Bornean lowland tropical forest, Hydrol. Process., 18, 2455–2474, https://doi.org/10.1002/hyp.1474, 2004.

Martinez-Meza, E. and Whitford, W.: Stemflow, throughfall and channelization of stemflow by roots in three Chihuahuan desert shrubs, J. Arid Environ., 32, 271–287, https://doi.org/10.1006/jare.1996.0023, 1996.

Mcclain, M.E., Boyer, E.W., Dent, C.L., Gergel, S.E., Grimm, N.B., Groffman, P.M., Hart, S.C., Harvey, J.W., Johnston, C.A. and Mayorga, E.: Biogeochemical hot spots and hot moments at the interface of terrestrial and aquatic ecosystems, Ecosystems, 6, 301–312, https://doi.org/10.1007/s10021-003-0161-9, 2003.

Návar, J.: Stemflow variation in Mexico's northeastern forest communities: Its contribution to soil moisture content and aquifer recharge, J. Hydrol., 408, 35–42, https://doi.org/10.1016/j.jhydrol.2011.07.006, 2011.

Owens, M.K., Lyons, R.K. and Alejandro, C.L.: Rainfall partitioning within semiarid juniper communities: effects of event size and canopy cover, Hydrol. Process., 20, 3179–3189, https://doi.org/10.1002/hyp.6326, 2006.

Reid, L.M. and Lewis, J.: Rates, timing, and mechanisms of rainfall interception loss in a coastal redwood forest, J. Hydrol., 375, 459–470, https://doi.org/10.1016/j.jhydrol.2009.06.048, 2009.

Schimmack, W., Förster, H., Bunzl, K., and Kreutzer, K.: Deposition of radiocesium to the soil by stemflow, throughfall and leaf-fall from beech trees, Radiat. Environ. Bioph., 32, 137–150, https://doi.org/10.1007/bf01212800, 1993.

Siegert, C.M. and Levia, D.F.: Seasonal and meteorological effects on differential stemflow funneling ratios for two deciduous tree species, J. Hydrol., 519, 446–454, https://doi.org/10.1016/j.jhydrol.2014.07.038, 2014.

Spencer, S.A. and van Meerveld, H.J.: Double funnelling in a mature coastal British Columbia forest: spatial patterns of stemflow after infiltration, Hydrol. Process., 30, 4185–4201, https://doi.org/10.1002/hyp.10936, 2016.

Sprenger, M., Stumpp, C., Weiler, M., Aeschbach, W., Allen, S.T., Benettin, P., Dubbert, M., Hartmann, A., Hrachowitz, M., Kirchner, J.W., McDonnell, J.J., Orlowski, N., Penna, D., Pfahl, S., Rinderer, M., Rodriguez, N., Schmidt, M. and Werner, C.: The Demographics of Water: A Review of Water Ages in the Critical Zone, Rev. Geophys., 57, 1–35, https://doi.org/10.1029/2018RG000633, 2019.

Staelens, J., De Schrijver, A., Verheyen, K. and Verhoest N.E.: Rainfall partitioning into throughfall, stemflow, and interception within a single beech (*Fagus sylvatica* L.) canopy: influence of foliation, rain event characteristics, and meteorology, Hydrol. Process., 22, 33–45, https://doi.org/10.1002/hyp.6610, 2008.

Teachey, M.E., Pound, P., Ottesen, E.A. and van Stan, J.T.: Bacterial community composition of throughfall and stemflow, Front. Plant. Sci., 1, 1–6, https://doi.org/10.3389/ffgc.2018.00007, 2018.

Uijlenhoet, R. and Sempere Torres, D.: Measurement and parameterization of rainfall microstructure, J. Hydrol., 328, 1, 1–7, https://doi.org/10.1016/j.jhydrol.2005.11.038, 2006.

van Stan, J.T. and Levia, D.F.: Inter- and intraspecific variation of stemflow production from *Fagus grandifolia* Ehrh. (American beech) and *Liriodendron tulipifera* L. (yellow poplar) in relation to bark microrelief in the eastern United States, Ecohydrology, 3, 11–19, https://doi.org/10.1002/eco.83, 2010.

van Stan, J.T., Siegert, C.M., Levia D.F. and Scheick, C.E.: Effects of wind-driven rainfall on stemflow generation between codominant tree species with differing crown characteristics, Agric. For. Meteorol., 151, 9, 1277–1286, https://doi.org/10.1016/j.agrformet.2011.05.008, 2011.

van Stan, J.T., Gay, T.E. and Lewis, E.S.: Use of multiple correspondence analysis (MCA) to identify interactive meteorological conditions affecting relative throughfall, J. Hydrol., 533, 452–460, https://doi.org/10.1016/j.jhydrol.2015.12.039, 2016.

Wang, X.P., Wang, Z.N., Berndtsson, R., Zhang, Y.F. and Pan, Y.X.: Desert shrub stemflow and its significance in soil moisture replenishment, Hydrol. Earth Syst. Sci., 15, 561–567, https://doi.org/10.5194/hess-15-561-2011, 2011.

Yang, Z.P.: Rainfall partitioning process and its effects on soil hydrological processes for sand-fixed shrubs in Mu us sandland, Northwest China. PhD Thesis. Beijing Normal University, Beijing, 123 pp (in Chinese with English abstract), 2010.

Yang, X.L., Shao, M.A. and Wei, X.H.: Stemflow production differ significantly among tree and shrub species on the Chinese Loess Plateau, J. Hydrol., 568, 427–436, https://doi.org/10.1016/j.jhydrol.2018.11.008, 2019.

Yuan, C., Gao, G.Y. and Fu, B.J.: Stemflow of a xerophytic shrub (*Salix psammophila*) in northern China: Implication for beneficial branch architecture to produce stemflow, J. Hydrol., 539, 577–588, https://doi.org/10.1016/j.jhydrol.2016.05.055, 2016.

Yuan, C., Gao, G.Y. and Fu, B.J.: Comparisons of stemflow and its bio-/abiotic influential factors between two xerophytic shrub species, Hydrol. Earth Syst. Sci., 21, 1421–1438, https://doi.org/10.5194/hess-21-1421-2017, 2017.

Zabret, K., Rakovec, J. and Šraj, M.: Influence of meteorological variables on rainfall partitioning for deciduous and coniferous tree species in urban area, J. Hydrol., 558, 29–41, https://doi.org/10.1016/j.jhydrol.2018.01.025, 2018.

Zhang, Y., Li, X.Y., Li, W., Wu, X.C., Shi, F.Z., Fang, W.W. and Pei, T.T.: Modeling rainfall interception loss by two xerophytic shrubs in the Loess Plateau, Hydrol. Process., 31, 1926–1937, https://doi.org/10.1002/hyp.11157, 2017.

Zhang, Y.F., Wang X.P., Hu, R., Pan Y.X. and Paradeloc, M.: Rainfall partitioning into throughfall, stemflow and interception loss by two xerophytic shrubs within a rain-fed re-vegetated desert ecosystem, northwestern China, J. Hydrol., 527, 1084–1095, https://doi.org/10.1016/j.jhydrol.2015.05.060, 2015.

Table 1. Branch morphologies of *C. korshinskii* and *S. psammophila* for stemflow recording.

Shrub species	BD categories (mm)	Amount	BD (mm)	BL (cm)	BA (°)	LA (cm^2)
C. korshinskii	5–10	2	6.6	131	61	837.1
	10–15	2	13.1	168	43	2577.3
	15–18	2	17.8	206	72	4243.1
	18–25	1	22.1	242	50	6394.7
	>25	NA	NA	NA	NA	NA
S. psammophila	5–10	2	7.5	248	69	626.3
	10–15	2	13.2	343	80	1683.5
	15–18	NA	NA	NA	NA	NA
	18–25	2	21.8	286	76	3468.3
	>25	1	31.3	356	60	7513.7

Notes: BD, BL and BA are branch basal diameter, length and inclination angle, respectively; LA is leaf area of individual branches; NA means not applicable.

Table 2. Rainfall characteristics during events with different intensity peak amounts.

Indicators	Event A	Event B	Event C	Others	Average
Event amount	17	11	15	11	13.5±1.5
RA (mm)	4.1 ab	5.2 b	11.7 c	0.6 a	5.4 ± 0.9
RD (h)	2.5 a	3.6 a	10.3 b	2.2 a	4.7 ± 0.8
RI (h)	48.5 ab	70.5 b	57.3 ab	26.1 a	50.6 ± 6.1
I ($mm \cdot h^{-1}$)	5.6 a	5.5 a	4.6 a	2.2 b	4.5 ± 1.0
I_{10} ($mm \cdot h^{-1}$)	15.5 a	12.7 ab	9.5 b	6.0 c	10.9 ± 2.1
I_{b10} ($mm \cdot h^{-1}$)	7.7 a	9.9 a	2.8 b	1.6 b	5.5 ± 1.4
I_{e10} ($mm \cdot h^{-1}$)	4.3 a	3.6 a	2.1 ab	1.2 b	2.8 ± 0.7
F ($mg \cdot m \cdot s^{-1}$)	17.1 a	17.6 a	17.2 a	12.5 b	16.1 ± 1.2
F_{10} ($mg \cdot m \cdot s^{-1}$)	27.8 a	26.6 a	24.2 ab	21.0 b	24.9 ± 1.4
F_{b10} ($mg \cdot m \cdot s^{-1}$)	19.7 ab	21.7 a	15.4 b	16.9 b	18.4 ± 1.4
F_{e10} ($mg \cdot m \cdot s^{-1}$)	17.3 a	16.6 a	13.4 b	16.8 a	16.0 ± 1.0
E (unitless)	0.9 ab	1.0 ab	0.4 a	1.7 b	0.9 ± 0.2

Note: Event A, Event B and Event C are events with the single, double and multiple rainfall intensity peaks, respectively; Others are the events that excluded from the categorization; RA, RD and RI are rainfall amount, duration and interval, respectively; I and I_{10} are the average and 10-min maximum rainfall intensities, respectively; I_{b10} and I_{e10} are the average rainfall intensities in 10 min after rain begins and before rain ends, respectively; F and F_{10} are the average and 10-min maximum raindrop momentums, respectively; F_{b10} and F_{e10} are the average raindrop momentums in 10 min after rain begins and before rain ends, respectively; E is evaporation coefficient; Different letters indicate significant differences of rainfall characteristics between event categories (p<0.05) (rows at the table).

Table 3. Stemflow variables of *C. korshinskii* and *S. psammophila* during rainfall events with different intensity peak amounts.

Species	Stemflow variables	Event A	Event B	Event C	Others	Average
C. korshinskii	SFV (mL)	134.1 a	203.7 a	560.8 b	7.6 c	226.6 ± 46.4
	SFI ($mm\cdot h^{-1}$)	672.9 a	552.4 b	527.0 b	317.8 c	517.5 ± 82.1
	SFI_{10} ($mm\cdot h^{-1}$)	2849.0 a	2399.3 a	1809.1 b	1173.2 c	2057.6 ± 399.7
	FR (unitless)	109.4 a	146.6 b	137.9 b	128.9 ab	130.7 ± 8.2
	TLG (min)	67.3 ab	56.2 a	67.0 ab	74.2 b	66.2 ± 10.6
	TLM (min)	81.1 a	75.5 a	202.1 b	78.8 a	109.4 ± 20.5
	TLE (min)	22.3 a	18.7 b	18.5 b	20.6 a	20.0 ± 5.3
	SFD (h)	1.4 a	3.1 a	9.1 b	1.4 a	3.8 ± 0.8
S. psammophila	SFV (mL)	102.6 a	145.7 a	435.2 b	4.7 c	172.1 ± 34.5
	SFI ($mm\cdot h^{-1}$)	648.1 a	421.5 b	246.6 c	153.2 c	367.3 ± 91.1
	SFI_{10} ($mm\cdot h^{-1}$)	1672.7 a	1582.8 a	888.4 b	384.7 c	1132.2 ± 214.3
	FR (unitless)	77.1 a	91.4 a	129.1 b	101.6 ab	101.6 ± 10.4
	TLG (min)	84.9 a	46.5 b	56.1 b	31.5 b	54.8 ± 11.7
	TLM (min)	64.3 a	93.4 a	235.8 b	88.4 a	120.5 ± 22.1
	TLE (min)	17.1 a	8.6 b	20.8 a	7.3 b	13.5 ± 17.2
	SFD (h)	1.2 a	3.4 a	8.3 b	0.7 a	3.4 ± 0.9

Note: Event A, Event B and Event C are events with the single, double and multiple rainfall intensity peaks, respectively; Others are the events that excluded from the categorization; TLG and TLM are time lags of stemflow generating and maximizing after rains begin, respectively; TLE is time lag of stemflow ending after rain ceases; SFD is stemflow duration; SFV is stemflow volume; SFI are the average stemflow intensities at incident rains, respectively; Different letters indicate significant differences of stemflow variables between event categories ($p<0.05$) (rows at the table).

Table 4. Comparisons of stemflow intensity and funnelling ratio at different basal diameter categories.

Species and stemflow variables		BD categories (mm)					
		5–10	10–15	15–18	18–25	>25	AVG
C. korshinskii	FR	163.7±12.2a	136±10.9b	119.5±13.0b	97.7±9.2b	NA	131±8.2
	SFI	716.2±118.7a	552.5±90.3b	619±103.3b	333.8±45.8b	NA	553.9±82.1
S. psammophila	FR	212±17.4a	84±6.4b	NA	44.2±3.0b	54.9±4.2b	100.6±7.9
	SFI	738.7±160.9a	360.7±82.7a	NA	197.2±44.9b	209.9±44.5b	372.2±79.4

Note: SFI and FR are the average stemflow intensity and funnelling ratio at incident rains, respectively; BD is branch basal diameter (mm); NA means not applicable; Different letters indicate significant differences of stemflow variables between event categories (p<0.05) (rows at the table).

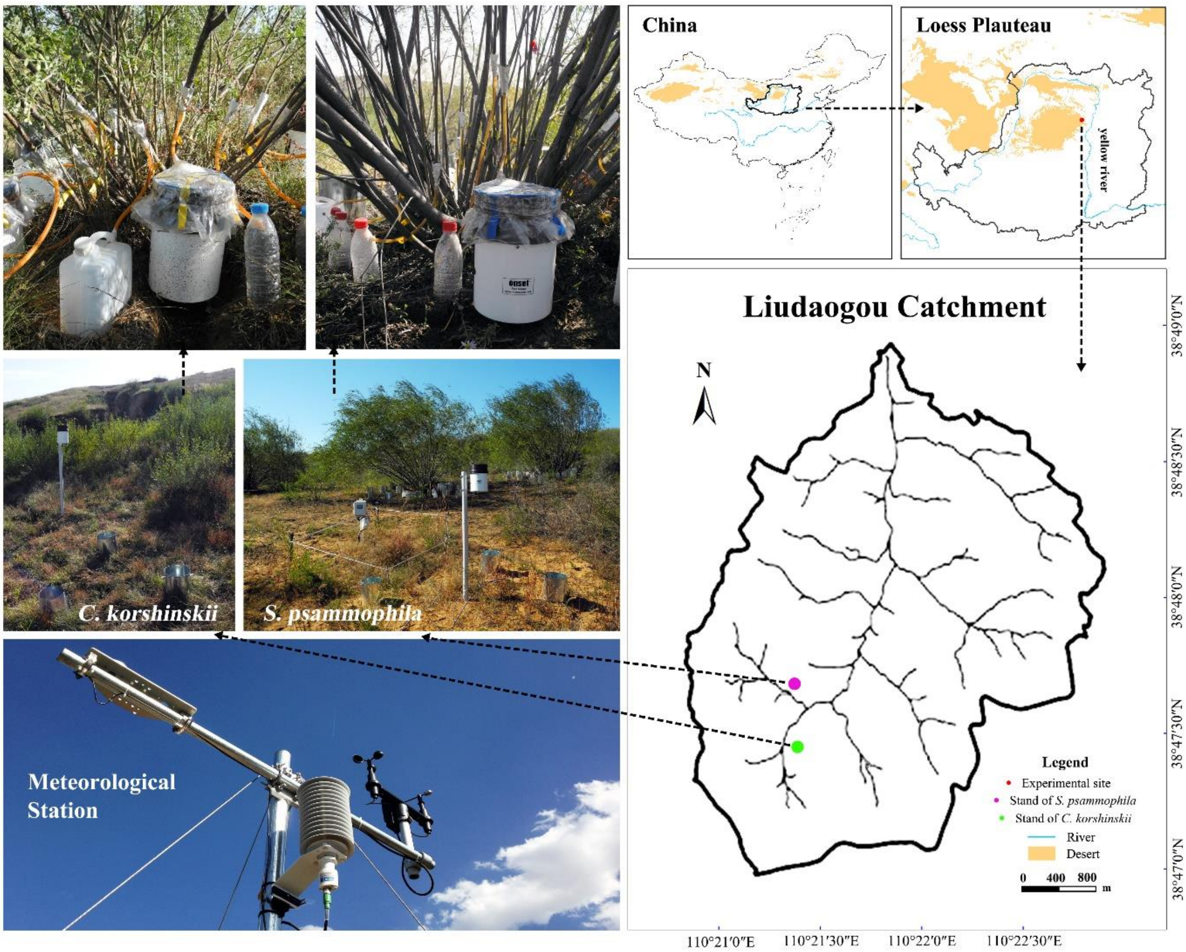

830

831 **Figure 1.** Locations and experimental settings in the plots of *C. korshinskii* and *S.*
832 *psammophila*.

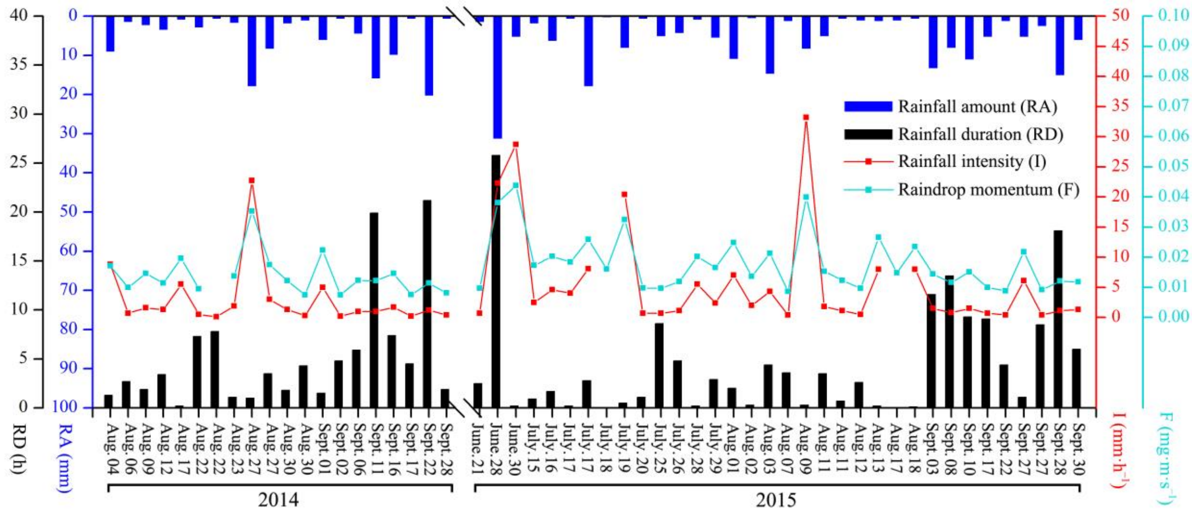

Figure 2. Inter-event variations in rainfall characteristics during the experimental period.

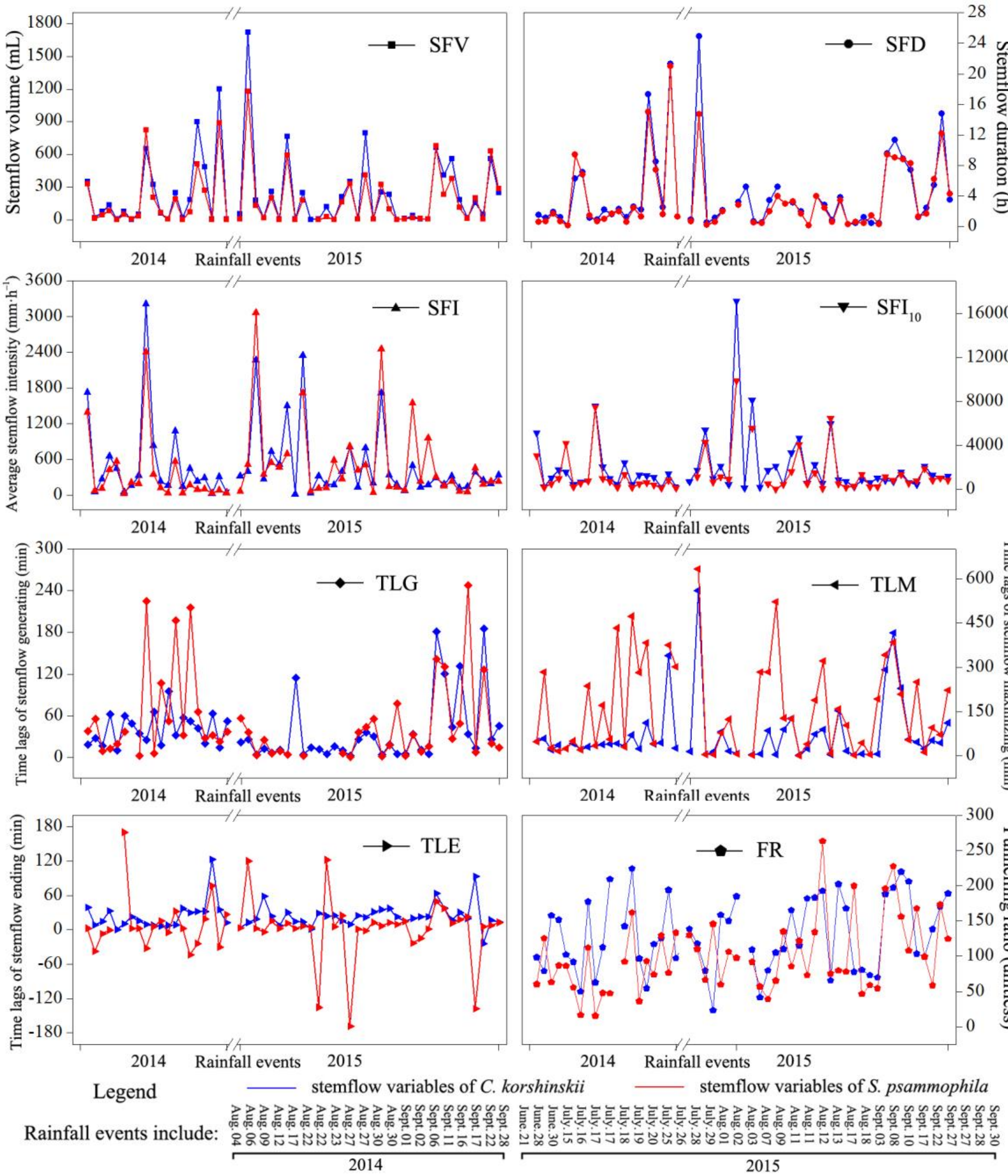

Figure 3. Inter-event variations in stemflow variables of *C. korshinskii* and *S. psammophila* during the experimental period.

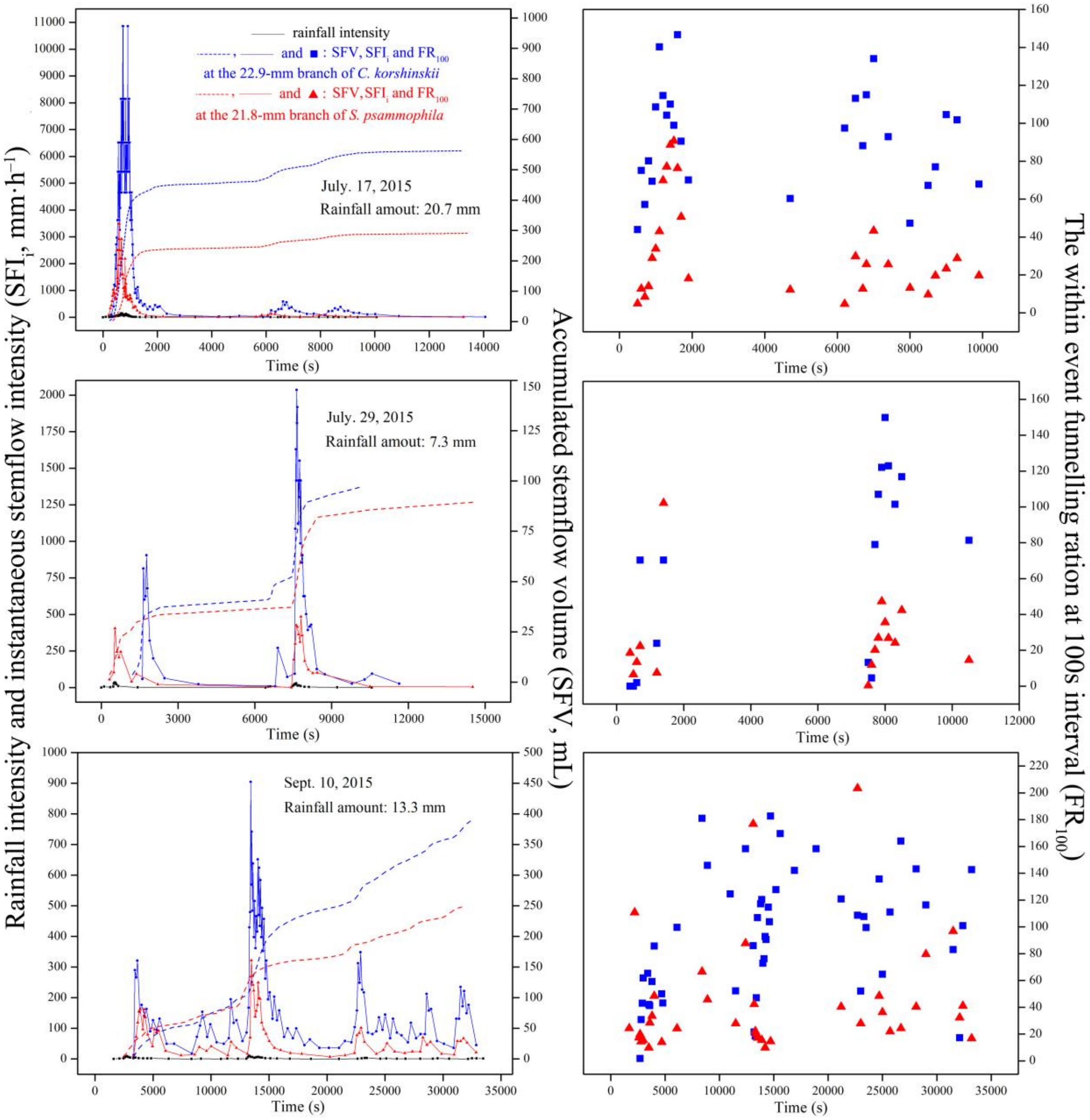

838

839 **Figure 4.** Stemflow synchronicity of *C. korshinskii* and *S. psammophila* to rains during

840 representative events with different rainfall-intensity peak amounts.

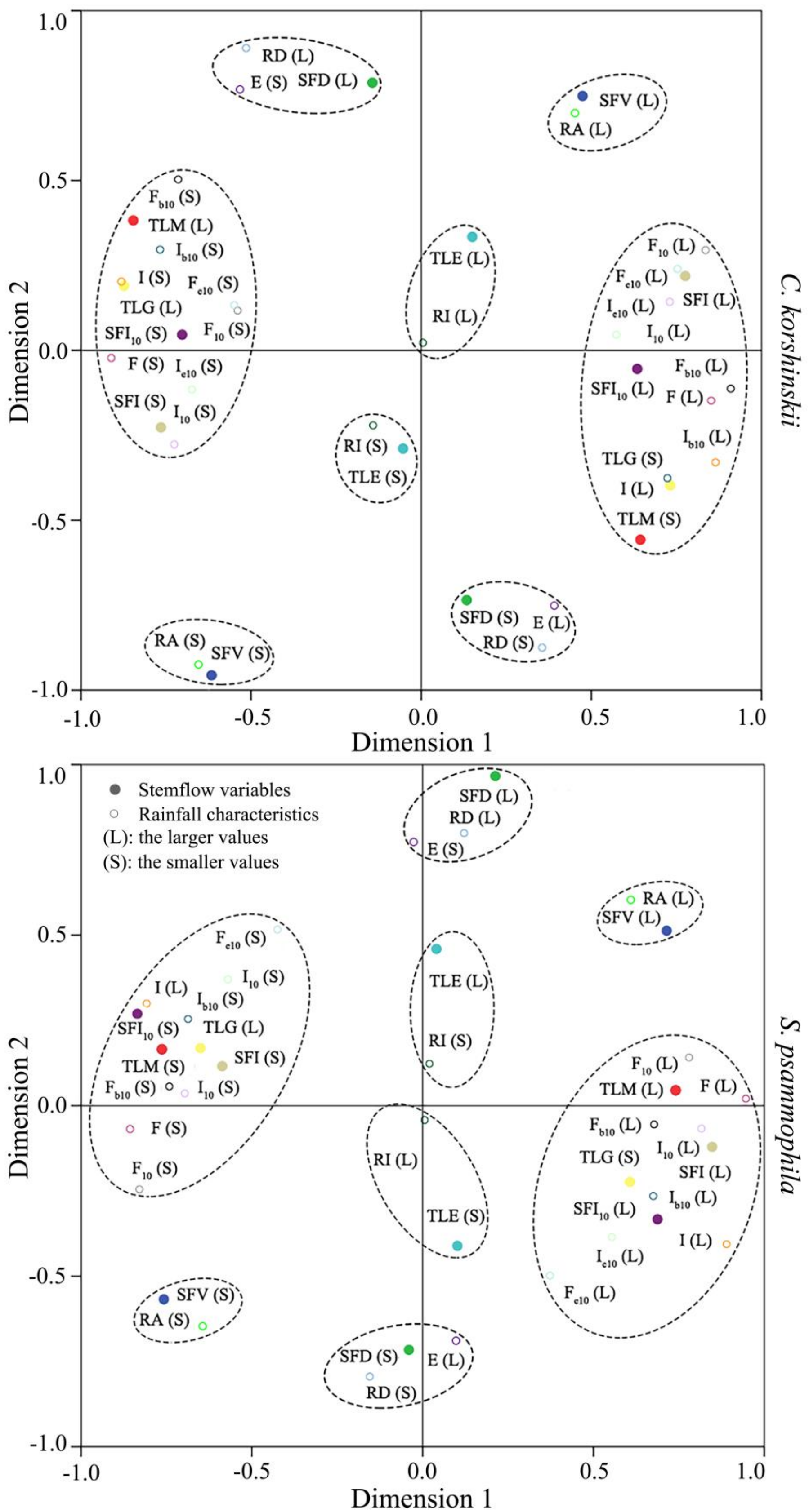

Figure 5. Correspondence maps of stemflow variables with rainfall characteristics for *C. korshinskii* and *S. psammophila*.

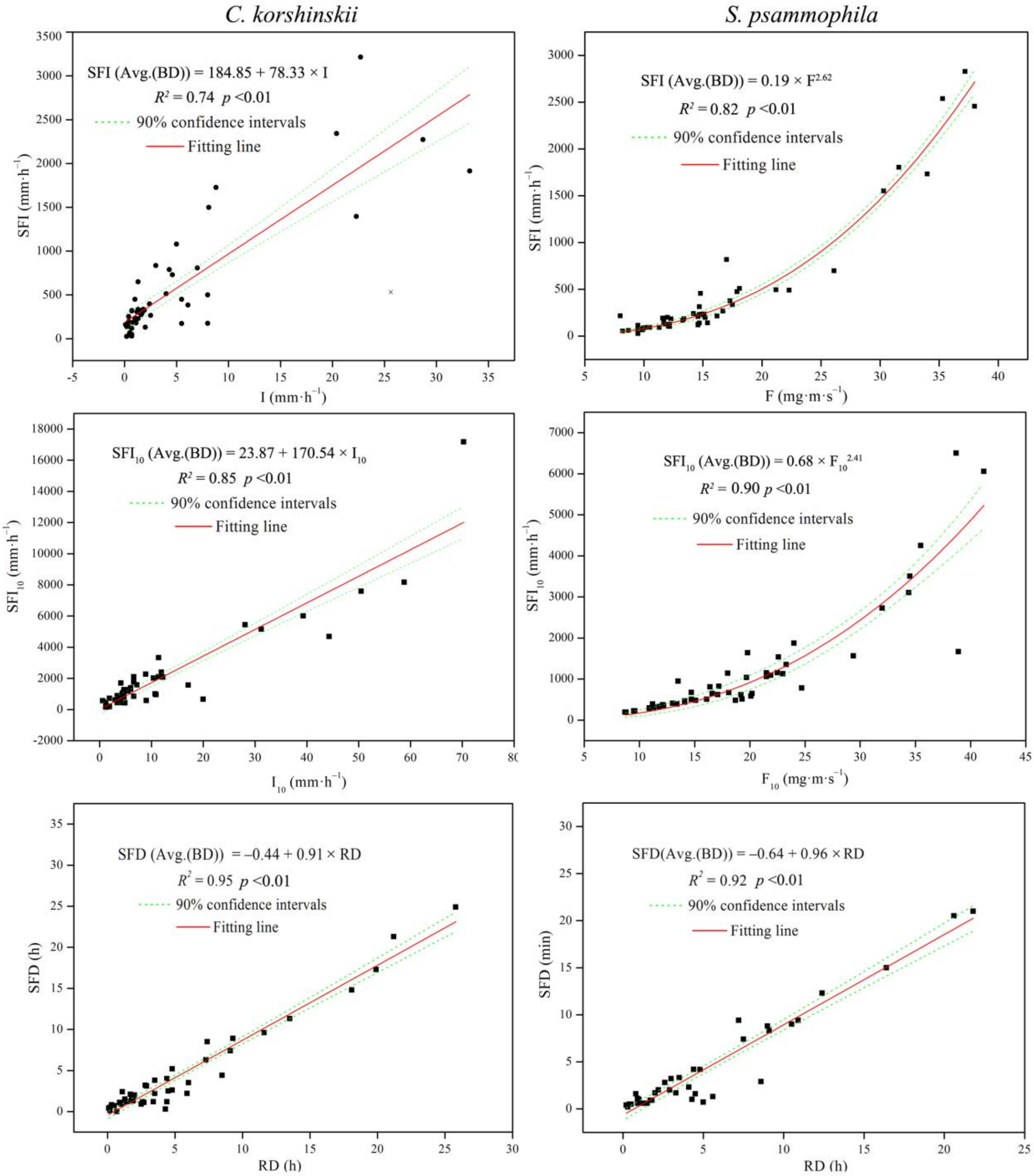

Figure 6. Relationships of stemflow intensity and duration with rainfall characteristics.

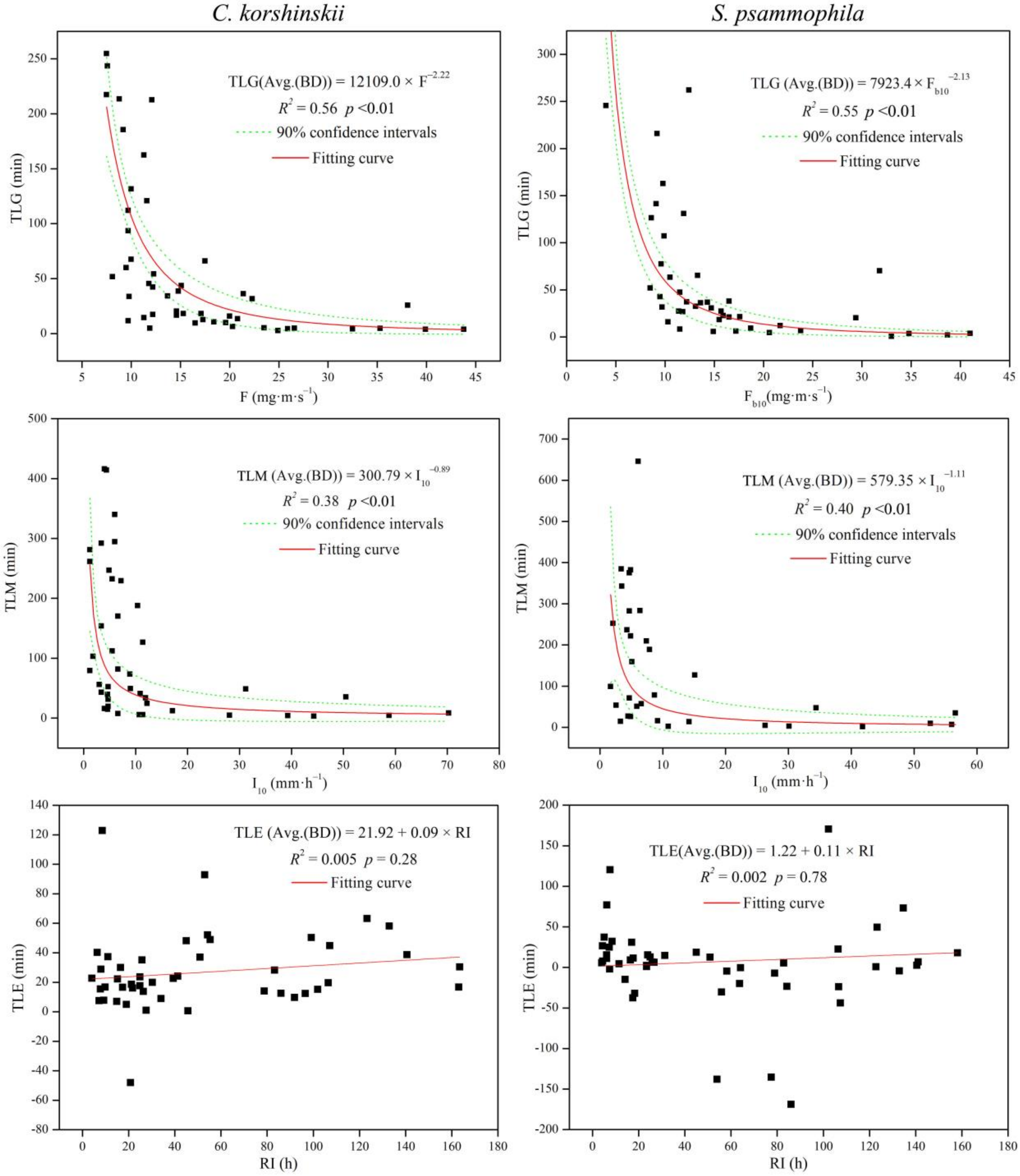

Figure 7. Relationships of stemflow time lags with rainfall characteristics.

Temporal-dependent effects of rainfall characteristics on inter-/intra-event branch-scaled stemflow variability in two xerophytic shrubs

Chuan Yuan[1, 2, 3], Guangyao Gao[2], Bojie Fu[2], Daming He[1, 3], Xingwu Duan[1, 3], and Xiaohua Wei[4]

[1]Institute of International Rivers and Eco–security, Yunnan University, Kunming 650091, China
[2]State Key Laboratory of Urban and Regional Ecology, Research Center for Eco-Environmental Sciences, Chinese Academy of Sciences, Beijing 100085, China
[3]Yunnan Key Laboratory of International Rivers and Trans-boundary Eco–security, Kunming 650091, China
[4]Department of Earth, Environmental and Geographic Sciences, University of British Columbia (Okanagan campus), Kelowna, British Columbia, V1V 1V7, Canada

Correspondence: Guangyao Gao **(**gygao@rcees.ac.cn)

Abstract

Stemflow is important for recharging root-zone soil moisture in arid regions. Previous studies have generally focused on stemflow volume, efficiency and influential factors but have failed to depict ~~temporal~~ stemflow processes and quantify their ~~relationships~~relations with rainfall characteristics within events, particularly for xerophytic shrubs. Here, we measured the stemflow volume, intensity, funnelling ratio, duration, and time lags to rain

~~events of~~at two ~~xerophytic~~dominant shrub species (*Caragana korshinskii* and *Salix psammophila*) and rainfall characteristics ~~for~~during 54 events ~~in~~at the semi-arid Liudaogou catchment of the Loess Plateau, China, during the 2014~~-~~–2015 rainy seasons. ~~The~~Funnelling ratio was calculated as the ratio between stemflow and rainfall intensities at the inter-/intra-event bases for the first time. Our results indicated that the stemflow ~~dynamics were well synchronized to rainfall processes. The stemflows~~ of *C. korshinskii* and *S. psammophila* were averagely started 66.2 and 54.8 min, maximized 109.4 and 120.5 min after rains began, and ended 20.0 and 13.5 min after rains ceased. They had shorter stemflow duration (3.8 and 3.4 h) and significantly larger ~~average~~stemflow intensities (517.5 and 367.3 mm·h^{-1}) than those of rains (4.7~~±1.5 and 4.8±1.6 mm·h^{-1}, respectively) than that of rain at the event scale (4.5±1.0 mm·h^{-1}), and the stemflows were even more intense (20.3±10.4 and 16.9±8.8 mm·~~ h~~$^{-1}$, respectively) than that of rain at 10-min intervals (10.9±2.1~~ and 4.5 mm·h^{-1}). ~~The average stemflow durations of *C. korshinskii* and *S. psammophila* (3.8±0.8 and 3.4±0.9 h, respectively) were shorter than the rainfall duration (4.7±0.8 h).~~ As branch size increased, both species shared the decreasing funnelling ratios (97.7–163.7 and 44.2–212.0) and stemflow intensities (333.8–716.2 mm·h^{-1} and 197.2–738.7 mm·h^{-1}). Tested by ~~a~~the multiple correspondence analysis and stepwise regression, rainfall amount and duration controlled stemflow volume and duration, respectively, at ~~the~~ event scale by linear ~~relationships~~relations (p<0.01). Rainfall intensity and raindrop momentum controlled stemflow intensity and time lags to rains for both species ~~at the intra-~~within event ~~scale~~ by linear or power relationships (p<0.01). Rainfall intensity was the key factor ~~for the~~affecting stemflow process of *C. korshinskii*, whereas raindrop

momentum had the greatest influence on ~~the~~ stemflow process of *S. psammophila*. ~~Rainfall~~Therefore, rainfall characteristics had temporal-dependent influences on corresponding stemflow variables, and the influence also depended on specific species.

1 Introduction

Stemflow directs the intercepted rains from ~~the~~ canopy to the trunk base. The funnel-shaped canopy and underground preferential paths, i.e., roots, worm paths and soil macropores, converge rains to recharge the root-zone moisture (Johnson and Lehmann, 2006; Li et al., 2008). Stemflow is important to concentrate water (Levia and Germer, 2015), nutrients (Dawoe et al., 2018), pathogens (Garbelotto et al., 2003) and bacteria (Bittar et al., 2018) from the phyllosphere into the pedosphere (Teachey et al., 2018), even though stemflow accounts for only a ~~minimal~~minor part of rainfall amount (RA) (6.2%) in contrast to throughfall (69.8%) and interception loss (24.0%) in ~~water-stressed regions~~dryland ecosystems with annual mean rainfall ranging in 154–900 mm (Magliano et al., 2019). Stemflow greatly contributes to the survival of xerophytic plant species (Návar, 2011), the maintenance of patch structures in arid areas (Kéfi et al., 2007), and the normal functioning of rainfed dryland ecosystems (Wang et al., 2011).

To quantify the ecohydrological importance of stemflow, numerous studies have been conducted on stemflow production and efficiency from various aspects, including stemflow volume (mL), depth (mm), percentage (%), funnelling ratio (unitless), and productivity ($mL \cdot g^{-1}$, the branch stemflow volume of unit biomass) (Herwitz, 1986; Yuan et al., 2016; Zabret et al., 2018; Yang et al., 2019). By ~~applying~~installing automatic recording devices, the stemflow process has been gradually determined at 1-h intervals (Spencer and van Meerveld, 2016), 5-min intervals (André et al., 2008; Levia et al., 2010) and 2-min intervals (Dunkerley, ~~2014~~2014b). This determination allowed ~~the calculation of~~to compute stemflow intensity (mm·h^{-1}) (Germer et al., 2010), ~~speed~~flux (mL·min^{-1}) (Yang, 2010) and time lag after rain (Cayuela et al., 2018). Differing from an event-based calculation, the stemflow process provided insights into the fluctuation of stemflow production at a high temporal resolution. ~~This process~~It permits a better interpretation of the “hot moment” and “hot spot” effects of many ecohydrological processes (Bundt et al., 2001; McClain et al., 2003). Quantifying the short-intensity burst and temporal characteristics~~ of stemflow~~ shed light on the dynamic process and pulse nature of stemflow (Dunkerley, 2019).

Stemflow cannot be ~~initialled after~~initiated until canopies were saturated by the rains (Martinez-Meza and Whitford, 1996). The minimal RA needed to start stemflow ~~is~~was usually calculated by regressing stemflow volume with RA ~~for~~at different plant species ~~or canopy states~~ (Levia and Germer, 2015). ~~In the leaf period, stemflow starts when rains are greater than~~It also varied with canopy states, i.e., 10.9 ~~mm~~ and 2.5~~-~~–3.~~4 mm~~4mm for the leafed oak and beech tress, ~~respectively, in Belgium,~~ and ~~in the leafless period, the minimal RA for stemflow generation is~~ 6.0 mm and 1.5~~-~~–1.9 mm for ~~these two species~~them in the leafless period (André et al., 2008; Staelens et al., 2008). ~~In comparison, a lower amount of rain,0.4-2.2 mm, can generally initiate stemflow of xerophytic shrubs (Yuan et al., 2017).~~ Stemflow also frequently ~~continues~~continued after rains ceased due to the rainwater retained on the canopy/branch surface (Iida et al., 2017). *Salix psammophila* and an open tropical forest ~~start~~started stemflow 5~~-~~–10 min and 15 min later than the beginning of a rain event in the Mu Us desert of China (Yang, 2010) and the Amazon basin of Brazil (Germer et al., 2010), respectively. However, 1 h and 1.5 h ~~are~~were needed to start stemflow after the beginning of a rain event for pine and oak trees in north-eastern Spain, respectively (Cayuela et al., 2018). For *S. psammophila*, stemflow ~~is~~flux was maximized 20~~-~~–210 min after the beginning of a rain event (Yang, 2010), and stemflow ceased 11 h after ~~rain stopped~~rains seaced in an open tropical forest (Germer et al., 2010). ~~Stemflow time~~Time lags ~~are critical indicators for depicting the~~ of stemflow generation, maximization and ending to rains depicted dynamic stemflow process~~ and are important for developing process-based~~ , and were conducive to better understand the hydrological process occurred at the interface between the intercepted rains and soil moisture (Sprenger et al., 2019). ~~models.~~It was important to discuss the temporal persistence in spatial patterns of soil moisture particularly at the intra-event scale (Gao et al., 2019). However, stemflow time lags have not been systematically studied for xerophytic shrubs.

The preferential paths at the underside of branches for delivering stemflow complicates stemflow processes within events (Dunkerley, ~~2014~~2014a). The influences of bark microrelief~~–~~ on stemflow are strongly affected by dynamic rain processes, such as rainfall intensity and raindrop striking within events (~~Van~~van Stan and Levia, 2010). While exceeding the holding capacity of branches, high rainfall intensity ~~can~~could overload and interrupt this preferential path (Carlyle-Mose and Price, 2006). Raindrops hit the canopy surface and create splashes on the surface. This process is conducive to wetting branches at the lower layers and accelerating the establishment of the preferential paths of stemflow transportation (Bassette and Bussière, 2008). Nevertheless, the interaction between the stemflow process and intra-event rainfall characteristics has not been substantially studied.

This study was designed at the event and process scales to investigate inter-/intra-event stemflow variability of two dominant xerophytic shrubs. Stemflow volume, intensity, funnelling ratio and temporal dynamics of *Caragana korshinskii* and *S. psammophila* were recorded during 54 rainfall events in the 2014–2015 rainy seasons on the Loess Plateau of China. Temporal dynamics were expressed as stemflow duration and time lags of stemflow generation, maximization and cessation to ~~the start of rain events.~~rains. Raindrop momentum was introduced to represent the comprehensive effects of raindrop size, velocity, inclination angle and kinetic energy ~~on~~at the stemflow process. Funnelling ratio had been calculated at the event base and the 100-s intervals to assess the convergence effects of stemflow. This study specifically aimed to (1) depict the stemflow process in terms of stemflow intensity and temporal dynamics, (2) identify the dominant rainfall characteristics influencing inter-/intra-event stemflow variables, and (3) quantify the relationships between stemflow process variables and rainfall characteristics. Achieving these objectives would advance our knowledge of the process-based stemflow production to better understand the pulse nature of stemflow and its interactions with dynamic rain processes.

2 Materials and Methods

2.1 Site description

This study was conducted in the Liudaogou catchment (110°21′–110°23′E, 38°46′–38°51′N) in Shenmu city, Shaanxi Province, China, during the 2014–2015 rainy seasons. This catchment is 6.9 km^2 and 1094–1273 m above sea level (m.a.s.l.). A semiarid continental climate prevails in this area. The mean annual precipitation (MAP) is 414 mm

(1971–2013). Most MAP (77%) occurs from July to September (Jia et al., 2013). The mean annual potential evaporation is 1337 mm (Yang et al., 2019). The mean annual temperature is 9.0 °C. The dominant shrubs include *C. korshinskii*, *S. psammophila*, and *Amorpha fruticosa*. The dominant grasses are *Artemisia capillaris*, *Artemisia sacrorum*, *Medicago sativa*, *Stipa bungeana*, etc.

C. korshinskii and *S.* ~~*psammophila* are two representative xerophytic shrub species. They~~*psammophila* are dominant shrub species at the arid and semi-arid regions of northwestern China (Hu et al., 2016; Liu et al., 2016). They were commonly planted for soil and water conservation, sand fixation and wind barrier, and had extensive distributions at this region (Li et al., 2016). The both species have inverted-cone crowns and no trunks, with multiple branches running obliquely from the base. As modular organisms and multi-stemmed shrub species, their branches live as independent individuals and compete with each other for water and light (Firn, 2004). Two plots were established in the southwestern catchment for these two xerophytic shrubs planted in the 1990s (Fig. 1). *C. korshinskii* and *S. psammophila* plots share similar stand conditions with elevations of 1179 and 1207 m.a.s.l., slopes of 13° and 18°, and sizes of 3294 and 4056 m^2, respectively. The *C. korshinskii* plot has a ground surface of loess and aspect of 224°, while the *S. psammophila* plot has a ground surface of sand and an aspect of 113°.

2.2 Meteorological measurements and calculations

A meteorological station was installed at the experimental plot of *S. psammophila* to record rainfall characteristics and wind speed (WS, $m \cdot s^{-1}$~~). The Onset® (Onset Computer Corp., USA) RG3-M tipping bucket rain gauges (with a diameter of 15.24 cm and a~~

~~resolution of 0.2 mm) recorded the rain amount and timing of incident rains. Discrete rainfall events were defined by a measurable RA of 0.2 mm (the resolution limit of the RG3-M rain gauge) and the smallest 4-h gap without rains (the analogue period of time to dry canopies from antecedent rains) (Giacomin and Trucchi, 1992; Zhang et al., 2015; Yang et al~~) (Model 03002, R. M. Young Company, USA), air temperature (T, °C) and relative humidity (H, %) (Model HMP 155, Vaisala, Finland). They were logged at 10-min intervals by a datalogger (Model CR1000, Campbell Scientific Inc., USA). Evaporation coefficient (E, unitless) was calculated to present the evaporation intensity (Equations 1–3) via aerodynamic approaches (Carlyle-Mose and Schooling, 2015). Tipping-bucket rain gauges (hereinafter referred to as “TBRG”) automatically recorded the volume and timing of rainfall and stemflow (Herwitz, 1986; Germer et al., 2010; Spencer and Meerveld, 2016; Cayuela et al., 2018). To mitigate the systematic errors for missing the records of inflow during tipping intervals (Groisman and Legates, 1994), we chose the Onset® (Onset Computer Corp., USA) RG3-M TBRG with the relatively smaller underestimation for its smaller bucket volume (3.73±0.01 mL) (Iida et al., 2012). Besides, three 20-cm-diameter standard rain gauges were placed around TBRG with a 0.5-m distance at the 120° separation (Fig. 1). The regression (R^2=0.98, p<0.01) between manual measurements and automatic recording further mitigated the understanding of inflow water by applying TBRG (Equation 4).~~., 2019). WS was recorded by wind sensors (Model 03002, R. M. Young Company, USA) and logged at 10-min intervals by a datalogger (Model CR1000, Campbell Scientific Inc., USA). For the 0.8 km distance between the two plots, the meteorological data were also applied to the *C. korshinskii* plot.~~

$$e_s = 0.611 \times \exp\left(17.27 \times T \Big/ (237.7 + T)\right) \quad (1)$$

$$VPD = e_s \times (1 - H) \quad (2)$$

$$E = WS \times VPD \quad (3)$$

where e_s is the saturation vapor pressure (kPa); T is air temperature (°C); H is air relative humidity (%); VPD is the vapor pressure deficit (kPa); and E is the evaporation coefficient (unitless).

$$IW_A = IW_R \times 1.32 + 0.16 \quad (4)$$

where IW_R is the recording of Inflow water (including rainfall and stemflow) via TBRG (mm), and IW_A is the adjusted inflow water (mm).

Discrete rainfall events were defined by a measurable RA of 0.2 mm (the resolution limit of the TBRG) and the smallest 4-h gap without rains. That was the same period of time to dry canopies from antecedent rains as reported by Giacomin and Trucchi (1992), Zhang et al. (2015), Zhang et al., (2017) and Yang et al. (2019). Rainfall interval (RI, h) was calculated to indirectly represent the bark wetness. Other rainfall characteristics were ~~calculated~~also computed, including the RA (mm), rainfall duration (RD, h), ~~rainfall interval (RI, h),~~ the average and 10-min maximum rainfall intensity of incident rains (I and I_{10}~~, respectively~~, mm·h^{-1}), and the 10-min average rainfall intensity after rain begins (I_{b10}, mm·h^{-1}) and before rain ends (I_{e10}, mm·h^{-1}). ~~Raindrop traits include diameter (D, mm) (Herwitz and Slye, 1995), terminal velocity (V, m·s^{-1}) (Carlyle-Moses and Schooling, 2015), and average inclination angle (θ, °) (Herwitz and Slye, 1995; Van Stan et al., 2011).~~ By assuming a perfect sphere of a raindrop (Uijlenhoet and Torres, 2006), ~~the average~~ raindrop momentum in the vertical direction (F, mg·m·s^{-1}) (Equation 8–9) was computed to comprehensively represent the effects of raindrop ~~morphology and energy~~size (D, mm) (Equation 5), terminal velocity (v, $m \cdot s^{-1}$) (Equation 6), average inclination angle (θ, °) (Equation 7) affecting stemflow process (Brandt, 1990; Kimble, 1996~~).~~

~~$D = 2.23 \times (0.03937 \times I)^{0.102}$ (1)~~

~~$V = 3.378 \times \ln(D) + 4.213$ (2)~~

~~$\tan\theta = WS / V$ (3)~~

~~$F_0 = M \times V = (1/6 \times \rho \times \pi \times D^3) \times V$ (4)~~

~~$F = F_0 \times \cos\theta$ (5)~~

~~where I is the average rainfall intensity of incident rains ($mm \cdot h^{-1}$), M is the average raindrop mass (g), and F_0 is the average raindrop momentum ($mg \cdot m \cdot s^{-1}$). ρ is the density of freshwater at standard atmospheric pressure and 20°C ($0.998\ g \cdot cm^{-3}$). WS is the average wind speed of incident rains ($m \cdot s^{-1}$~~; van Stan et al., 2011; Carlyle-Moses and Schooling, 2015). The 10-min maximum raindrop momentum (F_{10}, $mg \cdot m \cdot s^{-1}$) and the average raindrop momentum at the first and last 10 min (F_{b10} and F_{e10}, respectively, $mg \cdot m \cdot s^{-1}$) could ~~also~~ be calculated with I_{10}, I_{b10} and I_{e10} ~~during incident rains~~as indicated at Equation 5–9, respectively. For the 0.8-km distance between the two plots, the meteorological data were used at the *C. korshinskii* plot.

$$D = 2.23 \times (0.03937 \times I)^{0.102} \tag{5}$$

$$v = 3.378 \times \ln(D) + 4.213 \tag{6}$$

$$\tan\theta = {}^{WS}\!/_{v} \tag{7}$$

$$F_0 = m \times v = ({}^{1}\!/_{6} \times \rho \times \pi \times D^3) \times v \tag{8}$$

$$F = F_0 \times \cos\theta \tag{9}$$

where D is raindrop diameter (mm); I is the average rainfall intensity of incident rains ($mm \cdot h^{-1}$); v is raindrop velocity ($m \cdot s^{-1}$); θ is average inclination angle of raindrops (°); WS is the average wind speed of incident rains ($m \cdot s^{-1}$); F_0 is the average raindrop momentum ($mg \cdot m \cdot s^{-1}$); m is the average raindrop mass (g); ρ is the density of freshwater at standard atmospheric pressure and 20°C (0.998 $g \cdot cm^{-3}$).

2.3 Experimental branch selection and measurements

This study focused on the branch-scaled stemflow production of the 20-year-old *C. korshinskii* and *S. psammophila*. ~~By selecting four 20-year-old~~ Based on plot investigation, the canopy traits of standard shrubs ~~of~~were determined. Four shrubs were selected accordingly at each species with similar crown areas and heights (5.1±0.3 m^2 and 2.1±0.2 m for *C. korshinskii* and 21.4±5.2 m^2 and 3.5±0.2 m for *S. psammophila*, respectively~~), the variance in canopy traits was neglected.~~). The ~~isolated canopies~~approximately 10-m gap between them guaranteed ~~that they were exposed~~shrubs exposing to the similar ~~rainfall characteristics.~~meteorological conditions (Yuan et al., 2016). We measured branch morphologies of all 180 and 261 branches ~~of~~at experimental shrubs of *C. korshinskii* and *S. psammophila*, respectively~~. Branch basal~~, including BD (Basal diameter~~ (BD) was measured~~, mm) with a Vernier calliper (Model 7D-01150, Forgestar Inc., Germany~~). Branch~~), branch length (BL~~) and branch angle (BA) were estimated~~, cm) with a measuring tape, and branch angle (BA, °) with pocket geologic compass (Model DQL-8, Harbin Optical Instrument Factory, China), respectively. ~~Then, the branches were grouped into five~~Thus, BD categories ~~of~~were determined at 5–10 mm, 10–15 mm, 15–18 mm, 18–25 mm and >25 mm~~. Two~~ to guarantee the appropriate branch amounts within categories for meeting the statistical significance. Two representative branches with median BDs were selected in each category for stemflow recording. ~~These~~The experimental branches had no intercrossing with neighbouring ~~branches~~ones and no turning point in height from branch tip to base. The outlayer-of-canopy~~-skirt locations~~ positions avoided over-shading by the upper layer branches and permitted convenient measurements. Since ~~there were not sufficient~~the qualified branch with the >25-mm ~~branches~~size was not enough for ~~the~~ *C. korshinskii* ~~shrubs~~ and the ~~tipping-bucket rain gauges~~TBRG malfunctioned at the 15–18~~–25~~-mm branches of *S. psammophila*, stemflow data were not available in these BD categories. In total, ~~stemflow was automatically recorded at~~ 7 branches ~~for~~ were selected for stemflow measurements at each species (Table 1). As the important interface to intercept rains at the growing season, the well-verified allometric growth equations were performed to estimate the branch leaf area (LA, cm^2) of *C korshinskii* (LA=39.37×BD$^{1.63}$ R^2=0.98) (Yuan et al., 2017) and *S. psammophila* (LA=18.86×BD$^{1.74}$ R^2=0.90) (Yuan et al., 2016), respectively.

2.4 Stemflow measurements and calculations

~~We~~ A total of 14 TBRGs had been applied to automatically record the branch stemflow production of *C. korshinskii* and *S. psammophila*. The data of stemflow volume and timing were automatically recorded at dynamic intervals between neighboring tips. We installed aluminium foil collars to trap stemflow~~.~~ at branches nearly 40 cm off the ground, higher than TBRG orifice with height of 25.7 cm (Fig. 1). They were fitted around the entire branch circumference and sealed by neutral silicone caulking. The limited ~~external~~orifice diameter of ~~the~~ foil collars minimized the accessing of throughfall and rains ~~accessing~~into them~~. The RG3-M tipping-bucket rain gauges recorded the stemflow production and timing, thus computing the stemflow volume, duration, intensity and time lags to rain.~~ (Yuan et al., 2017). The 0.5-cm-diameter polyvinyl chloride hoses hung vertically and channelled stemflow from the collars to TBRGs with a minimum travel time. TBRGs were covered with the polyethylene ~~film-covered gauges preventing~~ films to prevent the accessing of throughfall and splash (Fig. ~~1). The hoses hung vertically to minimize the travel time to the rain gauges for an accurate recording of stemflow timing and intensity.~~1). These apparatuses were periodically checked ~~to avoid~~against leakages or blockages by insects and fallen leaves.

~~The stemflow~~ Stemflow variables ~~at the branches of C.~~ were computed ~~*korshinskii* and *S. psammophila* were calculated~~ as ~~follows~~follow.

(1) Stemflow volume (SFV, mL): the average stemflow volume of individual branches ~~of C.~~. Adjusted with Equation 4 firstly, SFV ~~*korshinskii* and *S. psammophila*. This variable~~ was ~~converted from~~computed with the ~~auto-~~TBRG recordings ~~of branch stemflow via the tipping-bucket rain gauges (~~(SF_{RG}, mm) by multiplying ~~the base~~its orifice area ~~of the RG3-M rain gauges (182~~(186.3 cm^2) (Equation 10).

$$SFV = SF_{RG} \times 18.63 \qquad (10)$$

(2) Stemflow intensity ~~(mm·h^{-1}):~~: the branch stemflow volume ~~in a certain time, including SFI, SFI$_{10}$~~ per branch basal area per unit time. SFI (mm·h^{-1}) is the average stemflow intensity of incident rains, which is computed by the event-based SFV (mL), branch basal area (BBA, mm^2) and RD (h) (Equation 11) (Herwitz, 1986; Spencer and Meerveld, 2016). SFI_{10} (mm·h^{-1}) is the 10-min

maximum stemflow intensity, which is calculated with the 10-min maximum stemflow volume (SFV_{10}, mL) and BBA (mm^2) (Equation 12). SFI_i ~~in this study. SFI and SFI10 are the average and 10-min maximum stemflow intensities during incident rains, which were computed by the branch stemflow as recorded by the tipping bucket rain gauges (mm) and rainfall duration (h). SFIi~~($mm \cdot h^{-1}$) is the instantaneous stemflow intensity, which ~~was~~is calculated ~~in terms of~~by the tip volume of ~~the RG3-M rain gauge (0.2 mm~~TBRG (3.73 mL), BBA (mm^2) and time intervals between neighbouring tips (t_i, h) (Equation 13). The comparison between SFI_i and the corresponding rainfall intensity depicted the synchronicity of stemflow with rains within event.

$$SFI = 1000 \times SFV / (BBA \times RD) \qquad (11)$$

$$SFI_{10} = 6000 \times SFV_{10} / BBA \qquad (12)$$

$$SFI_i = 3730 / (BBA \times t_i) \qquad (13)$$

(3) Stemflow temporal dynamics: stemflow duration and time lags ~~in response~~ to rains.

SFD (h): ~~the duration from~~ stemflow ~~beginning to its ending~~duration. It is computed by different timings between the first- and last-tips of stemflow via TBRG.

TLG (min): time lag of stemflow generation ~~to~~after rain begins. It is computed by different first-tip timings between rainfall ~~beginning~~and stemflow via TBRG.

TLM (min): time lag of stemflow ~~intensity peak to~~ maximization after rain begins. It is computed by different timings between the largest-SFI_i and first-rainfall ~~beginning~~tips via TBRG.

TLE (min): time lag of stemflow ending ~~to rainfall ceasing~~after rain ceases. It is computed by different last-tip timings between rainfall and stemflow via TBRG.

(4) ~~Ratio~~Funnelling ratio: the efficiency for capturing and delivering raindrops from the canopies to trunk/branch base (Siegert and Levia, 2014; Cayuela et al., 2018). By introducing RD at both numerator and denominator of the ~~intra-event stemflow intensity (RSFI,~~ original equation (Herwitz, 1986), FR (unitless~~):~~) was transformed as the ratio between stemflow ~~intensity~~ and rainfall ~~intensity at 100-s intervals~~ intensities at the event base (Equation 14). FR_{100} described the within~~events. Similar to the~~ -event funnelling ratio ~~(unitless) at the event scale (Herwitz, 1986; Siegert and Levia, 2014), the RSFI quantifies the convergence effect of stemflow by comparing stemflow intensity with rainfall intensity at a high temporal resolution (100 s) within events.~~at the 100-s interval after rain began (Equation 15).

~~We calculated stemflow volume, intensity and temporal dynamics for 54 rainfall events during the experimental period. While representative rains had RAs of 5–10 mm, 10–20 mm and >20 mm, RSFI was compared during events to illustrate the fluctuating convergence effects of stemflow. The comparison between SFI~~$_i$ ~~and rainfall intensity depicted the synchronicity between stemflow and rains.~~

$$FR = 1000 \times \frac{SFV}{BBA \times RA} = 1000 \times \frac{\frac{SFV}{BBA} / RD}{RA / RD} = \frac{SFI}{I} \qquad (14)$$

$$FR_{100_i} = {SFI_{100_i}}/{I_{100_i}} \qquad (15)$$

where SFV is branch stemflow volume (mL); RA is rainfall amount (mm); BBA is branch basal diameter (mm^2); RD is rainfall duration (h); SFI and I were stemflow and rainfall intensities (mm·h^{-1}), respectively; FR_{100i} is funnelling ratio at the number *i* interval of 100 s after rain begins.

2.5 Data analysis

~~The stemflow~~Stemflow variables were averaged ~~among~~at different BD categories to analyse the ~~influences of~~ most influential rainfall characteristics ~~on~~affecting them. ~~The~~ Pearson correlation analyses ~~tested~~were firstly performed to test the relationships between rainfall characteristics ~~and stemflow variables. This analysis includes the intra-event rainfall characteristics (~~(RA, RD, RI, I, I_{10}, I_{b10}, I_{e10}, F, F_{10}, F_{b10}~~ and~~, F_{e10}~~) and stemflow variables (SFI, SFI_{10}, TLG, TLM and TLE), and the inter-event rainfall characteristics (RA, RD and RI~~ and E) and stemflow variables (SFV, SFI, SFI_{10}, FR, TLG, TLM, TLE and SFD). The significantly related factors were grouped ~~according to the~~ in terms of median value~~. These factors were then~~ , and compiled into indicator matrices~~ and~~. They were standardized for a cross-tabulation check as required by ~~a~~the multiple correspondence analysis (MCA) (Levia et al., 2010; ~~Van~~van Stan et al., 2011, 2016). All qualified data were restructured into orthogonal dimensions (Hair et al., 1995), where distances between row and column points were maximized (Hill and Lewicki, 2007). As shown ~~in the~~at correspondence maps, ~~rainfall feature~~ the clustering ~~is~~rainfall characteristics tightly related to the centred stemflow variable. ~~The~~ Finally, stepwise regressions were operated to identify the most influential rainfall ~~factor could then be identified with stepwise~~

~~regression~~characteristics (Carlyle-Moses and Schooling, 2015). ~~We built regression models~~The quantitative relations were established in terms of the qualified level of significance (p <0.05) and the highest coefficient of determination (R^2). One-way analysis of variance (ANOVA) with LSD post hoc test was used to determine whether rainfall characteristics， and stemflow variables significantly differed among event categories, and whether funnelling ratio and stemflow intensity significantly differed among BD categories for *C. korshinskii* and *S. psammophila*. The level of significance was set at 95% confidence interval (p=0.05). SPSS 21.0 (IBM Corporation, USA), Origin 8.5 (OriginLab Corporation, USA) and Excel 2019 (Microsoft Corporation, USA) were used for data analysis.

3 Results

3.1 Rainfall characteristics

~~Stemflow was automatically recorded for 54 rainfall events during the experimental period (Fig. 2). There were~~ A total of 20, 8, 10, 8, 4 and 4 rainfall events were recorded in the RA categories of ≤2 mm, 2–5 mm, 5–10 mm, 10–15 mm, 15–20 mm and >20 mm, respectively. The ~~corresponding~~ total RAs ~~of the above five rainfall~~at these categories were 22.1 mm, 26.1 mm, 68.8 mm, 93.3 mm, 74.8 mm and 110.0 mm, respectively. ~~The~~ During these events, the average I, I_{10}, I_{b10} and I_{e10} ~~of the 54 rainfall events~~ were 4.~~6~~5±1.0 mm·h^{-1}, ~~11.5~~10.9±2.1 mm·h^{-1}, 5.~~8~~5±1.~~5~~4 mm·h^{-1} and 2.~~9~~8±0.7 mm·h^{-1}, respectively. The average F, F_{10}, F_{b10} and F_{e10} were 16.~~3±8.7~~1±1.2 mg·m·s^{-1}, ~~25.7±~~24.9~~.6~~±1.4 mg·m·s^{-1}, 18.~~5±9.9~~4±1.4 mg·m·s^{-1} and ~~15.8±7~~16.0±1.0 mg·m·s^{-1}, respectively. RD, RI and R~~I~~E averaged 4.~~9~~7±0.8 h ~~and~~, 50.~~9~~6±6.1 h, and 0.9±0.2, respectively~~.~~ (Table 2).

Rainfall events were further categorized in terms of rainfall-intensity peak amount, including Events A~~, B and C, with~~ (the single~~,~~-peak events), B (the double-peak events) and C (the multiple~~-peaks (~~-peak events). There were 17, 11 and 15 events at Event A, B and C, respectively~~) (Table 2). The~~. Because the remaining 11 events had the average RA of 0.6 mm, no more than three recordings had been observed within event which was limited by 0.2-mm resolution of TBRGs. Therefore, they could not be categorized ~~due to less than three intra-event recordings.~~and grouped as Event others (Table 2). Compared with Events A and B, Event C possessed significantly different rainfall characteristics, e.g., ~~a~~the significantly larger RA (11.7 vs. 4.1 and 5.2 mm) and RD (10.3 vs. 2.5 and 3.6 h) but ~~a~~the significantly smaller I_{10} (9.5 vs. 15.5 and 12.7 mm·h^{-1}), I_{b10} (2.8 vs. 7.7 and 9.9 mm·h^{-1}), ~~I_{e10} (2.1 vs. 4.3 and 3.6 mm·h^{-1}), F_{10} (24.2 vs. 27.8 and 26.6 mg·m·s^{-1}),~~ F_{b10} (15.4 vs. 19.7 and 21.7 mg·m·s^{-1}) and F_{e10} (13.4 vs. 17.3 and 16.6 mg·m·s^{-1}), the non-significantly smaller I_{e10} (2.1 vs. 4.3 and 3.6 mm·h^{-1}), F_{10} (24.2 vs. 27.8 and 26.6 mg·m·s^{-1}~~,~~) and E (0.4 vs. 0.9 and 1.0), respectively~~)~~ (Table 2).

In general, ~~the~~rainfall events were ~~skewed in their distributions~~skewedly distributed in terms of RA~~ during the experimental period~~. The occurrences of events with a RA≤2 mm dominated the experimental period (40.7%), but the events with ~~RAs~~RA>20 mm were the greatest contributor to the total RA (28.0%). However, a relatively equal distribution was noted during events with single (17 events), double (11 events) and multiple (15 events) rainfall-intensity peaks. ~~In contrast~~Comparatively, the multiple-~~intensity ~~peak events had significantly larger rainfall amounts, durations, intensities and raindrop momentums~~ (Table 2). Therefore, grouping events in terms of rainfall-intensity peak amounts was justified~~.

3.2 Stemflow volume, intensity, funnelling ratio and temporal dynamics

~~The stemflow~~Stemflow variables of *C. korshinskii* and *S. psammophila* showed great inter-event variations during the experimental period (Fig. 3). *C. korshinskii* had larger SFV, SFI, SFI_{10}, FR, SFD, TLG and TLE (~~1658~~226.6±46.4~~±320.9~~ mL, ~~20.3±10.4~~517.5±82.1 mm·h^{-1}, 2057.6±399.7 mm·h^{-1}, 130.7±8.2, 3.8±0.8 h, 66.2±10.6 min and 20.0±5.3 min, respectively) but ~~significantly~~ smaller TLM (109.4±20.5 min) ~~and slightly smaller SFI (4.7±1.5 mm·h^{-1})~~ than those of *S. psammophila* (~~1014.0±174~~172.1±34.5 mL, ~~16.9±8.8~~367.3±91.1 mm·h^{-1}, 1132.2±214.3 mm·h^{-1}, 101.6±10.4, 3.4±0.9 h, 54.8±11.7 min, 13.5±17.2 min, and 120.5±22.1 min, ~~4.8±1.6 mm·h^{-1},~~ respectively) (Table 3). ~~The positive TLG, TLE~~During the 54 events, no negative values were observed for TLG and TLM but TLE. It indicated that ~~both species~~stemflow generally ~~started,~~ initiated and maximized ~~and~~ after rains started for both species. However, stemflow might be ended before (negative TLE) and after (positive TLE) rains ceased ~~stemflow later than the rains~~.

~~As shown in Fig. 4, stemflow was~~ Stemflow well synchronized to rains with similar intensity peak shapes, amounts and positions for ~~the two~~both species. ~~This result was~~ These results were vividly demonstrated ~~during~~at representative ~~events~~rains with different intensity peak amounts and RAs, including ~~the rainfall~~ events on July 17, 2015 (Event A, 20.7 mm~~, Event A), on~~), July 29, 2015 (~~7.3 mm,~~ Event B, 7.3 mm), and ~~on~~ September 10, 2015 (Event C, 13.3 mm~~, Event C). For these three events,~~) (Fig. 4). *C. korshinskii* had larger ~~RSFIs (2,~~ FR_{100} (91.7, 76.1~~.8~~ and ~~2.1~~94.0, respectively) than those of *S. psammophila* (~~1.4, 0.9~~32.8, 26.3 and ~~1.4~~43.7, respectively~~). Comparatively, the RSFI~~) during representative events. It indicated a comparatively greater ability of ~~*S. psammophila* fluctuated more dramatically around the value of 1.~~ converging rains for *C. korshinskii* within event.

Stemflow variables varied between rainfall event categories~~ (Table 3)~~. For Event C in comparison to Events A and B, *S. psammophila* had significantly larger SFV (~~2469.0~~435.2 vs. ~~616.5~~102.6 and ~~907.0~~145.7 mL), SFD (8.~~2~~3 vs. 1.2 and 3.4 h), TLM (235.8 vs. 64.3 and 93.4 min~~) and~~), FR (129.1 vs. 77.1 and 91.4), non-significantly larger TLE (20.8 vs. 17.1 and 8.6 min) but significantly smaller SFI (~~2.4~~246.6 vs. ~~7.2~~648.1 and ~~6.0~~421.5 mm·h^{-1}) and SFI$_{10}$ (~~8.8~~888.4 vs. ~~24.8~~1672.7 and ~~24.5~~1582.8 mm·h^{-1}~~;~~), respectively~~). For Event C in comparison to~~ (Table 3). SFI decreased at events with increasing intensity peak amounts as shown at Events A~~ and B,~~ C. The drop of SFI was offset by the decreasing I to some extent (Table 2), which might partly explain the increasing trend of FR from Event A to C. *C. korshinskii* shared similar changing trends ~~for its~~of stemflow variables between event categories with those of *S. psammophila*, except for the ~~slightly~~non-significantly smaller TLE (18.5 ~~vs.~~ min) at Event C in contrast to TLE at Event A and B (22.3 ~~and 18~~and18.7 min~~)~~).

Funnelling ratio and ~~SFI (5.1 vs. 5.7~~ stemflow intensity negatively related with branch size. *C. korshinskii* and ~~6.0~~*S. psammophila* had significantly greater FR, SFI, and SFI$_{10}$ at the 5–10 mm~~·h~~$^{-1}$ branches than those at the larger branches (Table 4). For *C. korshinskii*, FR decreased from 163.7±12.2 at the 5–10-mm branches to 97.7±9.2 at the 18–25-mm branches, respectively~~)~~. It was consistent with decreasing SFI (333.8–716.2 mm·h^{-1}) at the corresponding BD categories (Table 4). As branch size increased, *S. psammophila* shared similar decreasing trends of FR (44.2–212.0) and SFI (197.2–738.7 mm·h^{-1}), respectively.

3.3 Relationships between stemflow variables and rainfall characteristics

~~Correspondence had been established~~*C. korshinskii* and *S. psammophila* had similar correspondence patterns between rainfall characteristics and stemflow variables~~ for *C. korshinskii* and *S. psammophila* (Fig. 5). These two species had similar correspondence patterns.~~. As shown in Fig. 5, the one-to-one correspondences were observed for SFV~~, SFD~~ and TLE. The larger (or smaller) SFV~~, SFD~~ and TLE corresponded to the larger (or smaller) RA~~, RD~~ and RI, respectively. This result ~~clearly~~ demonstrated the dominant influences of RA~~, RD~~ and RI on SFV~~, SFD~~ and TLE, respectively. ~~Nevertheless,~~The one-to-two correspondences was noted for SFD with RD and E. The larger (or smaller) SFD corresponded to the larger (or smaller) RD and smaller (or larger) E. RA had been identified as the dominant rainfall characteristic affecting FR based on the analysis for 53 branches of *C. korshinskii* and 98 branches of *S. psammophila* at the same plots during the same experimental period (Yuan et al., 2017). It seemed that event-based stemflow production (the volume, duration and efficiency) were strongly influenced by rainfall characteristics at inter-event scale (the rainfall amount and duration).

The one-to-more correspondences were ~~noted~~observed for TLM, TLG, SFI and SFI_{10}. The larger (or smaller) TLM ~~and TLG were, the smaller SFI and SFI_{10} were, and all~~ corresponded to the smaller (or larger) rainfall characteristics of I, I_{10}, I_{b10}, I_{e10}, F, F_{10}, F_{b10} and F_{e10}. ~~In contrast, the~~T he same correspondences were applied to the larger (or smaller ~~TLM~~) TLG, and ~~TLG were,~~ the smaller (or larger) SFI and SFI_{10}~~ were, and all corresponded to the larger rainfall characteristics of I, I_{10}, I_{b10}, I_{e10}, F, F_{10}, F_{b10} and F_{e10}. This result indicated~~. It seemed that the within-event stemflow processes (SFI, SFI_{10}, TLG and TLM) were strongly affected by rainfall characteristics at intra-event scale (the rainfall intensity and raindrop momentum~~. The~~). Therefore, these results indicated that rainfall characteristics influenced~~ the~~ stemflow variables at the corresponding temporal scales. This influence occurred at the inter-event scale between SFV and RA, FR and RA, SFD and RD, ~~while this influence occurred~~and at the intra-event scale for stemflow time lags (TLG and TLM) and intensities (SFI and SFI_{10}) with rainfall intensity (I, I_{10}, I_{b10} and I_{e10}) and raindrop momentum (F, F_{10}, F_{b10} and F_{e10}). The only exception ~~of mismatched temporal sales~~ was noted between TLE and RI for the mismatched temporal sales.

~~To identify~~Stepwise regression analysis identified the most influential rainfall characteristics affecting stemflow intensities and ~~time lags, stepwise regression~~ temporal dynamics. RD was ~~performed and indicated that~~the dominant rainfall characteristics affecting SFD. I_{10} significantly affected the TLM of the both ~~shrub~~ species. For *C. korshinskii*, I, I_{10} and F were the most influential factors on SFI, SFI_{10} and TLG, respectively. However, for *S. psammophila*, F, F_{10} and F_{b10} significantly affected SFI, SFI_{10} and TLG, respectively. ~~There~~The results of multiple regression analysises indicated that there were linear relationships between SFI and I (R^2=0.~~85~~74, p<0.01) and SFI_{10} and I_{10} (R^2=0.~~90~~85, p~~-~~<0.01) for *C. korshinskii* and between SFD and RD for *C. korshinskii* (R^2=0.95, p<0.01) and *S. psammophila* (R^2=0.92, p<0.01) (Fig. 6). Moreover, power functional relations were found between SFI and F (R^2=0.82, p<0.01), SFI_{10} and F_{10} (R^2=0.90, p<0.01) (Fig. 6), TLG and F_{b10} (R^2=0.55, p<0.01) and TLM and I_{10} (R^2=0.40, p<0.01) (Fig. 7) for *S. psammophila*, and TLG and F (R^2=0.56, p <0.01) and TLM and I_{10} (R^2=0.38, p<0.01) (Fig. 7) for *C. korshinskii*. However, there was no significant quantitative relationship between TLE and RI for *C. korshinskii* (R^2=0.005, p=0.28) or *S.*

psammophila (R^2=0.002, p=0.78) (Fig. 7).

4 Discussion

4.1 Stemflow intensity and funnelling ratio

Stemflow intensity is generally greater than rainfall intensity ~~for~~at different plant life forms. The xerophytic shrubs of *C. korshinskii* and *S. psammophila* had larger average stemflow intensities than the average rainfall intensity (~~4.7±1~~517.5 and ~~4.8±1.6~~367.3 mm·h^{-1}~~, respectively,~~ vs. 4.5~~±1.0~~ mm·h^{-1}~~) in this study.~~). Broadleaf and coniferous species (*Quercus pubescens* Willd. and *Pinus sylvestris* L., respectively) also have larger ~~average~~ maximum stemflow intensities than the maximum rainfall intensity in north-eastern Spain (Cayuela et al., 2018). The gap between stemflow and rainfall ~~intensity~~intensities generally increased as the recording time intervals decreased. While recording at the 1-h intervals, approximately 20-, 17-, 13- and 2.5-fold greater peak stemflow intensities had been observed for trees of Cedar, Birch, Douglas Fir and Hemlock, respectively, at the coastal British Columbia forest (Spencer and Meerveld, 2016). For *C. korshinskii* and *S. psammophila*, in comparison to I_{10} (10.9~~±2.1~~ mm·h^{-1}) at 10-min intervals, the SFI_{10} (~~20.3±10.4~~2057.6 and ~~16.9±8.8~~1132.2 mm·h^{-1}, respectively) was ~~1.5-fold greater. When recorded at 5-min intervals, SFI~~$_5$ ~~(1232 mm·h~~$^{-1}$~~) is as much as 15~~over 103.9-fold greater~~-~~. The recordings at 6-min interval indicated a 157-fold larger of stemflow intensity (18840 mm·h^{-1}) than rainfall intensity (120 mm·h^{-1}) in the ~~open~~cyclone-prone tropical rainforest ~~of Brazil (Germer et al., 2010).~~with extremely high MAP of 6570 mm (Herwitz, 1986). While calculating the dynamic time interval between neighbouring tips of ~~the tipping-bucket rain gauges~~TBRG, SFI_i (~~240~~10816.2 mm·h^{-1}) was ~~3.3~~150.2-fold greater than the corresponding rainfall intensity (72 mm·h^{-1}). Therefore, stemflow recorded at a higher temporal resolution ~~provided~~might provide more information into the dynamic nature of stemflow and real-time responses to rainfall characteristics within events.

Greater stemflow intensity than rainfall intensity is hydrologically significant ~~in~~at terrestrial ecosystems. This scenario indicates the convergence of the canopy-intercepted rains into the limited area around ~~the~~ trunk or branch bases within a certain time period~~.~~ ~~The funnelling ratio~~, i.e., 8.0% and 3.5% of rains being directed to the trunk base only accounting for 0.3% and 0.4% of plot area in the open rainforest (Germer et al., 2010) and undisturbed lowland tropical rainforest (Manfroi et al., 2004), respectively. Besides, FR, which ~~quantifies the efficiency of individual plants in capturing and delivering raindrops~~compared SFV with RA that would have been collected at the same area as the basal area at an event scale (~~Siegert and Levia, 2014~~Herwitz, 1986), is commonly applied to assess the convergence effect ~~(Herwitz, 1986; Wang et al., 2013~~via stemflow volume, rainfall amount and basal area (Carlyle-Moses et al., 2010; Siegert and Levia, 2014; Fan et al., 2015~~).~~; Yang et al., 2019). If ~~the funnelling ratio~~FR is greater than 1, ~~then~~ more water is collected at the trunk or branch base than at the clearings ~~during incident rains.~~. Both methods successfully quantified the convergence effects of stemflow. However, the ~~process~~former provided a possibility to assess ~~the convergence effect of stemflow~~ it at high temporal resolutions within ~~events has still not been adequately studied~~event.

~~RSFI depicted the intra-event convergence effects of stemflow by comparing stemflow and rainfall intensities at 100 s intervals starting from the beginning to the ending of incident rains. We found that RSFI fluctuated around the value of 1 for both shrub species~~

~~(Fig. 4). The RSFI was generally greater than 1 for *C. korshinskii*, whereas the RSFI for *S. psammophila* fluctuated more dramatically. This result indicated that comparatively more rainwater was delivered within a short period to the branch base of *C. korshinskii* during the rain process. This result agreed with the results of reports related to the more efficient stemflow production of *C. korshinskii* at the event scale, as expressed by its larger stemflow productivity (1.95 mL·g^{-1}) and funnelling ratio (173.3) than those of *S. psammophila* (1.19 mL·g^{-1} and 69.3, respectively) (Yuan et al., 2017). Therefore, RSFI demonstrated the process-based estimation of stemflow efficiency. Carlyle-Moses et al. (2018) have addressed the importance of studying stemflow convergence effects by employing the funnelling ratio at the stand scale. We highly recommended that future studies evaluate convergence effects during rain events by combining the results of the funnelling ratio and RSFI.~~

This study established the quantitative connection between FR and stemflow intensity for the first time. As per Equation 14 and the average stemflow and rainfall intensities listed at Table 2 and 3, FR could be estimated to be 115.0 and 81.6 for *C. korshinskii* and *S. psammophila*, respectively. Those results approximately agreed with FR of 173.3 and 69.3 (Yuan et al., 2017) and 124.9 and 78.2 (Yang et al., 2019) for the two species by applying the traditional calculation based on SFV and RA (Herwitz, 1986). As branch size increased, FR of *C. korshinskii* decreased from 163.7 at the 5–10-mm branches to 97.7 at the 18–25-branches. The decreasing trend of FR of *S. psammophila* were also noted in the range of 44.2–212.0 with increasing BD. The negative relation between BD and FR agreed with the reports for trees and babassu palms in an open tropical rainforest in Brazil (Germer et al., 2010), the mixed-species coastal forest at British Columbia of Canada (Spencer and Meerveld, 2016), for trees (*Pinus tabuliformis* and *Armeniaca vulgaris*) and shrubs (*C. korshinskii* and *S. psammophila*) on the Loess Plateau of China (Yang et al., 2019). It might be partly explained by the decreasing stemflow intensities with increasing branch size as per Equation 14. Our results found that SFI decreased from 716.2 to 333.8 for *C. korshinskii*, and 738.7 to 197.2 for *S. psammophila* as branch size increased (Table 4). It well justified the importance of branch size on stemflow intensity. Associated with the infiltration rate, the stemflow-induced hydrological process might be strongly affected, i.e., soil moisture recharge, Hortonian overland flow (Herwitz, 1986), Saturation overland flow (Germer et al., 2010), soil erosion (Liang et al., 2011), nutrient leaching (Corti et al., 2019), etc. Therefore, more attention should be paid to tree/branch size and size-related stand age at future studies while modeling the stemflow-induced terrestrial hydrological fluxes.

The importance had been addressed to study the funnelling ratio at the stand scale (Carlyle-Moses et al., 2018); however, it had not been adequately studied at the intra-event scale. This study calculated the average funnelling ratio at the event base and the 100-s intervals after rain began. Thus, the convergence effect of stemflow could be better understood at the inter-/intra-event scales. Our results found that FR_{100} were over 1.8-fold greater than FR of *C. korshinskii* (282.7 vs. 130.7) and *S. psammophila* (203.4 vs. 101.6), respectively. It indicated that funnelling ratio fluctuated dramatically within event. Therefore, computing FR at event and ignoring it at high temporal resolutions within event might underestimate the eco-hydrological significance of stemflow.

In general, stemflow intensity highly related to funnelling ratio. For addressing its eco-hydrological importance, stemflow intensity should be precisely defined. It had been expressed as the stemflow volume per basal area of branches/trunks per unit time with the unit of mm·h^{-1} (Herwitz, 1986; Spencer and Meerveld, 2016) and mm·5 min^{-1} (Cayuela et al., 2018). However, stemflow intensity had also been described as stemflow volume per unit time with the unit of L·week^{-1} (Schimmack et al., 1993) and L·h^{-1} (Liang et al., 2011; Germer et al., 2013). We highly recommended the former definition. Because of its highly spatial-related (Herwitz, 1986; Liang et al., 2011; 2014), the eco-hydrological significance of stemflow would be underestimated by ignoring the basal area, over which stemflow was received. Moreover, as per this definition, stemflow intensity quantitively connected with funnelling ratio via Equation 14. Thus, funnelling ratio could be used to assess the convergence effect of stemflow at both inter- and intra-event scales.

4.2 Stemflow temporal dynamics

Stemflow ~~was~~ well synchronized to the rains. ~~This result~~It agreed with ~~those~~the report of Levia et al. (2010), who demonstrated a marked synchronicity between ~~stemflow volume~~SFV and RA in 5-min intervals for *Fagus. grandifolia*. The duration and time lags to rains were critical to describe stemflow temporal dynamics. Our results indicated that in comparison to *S. psammophila*, *C. korshinskii* takes a longer time to initiate (66.2 vs. 54.8 min), end (20.0 vs. 13.5 min) and produce stemflow (3.8 vs. 3.4 h) but a shorter time to maximize stemflow (109.4 vs. 120.5 min, respectively). Moreover, the TLMs of both ~~shrub~~ species were in the range of the TLMs for *S. psammophila* (20–210 min) in the Mu Us desert of China (Yang, 2010).

Varying TLGs were documented for different species. Approximately 15 min, 1 h and

1.5 h ~~are~~were needed to initiate the stemflow of palms (Germer, 2010), pine trees and oak trees (Cayuela et al., 2018), respectively. In addition, an almost instantaneous start of stemflow ~~has~~had also been observed as rain began for *Quercus rubra* (Durocher, 1990), *Fagus grandifolia* and *Liriodendron tulipifera* (Levia et al., 2010). ~~In contrast~~Compared to the positive TLE dominating xerophytic shrubs, the TLE greatly ~~varies~~varied with tree species. TLE ~~is~~was as much as 48 h for Douglas fir, oak and redwood in California, USA (Reid and Levia, 2009), and almost 11 h for palm trees in Brazil (Germer, 2010). However, for sweet chestnut and oak, almost no stemflow ~~continues~~continued when rains ~~cease~~ceased in Bristol, England (Durocher, 1990). These scenarios might occur due to the sponge effect of the canopy surface (Germer, 2010), which ~~buffers~~buffered stemflow generation, maximization and cessation before saturation. These conclusions were consistent with the smaller stemflow intensities of *C. korshinskii* and *S. psammophila* than the rainfall intensity when rain began, as part of the rains was used to wet canopies (Fig. 4). The hydrophobic bark traits ~~benefit~~benefited stemflow initiation with the limited time lags to rains. In contrast, the hydrophilic bark traits ~~are~~were conducive for continuing stemflow after rain ~~stops~~ceased, which ~~keep~~kept the preferential flow paths wetter for longer time periods (Levia and Germer, 2015). As a result, it ~~takes~~took time to transfer intercepted rains from the leaf, branch and trunk to the base. This process strongly affects the stemflow volume, intensity and loss as evaporation.

The dynamics of intra-event rainfall intensity ~~complicates~~complicated the stemflow time lags to rains. A 1-h lag to begin and stop stemflow with the beginning and ending of rains ~~was~~had been observed for ashe juniper trees during high-intensity events, but no stemflow was generated at low-intensity storms (Owens et al., 2006). Rainfall intensity was an important dynamic rainfall characteristic affecting stemflow volume. Owens et al. (2006) found the most significant difference between various rainfall intensities located in the stemflow patterns other than throughfall and interception loss. During events with a front-positioned, single rainfall-intensity peak, *S. psammophila* maximized stemflow in a shorter time than *C. korshinskii* did in the Mu Us desert (30 and 50 min) (Yang, 2010). ~~During these events, a smaller SFD (1.5 h) and a larger TLE (55.8 min) and SFI (11.5 mm·h^{-1}) were also observed for *C. korshinskii* than for *S. psammophila* in this study. This result~~These results highlighted the amounts and occurrence time of rainfall-intensity peak affecting the stemflow process, which was consistent with the finding of Dunkerley (~~2014~~2014b).

Raindrops presented rainfall characteristics at finer temporal-spatial scales. They ~~are~~were usually ignored because rains were generally regarded as a continuum rather than a discrete process consisting of individual raindrops of various sizes, velocities, inclination angles and kinetic energies. Raindrops hit the canopy surface and ~~create~~created splashes at different canopy layers (Bassette and Bussière, 2008; Li et al., 2016). This process ~~accelerates~~accelerated canopy wetting and ~~increases the~~increased water supply for stemflow production. Therefore, raindrop momentum was introduced in this study to represent the comprehensive effects of raindrop attributes. Our results indicated that raindrop momentum was sensitive to predicting the variations in stemflow intensity and temporal dynamics with significant linear or power functional relations (Figs. 6 and 7). Compared with the importance of rainfall intensity for *C. korshinskii*, raindrop momentum more significantly affected the stemflow process of *S. psammophila.* This result might be related to the larger canopy size and height of *S. psammophila* (21.4±5.2 m^2 and 3.5±0.2 m) than that of *C. korshinskii* (5.1±0.3 m^2 and 2.1±0.2 m, respectively). ~~Thus, more~~More layers ~~are~~were available within canopies of *S. psammophila* to intercept the splashes created by raindrop striking (Bassette and Bussière, 2008; Li et al., 2016), thus shortening the paths and having more water supply for stemflow production.

4.3 Temporal-dependent influence of rainfall characteristics

This study discussed stemflow variables and rainfall characteristics at ~~different temporal scales. Stemflow variables were further categorized into volume, intensity and temporal dynamics. The last two variables depicted the stemflow process with a high temporal resolution. The influences of rainfall characteristics were explored at a fine temporal scale by introducing raindrop momentum, rainfall-intensity peak amounts and intra-event positions.~~inter-/intra-event scales. We found that rainfall characteristics affected stemflow variables at the corresponding temporal scales. RA and RD controlled SFV, FR and SFD, respectively, at the inter-event scale. However, stemflow intensity (e.g., SFI and SFI_{10}) and temporal dynamics (e.g., TLG and TLM) were strongly influenced by rainfall intensity (e.g., I, I_{10} and I_{b10}) and raindrop momentum (e.g., F, F_{10} and F_{b10}) at the intra-event scales. These results were verified by the well-fitting linear or power functional equations among them (Figs. 6 and 7). Furthermore, the influences of rainfall intensity and raindrop momentum on stemflow process were species-specific. In contrast to the significance of rainfall intensity on the stemflow process of *C. korshinskii*, raindrop momentum imposed a greater influence on the stemflow process of *S. psammophila*.

In general, rainfall characteristics had temporal-dependent influences on the corresponding stemflow variables. The only exception was found between TLE and RI. RI tightly corresponded to TLE for both species tested by the MCA, but there was no significant quantitative relationship between them (R^2=0.005, p=0.28 for *C. korshinskii*, and R^2=0.002, p=0.78 for *S. psammophila*). This result might be related to the mismatched temporal scales between TLE and RI. TLE represented stemflow temporal dynamics at the intra-event scale, while RI was the interval times between neighbouring rains at the inter-event scale. The mismatched temporal scales might also partly explain the long-standing debates on the controversial positive, negative and even no significant influences of rainfall intensity (depicting raining process at 5 min, 10 min, 60 min, etc.) on event-based stemflow volume (Owens et al., 2006; André et al., 2008; Zhang et al., 2015).

5 Conclusions

Stemflow intensity and temporal dynamics are important in depicting the stemflow process and its interactions with rainfall characteristics within events. We categorized stemflow variables into the volume, intensity, funnelling ratio and temporal dynamics, thus to representing the stemflow yield, efficiency and process. Funnelling ratio had been calculated as the ratio between stemflow and rainfall intensities for the first time. It enabled it to assess the convergence of stemflow at ~~different~~the inter-/intra-event scales. Over 1.8-fold greater FR_{100} were noted than FR at representative events for *C. korshinskii* and *S. psammophila*, respectively. The eco-hydrological significance of stemflow might be underestimated by ignoring stemflow production at high temporal ~~scales.~~resolutions within event. FR decreased with increasing branch size of both species. It could be partly explained by the decreasing trends of SFI as branch size increased. The influences of rainfall characteristics were quantified at a fine temporal scale by introducing SFI_i, ~~RSFI~~FR_{100}, raindrop momentum, rainfall-intensity peak amounts and intra-event positions. The results indicated that rainfall characteristics had temporal-dependent influences on stemflow variables. RA and RD controlled SFV, FR and SFD at the inter-event scale. Rainfall intensity and raindrop momentum significantly affected stemflow intensity and time lags to rains at the intra-event scale except for TLE. Although there was tight correspondence between TLE and RI by MCA, there was no significant quantitative relationship (R^2<0.005, p>0.28) due to the mismatched temporal scale between them. These findings advance our understanding of the stemflow process and its influential mechanism and help model the critical process-based hydrological fluxes of terrestrial ecosystems.

Data availability. The data collected in this study are available upon request to the authors.

Author contributions. GYG and CY set up the research goals and designed field experiments. CY measured and analyzed the data. GYG and BJF provided the financial support for the experiments, and supervised the execution. CY created the figures and wrote the original draft. GYG, BJF, DMH, XWD and XHW reviewed and edited the draft in serval rounds of revision.

Competing interests. The authors declare that they have no conflict of interest.

Acknowledgements. This research was sponsored by the National Natural Science Foundation of China (nos. 41390462~~ and~~, 41822103 and 41901038), the National Key Research and Development Program of China (no. 2016YFC0501602), the Chinese Academy of Sciences (no. QYZDY-SSW-DQC025), the Youth Innovation Promotion Association CAS (no. 2016040), and the China Postdoctoral Science Foundation (no. 2018M633427). We appreciate Prof. D. F. Levia in University of Delaware for reviewing and improving this manuscript. Thanks to Liwei Zhang for the catchment GIS mapping. Special thanks are given to Shenmu Erosion and Environment Research Station for experimental support to this research.

Appendix

List of symbols

Abbreviation	Descriptions	Unit
a.s.l.	above sea level	NA
BA	Branch angle	°
BBA	Branch basal area	mm^2
BD	Branch diameter	mm
BL	Branch length	cm
D	Diameter of rain drop	mm
e_s	Saturation vapor pressure	kPa
E	Evaporation coefficient	unitless
F	Average raindrop momentum in the vertical direction of incident event	$mg \cdot m \cdot s^{-1}$
F_0	Average raindrop momentum of incident event	$mg \cdot m \cdot s^{-1}$
F_{10}	The 10-min maximum raindrop momentum	$mg \cdot m \cdot s^{-1}$
F_{b10}	Average raindrop momentum at the first 10 min	$mg \cdot m \cdot s^{-1}$
F_{e10}	Average raindrop momentum at the last 10 min	$mg \cdot m \cdot s^{-1}$
FR	Average funnelling ratio of incident event	unitless
FR_{100}	Funnelling ratio at the 100-s intervals after rain begins	unitless
H	Air relative humidity	%
I	Average rainfall intensity of incident event	$mm \cdot h^{-1}$
I_{10}	The 10-min maximum rainfall intensity	$mm \cdot h^{-1}$
I_{b10}	Average rainfall intensity at the first 10-min of incident event	$mm \cdot h^{-1}$
I_{e10}	Average rainfall intensity at the last 10-min of incident event	$mm \cdot h^{-1}$

IW_A	The adjusted inflow water at TBRG	mm
IW_R	The recorded inflow water at TBRG	mm
LA	Leaf area of individual branch	cm^2
MAP	Mean annual precipitation	mm
MCA	Multiple correspondence analysis	NA
NA	Not applicable	NA
p	Level of significance	NA
R^2	Coefficient of determination	NA
RA	Rainfall amount	mm
RD	Rainfall duration	h
RI	Rainfall interval	h
SE	Standard error	NA
SFD	Stemflow duration from its beginning to ending	h
SFI	Average stemflow intensity of incident event	$mm \cdot h^{-1}$
SFI_{10}	The 10-min maximum stemflow intensity of incident event	$mm \cdot h^{-1}$
SFI_i	Instantaneous stemflow intensity	$mm \cdot h^{-1}$
SF_{RG}	Stemflow depth recorded by TBRG	mm
SFV	Stemflow volume	mL
t_i	Time intervals between neighboring tips	h
T	Air temperature	°C
TBRG	Tipping bucket rain gauge	NA
TLE	Time lag of stemflow ending to rainfall ceasing	min
TLG	Time lag of stemflow generation to rainfall beginning	min
TLM	Time lag of stemflow maximization to rainfall beginning	min
v	Terminal velocity of rain drop	$m \cdot s^{-1}$
VPD	Vapor pressure deficit	kPa
WS	Wind speed	$m \cdot s^{-1}$
ρ	Density of freshwater at standard atmospheric pressure and 20°C	$g \cdot cm^{-3}$
θ	Inclination angle of rain drop	°

References

André, F., Jonard, M. and Ponette, Q.: Influence of species and rain event characteristics on stemflow volume in a temperate mixed oak-beech stand, Hydrol. Process., 22, 4455–4466. https://doi.org/10.1002/hyp.7048, 2008.

Bassette, C. and Bussière, F.: Partitioning of splash and storage during raindrop impacts on banana leaves, Agr., Forest Meteorol., 148, 991–1004, https://doi.org/10.1016/j.agrformet.2008.01.016, 2008.

Bittar, T.B., Pound, P., Whitetree, A., Moore, L.D. and ~~Van~~van Stan John, T.: Estimation of throughfall and stemflow bacterial flux in a subtropical oak-cedar forest. Geophys. Res. Lett., 45, 1410–1418, https://doi.org/10.1002/2017GL075827, 2018.

Brandt, C.J.: Simulation of the size distribution and erosivity of raindrops and throughfall drops. Earth. Surf. Proc. Land., 15, 687–698, https://doi.org/10.1002/esp.3290150803, 1990.

Bundt, M., Widmer, F., Pesaro, M., Zeyer, J. and Blaser, P.: Preferential flow paths: biological 'hot spots' in soils. Soil. Biol. Biochem., 33, 729–738, https://doi.org/10.1016/S0038-0717(00)00218-2, 2001.

Carlyle-Moses, D.E., Iida, S.I., Germer, S., Llorens, P., Michalzik, B., Nanko, K., Tischer, A. and Levia, D.F.: Expressing stemflow commensurate with its ecohydrological importance, Adv. Water Resources, 121, 472–479, https://doi.org/10.1016/j.advwatres.2018.08.015, 2018.

Carlyle-Moses, D.E. and Price, A.G.: Growing-season stemflow production within a deciduous forest of southern Ontario, Hydrol. Process., 20, 3651–3663, https://doi.org/10.1002/hyp.6380, 2006.

Carlyle-Moses, D.E. and Schooling, J.: Tree traits and meteorological factors influencing the initiation and rate of stemflow from isolated deciduous trees, Hydrol. Process., 29, 4083–4099, https://doi.org/10.1002/hyp.10519, 2015.

Carlyle-Moses, D.E., Park, A.D. and Cameron, J.L.: Modelling rainfall interception loss in forest restoration trials in Panama, Ecohydrology, 3, 272–283, https://doi.org/10.1002/eco.105, 2010.

Cayuela, C., Llorens, P., Sánchez-Costa, E., Levia, D.F. and Latron, J.: Effect of biotic and abiotic factors on inter- and intra-event variability in stemflow rates in oak and pine stands in a Mediterranean mountain area, J. Hydrol., 560, 396–406, https://doi.org/10.1016/j.jhydrol.2018.03.050, 2018.

Corti, G., Agnelli, A., Cocco, S., Cardelli, V., Masse, J. and Courchesne, F.: Soil affects throughfall and stemflow under Turkey oak (*Quercus cerris* L.), Geoderma, 333, 43–56, https://doi.org/10.1016/j.geoderma.2018.07.010, 2019.

Dawoe, E.K., Barnes, V.R. and Oppong, S.K.: Spatio-temporal dynamics of gross rainfall partitioning and nutrient fluxes in shaded-cocoa (*Theobroma cocoa*) systems in a tropical semi-deciduous forest, Agroforst. Syst., 92, 397–413, https://doi.org/10.1007/s10457-017-0108-3, 2018.

Dunkerley, D.L.: Stemflow production and intrastorm rainfall intensity variation: an experimental analysis using laboratory rainfall simulation, Earth. Surf. Proc. Land., 39, 1741–1752, https://doi.org/10.1002/esp.3555, 2014.

Dunkerley, D.L.: Stemflow on the woody parts of plants: dependence on rainfall intensity and event profile from laboratory simulations, Hydrol. Process., 28, 5469–5482, https://doi.org/10.1002/hyp.10050, 2014.

Dunkerley, D.L.: Rainfall intensity bursts and the erosion of soils: an analysis highlighting the need for high temporal resolution rainfall data for research under current and future climates, Earth Surf. Dynam., 7, 345–360, https://doi.org/10.5194/esurf-7-345-2019, 2019.

Durocher, M.G.: Monitoring spatial variability of forest interception, Hydrol. Process., 4, 215–229, https://doi.org/10.1002/hyp.3360040303, 1990.

Fan, J.L., Baumgartl, T., Scheuermann, A. and Lockington, D.A.: Modeling effects of canopy and roots on soil moisture and deep drainage. Vadose. Zone. J., 14, 1–18, https://doi.org/10.2136/vzj2014.09.0131, 2015.

Firn, R.: Plant intelligence: an alternative point of view, Ann. Bot., 93, 345–351, https://doi.org/10.1093/aob/mch058, 2004.

Gao, X.D., Zhao, X.N., Pan, D.L., Yu, L.Y. and Wu, P.T.: Intra-storm time stability analysis of surface soil water content, Geoderma, 352, 33–37, https://doi.org/10.1016/j.geoderma.2019.06.001, 2019.

Garbelotto, M.M., Davidson, J.M., Ivors, K., Maloney, P.E., Hüberli, D., Koike, S.T. and Rizzo, D.M.: Non-oak native plants are main hosts for sudden oak death pathogen in California, Calif. Agric, 57, 18–23, https://doi.org/10.3733/ca.v057n01p18, 2003.

Germer, S.: Development of near-surface perched water tables during natural and artificial stemflow generation by babassu palms, J. Hydrol., 507, 262–272, http://dx.doi.org/10.1016/j.jhydrol.2013.10.026, 2013.

~~Giacomin, A. and Trucchi, P.: Rainfall interception in a beech coppice (Acquerino, Italy). J. Hydrol., 137, 141–147, https://doi.org/10.1016/0022-1694(92)90052-W, 1992.~~

Germer, S., Werther, L. and Elsenbeer, H.: Have we underestimated stemflow? Lessons from an open tropical rainforest, J. Hydrol., 395, 169–179, https://doi.org/10.1016/j.jhydrol.2010.10.022, 2010.

Giacomin, A. and Trucchi, P.: Rainfall interception in a beech coppice (Acquerino, Italy). J. Hydrol., 137, 141–147, https://doi.org/10.1016/0022-1694(92)90052-W, 1992.

Groisman, P.Y. and Legates, D.R.: The accuracy of United States precipitation data, B. Am. Meteorol. Soc., 75, 215–227, https://doi.org/10.1175/1520-0477(1994)075<0215:TAOUSP>2.0.CO;2, 1994.

Hair, J.F., Anderson, R.E., Tatham, R.L. and Black, W.C.: Multivariate Data Analysis, fourth ed. Prentice Hall College Division, 745 p, 1995.

Herwitz, S.R.: Infiltration-excess caused by Stemflow in a cyclone-prone tropical rainforest, Earth Surf. Proc. Land, 11, 401–412, https://doi.org/10.1002/esp.3290110406, 1986.

~~Herwitz, S.R. and Slye, R.E.: Three-dimensional modeling of canopy tree interception of wind-driven rainfall, J. Hydrol., 168, 1–4, https://doi.org/10.1016/0022-1694(94)02643-P, 1995.~~

Hill, T. and Lewicki, P.: Statistics: Methods and Applications. Statsoft, Tulsa, 800 p, 2007.

Hu, R., Wang, X.P., Zhang, Y.F., Shi, W., Jin, Y.X. and Chen, N.: Insight into the influence of sand-stabilizing shrubs on soil enzyme activity in a temperate desert, Catena, 137, 526–535, http://dx.doi.org/10.1016/j.catena.2015.10.022, 2016.

Iida, S.~~I~~., Levia, D.F., Shimizu, A., Shimizu, T., Tamai, K., Nobuhiro, T., Kabeya, N., Noguchi, S., Sawano, S. and Araki, M.: Intrastorm scale rainfall interception dynamics in a mature coniferous forest stand, J. Hydrol., 548, 770–783, https://doi.org/10.1016/j.jhydrol.2017.03.009, 2017.

Iida, S., Shimizu, T., Kabeya, N., Nobuhiro, T., Tamai, K., Shimizu, A., Ito, E., Ohnuki, Y., Abe, T., Tsuboyama, Y., Chann, S. and Keth, N.: Calibration of tipping-bucket flow meters and rain gauges to measure gross rainfall, throughfall, and stemflow applied to data from a Japanese temperate coniferous forest and a Cambodian tropical deciduous forest, Hydrol. Process., 26, 2445–2454, https://doi.org/10.1002/hyp.9462, 2012.

Jia, X.X., Shao, M.A., Wei, X.R. and Wang, Y. Q.: Hillslope scale temporal stability of soil water storage in diverse soil layers, J. Hydrol., 498, 254–264, https://doi.org/10.1016/j.jhydrol.2013.05.042, 2013.

Johnson, M.S. and Lehmann, J.: Double-funneling of trees: Stemflow and root-induced preferential flow, Ecoscience, 13, 324–333, https://doi.org/0.2980/i1195-6860-13-3-324.1, 2006.

Kéfi, S., Rietkerk, M., Alados, C.L., Pueyo, Y., Papanastasis, V.P., ElAich, A. and De Ruiter, P.C.: Spatial vegetation patterns and imminent desertification in Mediterranean arid ecosystems, Nature, 449, 213–217, https://doi.org/10.1038/nature06111, 2007.

Kimble, P.D.: Measuring the momentum of throughfall drops and raindrops. Master Thesis. Western Kentucky University, Bowling Green, 126 pp, 1996.

Levia, D.F. and Germer, S.: A review of stemflow generation dynamics and stemflow-environment interactions in forests and shrublands, Rev. Geophys., 53, 673-714, 2015, https://doi.org/10.1002/2015RG000479, 2015.

Levia, D.F., ~~Van~~van Stan, J.T., Mage, S.M. and Kelley-Hauske, P.W.: Temporal variability of stemflow volume in a beech-yellow poplar forest in relation to tree species and size, J. Hydrol., 380, 112–120, https://doi.org/10.1016/j.jhydrol.2009.10.028, 2010.

Liang, W.L., Kosugi, K. and Mizuyama, T.: Soil water dynamics around a tree on a hillslope with or without rainwater supplied by stemflow, Water Resour. Res., https://doi.org/10.1029/2010WR009856, 2011.

Liang, W.L., Kosugi, K. and Mizuyama, T.: Soil water redistribution processes around a tree on a hillslope: the effect of stemflow on the drying process, Ecohydrology, 8, 1381–1395, https://doi.org/10.1002/eco.1589, 2014.

Li X., Xiao, Q.F., Niu, J.Z., Dymond, S., van Doorn, N.S., Yu, X.X., Xie, B.Y., Lv, X.Z., Zhang, K.B. and Li, J.: Process-based rainfall interception by small trees in Northern China: The effect of rainfall traits and crown structure characteristics, Agric. For. Meteorol., 218–219, 65–73, https://doi.org/10.1016/j.agrformet.2015.11.017, 2016.

Li, X.Y., Liu, L.Y., Gao, S.Y., Ma, Y.J. and Yang, Z.P.: Stemflow in three shrubs and its effect on soil water enhancement in semiarid loess region of China, Agric. For. Meteorol., 148, 1501–1507, https://doi.org/10.1016/j.agrformet.2008.05.003, 2008.

Li, Y.Y., Chen, W.Y., Chen, J.C. and Shi, H.: Contrasting hydraulic strategies in *Salix psammophila* and *Caragana korshinskii* in the southern Mu Us Desert, China, Ecol. Res., 31, 869–880, https://doi.org/10.1007/s11284-016-1396-1, 2016.

Liu, Y.X., Zhao, W.W., Wang, L.X., Zhang, X., Daryanto, S. and Fang, X.N.: Spatial variations of soil moisture under *Caragana korshinskii* kom. from different precipitation zones: field based analysis in the Loess Plateau, China, Forests, 7, https://doi.org/10.3390/f7020031, 2016.

Magliano, P.N., Whitworth-Hulse, J.I. and Baldi, G.: Interception, throughfall and stemflow partition in drylands: Global synthesis and meta-analysis, J. Hydrol., 568, 638–645, https://doi.org/10.1016/j.jhydrol.2018.10.042, 2019.

Manfroi, O.J., Koichiro, K., Nobuaki, T., Masakazu, S., Nakagawa, M., Nakashizuka, T. and Chong, L.: The stemflow of trees in a Bornean lowland tropical forest, Hydrol. Process., 18, 2455–2474, https://doi.org/10.1002/hyp.1474, 2004.

Martinez-Meza, E. and Whitford, W.: Stemflow, throughfall and channelization of stemflow by roots in three Chihuahuan desert shrubs, J. Arid Environ., 32, 271–287, https://doi.org/10.1006/jare.1996.0023, 1996.

Mcclain, M.E., Boyer, E.W., Dent, C.L., Gergel, S.E., Grimm, N.B., Groffman, P.M., Hart, S.C., Harvey, J.W., Johnston, C.A. and Mayorga, E.: Biogeochemical hot spots and hot moments at the interface of terrestrial and aquatic ecosystems, Ecosystems, 6, 301–312, https://doi.org/10.1007/s10021-003-0161-9, 2003.

Návar, J.: Stemflow variation in Mexico's northeastern forest communities: Its contribution to soil moisture content and aquifer recharge, J. Hydrol., 408, 35–42, https://doi.org/10.1016/j.jhydrol.2011.07.006, 2011.

Owens, M.K., Lyons, R.K. and Alejandro, C.L.: Rainfall partitioning within semiarid juniper communities: effects of event size and canopy cover, Hydrol. Process., 20, 3179–3189, https://doi.org/10.1002/hyp.6326, 2006.

Reid, L.M. and Lewis, J.: Rates, timing, and mechanisms of rainfall interception loss in a coastal redwood forest, J. Hydrol., 375, 459–470, https://doi.org/10.1016/j.jhydrol.2009.06.048, 2009.

Schimmack, W., Förster, H., Bunzl, K., and Kreutzer, K.: Deposition of radiocesium to the soil by stemflow, throughfall and leaf-fall from beech trees, Radiat. Environ. Biophys., 32, 137–150, https://doi.org/10.1007/bf01212800, 1993.

Siegert, C.M. and Levia, D.F.: Seasonal and meteorological effects on differential stemflow funneling ratios for two deciduous tree species, J. Hydrol., 519, 446–454, https://doi.org/10.1016/j.jhydrol.2014.07.038, 2014.

Spencer, S.A. and van Meerveld, H.J.: Double funnelling in a mature coastal British Columbia forest: spatial patterns of stemflow after infiltration, Hydrol. Process., 30, 4185–4201, https://doi.org/10.1002/hyp.10936, 2016.

Sprenger, M., Stumpp, C., Weiler, M., Aeschbach, W., Allen, S.T., Benettin, P., Dubbert, M., Hartmann, A., Hrachowitz, M., Kirchner, J.W., McDonnell, J.J., Orlowski, N., Penna, D., Pfahl, S., Rinderer, M., Rodriguez, N., Schmidt, M. and Werner, C.: The Demographics of Water: A Review of Water Ages in the Critical Zone, Rev. Geophys., 57, 1–35, https://doi.org/10.1029/2018RG000633, 2019.

Staelens, J., De Schrijver, A., Verheyen, K. and Verhoest N.E.: Rainfall partitioning into throughfall, stemflow, and interception within a single beech (*Fagus sylvatica* L.) canopy: influence of foliation, rain event characteristics, and meteorology, Hydrol. Process., 22, 33–45, https://doi.org/10.1002/hyp.6610, 2008.

Teachey, M.E., Pound, P., Ottesen, E.A. and ~~Van~~van Stan, J.T.: Bacterial community composition of throughfall and stemflow, Front. Plant. Sci., 1, 1–6, https://doi.org/10.3389/ffgc.2018.00007, 2018.

Uijlenhoet, R. and Sempere Torres, D.: Measurement and parameterization of rainfall microstructure, J. Hydrol., 328, 1, 1–7, https://doi.org/10.1016/j.jhydrol.2005.11.038, 2006.

~~Van~~van Stan, J.T. and Levia, D.F.: Inter- and intraspecific variation of stemflow production from *Fagus grandifolia* Ehrh. (American beech) and *Liriodendron tulipifera* L. (yellow poplar) in relation to bark microrelief in the eastern United States, Ecohydrology, 3, 11–19, https://doi.org/10.1002/eco.83, 2010.

~~Van~~van Stan, J.T., Siegert, C.M., Levia D.F. and Scheick, C.E.: Effects of wind-driven rainfall on stemflow generation between codominant tree species with differing crown characteristics, Agric. For. Meteorol., 151, 9, 1277–1286, https://doi.org/10.1016/j.agrformet.2011.05.008, 2011.

~~Van~~van Stan, J.T., Gay, T.E. and Lewis, E.S.: Use of multiple correspondence analysis (MCA) to identify interactive meteorological conditions affecting relative throughfall, J. Hydrol., 533, 452–460, https://doi.org/10.1016/j.jhydrol.2015.12.039, 2016.

Wang, X.P., Wang, Z.N., Berndtsson, R., Zhang, Y.F. and Pan, Y.X.: Desert shrub stemflow and its significance in soil moisture replenishment, Hydrol. Earth Syst. Sci., 15, 561–567, https://doi.org/10.5194/hess-15-561-2011, 2011.

~~Wang, X.P., Zhang, Y.F., Wang, Z.N., Pan, Y.X., Hu, R., Li, X.J. and Zhang, H.: Influence of shrub canopy morphology and rainfall characteristics on stemflow within a revegetated sand dune in the Tengger Desert, NW China, Hydrol. Process., 27, 1501–1509, https://doi.org/10.1002/hyp.9767, 2013.~~

Yang, Z.P.: Rainfall partitioning process and its effects on soil hydrological processes for sand-fixed shrubs in Mu us sandland, Northwest China. PhD Thesis. Beijing Normal University, Beijing, 123 pp (in Chinese with English abstract), 2010.

Yang, X.L., Shao, M.A. and Wei, X.H.: Stemflow production differ significantly among tree and shrub species on the Chinese Loess Plateau, J. Hydrol., 568, 427–436, https://doi.org/10.1016/j.jhydrol.2018.11.008, 2019.

Yuan, C., Gao, G.Y. and Fu, B.J.: Stemflow of a xerophytic shrub (*Salix psammophila*) in northern China: Implication for beneficial branch architecture to produce stemflow, J.

Hydrol., 539, 577–588, https://doi.org/10.1016/j.jhydrol.2016.05.055, 2016.

Yuan, C., Gao, G.Y. and Fu, B.J.: Comparisons of stemflow and its bio-/abiotic influential factors between two xerophytic shrub species, Hydrol. Earth Syst. Sci., 21, 1421–1438, https://doi.org/10.5194/hess-21-1421-2017, 2017.

Zabret, K., Rakovec, J. and Šraj, M.: Influence of meteorological variables on rainfall partitioning for deciduous and coniferous tree species in urban area, J. Hydrol., 558, 29–41, https://doi.org/10.1016/j.jhydrol.2018.01.025, 2018.

Zhang, Y., Li, X.Y., Li, W., Wu, X.C., Shi, F.Z., Fang, W.W. and Pei, T.T.: Modeling rainfall interception loss by two xerophytic shrubs in the Loess Plateau, Hydrol. Process., 31, 1926–1937, https://doi.org/10.1002/hyp.11157, 2017.

Zhang, Y.F., Wang X.P., Hu, R., Pan Y.X. and Paradeloc, M.: Rainfall partitioning into throughfall, stemflow and interception loss by two xerophytic shrubs within a rain-fed re-vegetated desert ecosystem, northwestern China, J. Hydrol., 527, 1084–1095, https://doi.org/10.1016/j.jhydrol.2015.05.060, 2015.

Table 1. Branch morphologies of *C. korshinskii* and *S. psammophila* for stemflow recording.

Shrub species	BD categories (mm)	Amount	BD (mm)	BL (cm)	BA (°)	LA (cm^2)
	5–10	2	6.6	131	61	837.1
	10–15	2	13.1	168	43	2577.3
C. korshinskii	15–18	2	17.8	206	72	4243.1
	18–25	1	22.1	242	50	6394.7
	>25	NA	NA	NA	NA	NA
	5–10	2	7.5	248	69	626.3
	10–15	2	13.2	343	80	1683.5
S. psammophila	15–18	NA	NA	NA	NA	NA
	18–25	2	21.8	286	76	3468.3
	>25	1	31.3	356	60	7513.7

Notes: BD, BL and BA are branch basal diameter, length and inclination angle, respectively~~.~~; LA is leaf area of individual branches; NA means not applicable.

Table 2. Rainfall characteristics during events with different intensity peak amounts.

Indicators	Event A	Event B	Event C	Others	Average
Event amount	17	11	15	11	13.5±1.5
RA (mm)	4.1 ab	5.2 b	11.7 c	0.6 a	5.4 ± 0.9
RD (h)	2.5 a	3.6 a	10.3 b	2.2 a	4.7 ± 0.8
RI (h)	48.5 ab	70.5 b	57.3 ab	26.1 a	50.6 ± 6.1
I ($mm·h^{-1}$)	5.6 a	5.5 a	4.6 a	2.2 b	4.5 ± 1.0
I_{10} ($mm·h^{-1}$)	15.5 a	12.7 ab	9.5 b	6.0 c	10.9 ± 2.1
I_{b10} ($mm·h^{-1}$)	7.7 a	9.9 a	2.8 b	1.6 b	5.5 ± 1.4
I_{e10} ($mm·h^{-1}$)	4.3 a	3.6 a	2.1 ab	1.2 b	2.8 ± 0.7
F ($mg·m·s^{-1}$)	17.1 a	17.6 a	17.2 a	12.5 b	16.1 ± 1.2
F_{10} ($mg·m·s^{-1}$)	27.8 a	26.6 a	24.2 ab	21.0 b	24.9 ± 1.4
F_{b10} ($mg·m·s^{-1}$)	19.7 ab	21.7 a	15.4 b	16.9 b	18.4 ± 1.4
F_{e10} ($mg·m·s^{-1}$)	17.3 a	16.6 a	13.4 b	16.8 a	16.0 ± 1.0
E (unitless)	0.9 ab	1.0 ab	0.4 a	1.7 b	0.9 ± 0.2

Note: Event A, Event B and Event C are events with the single, double and multiple rainfall intensity peaks, respectively~~, and~~; Others are the events that excluded from the categorization~~.~~; RA~~ is the rainfall amount.~~, RD and RI are rainfall amount, duration and interval, respectively~~.~~; I and I_{10} are the average and 10-min maximum rainfall ~~intensity~~intensities, respectively~~.~~; I_{b10} and I_{e10} are the average rainfall ~~intensity~~intensities in 10 min after rain ~~beginning~~begins and before rain ~~ending~~ends, respectively~~.~~; F and F_{10} are the average and 10-min maximum raindrop ~~momentum~~momentums, respectively~~.~~; F_{b10} and F_{e10} are the average raindrop ~~momentum~~momentums in 10 min after rain ~~beginning~~begins and before rain ~~ending~~ends, respectively~~.~~; E is evaporation coefficient; Different letters indicate significant differences of rainfall characteristics between event categories (p<0.05) (rows at the table).

Table 3. Stemflow variables of *C. korshinskii* and *S. psammophila* during rainfall events with different intensity peak amounts.

Species	Stemflow	Event A	Event B	Event C	Others	Average
C. korshinskii	SFV (mL)	~~934~~134.1	~~1552.5~~203.	~~3719.7~~560.	~~67.3~~7.6	~~1658~~226.6 ±
	SFI (mm·h^{-1})	~~5.7~~672.9	~~6.0~~552.4 b	~~5.1~~527.0 b	~~1.9~~317.8	~~4.7 ± 1~~517.5
	SFI$_{10}$ (mm·h^{-1})	~~30.2~~2849.	~~26.4~~2399.3	~~15.3~~1809.1	~~9.1~~1173.	~~20.3 ±~~
	FR (unitless)	109.4 a	146.6 b	137.9 b	128.9 ab	130.7 ± 8.2
	TLG (min)	67.3 ab	56.2 a	67.0 ab	74.2 b	66.2 ± 10.6
	TLM (min)	81.1 a	75.5 a	202.1 b	78.8 a	109.4 ± 20.5
	TLE (min)	22.3 a	18.7 b	18.5 b	20.6 a	20.0 ± 5.3
	~~TLM (min)~~	~~81.1~~	~~75.5~~	~~202.1~~	~~78.8~~	~~109.4 ± 20.5~~
	SFD (h)	1.4 a	3.1 a	9.1 b	1.4 a	3.8 ± 0.8
S. psammophila	SFV (mL)	~~616.5~~102.	~~907.0~~145.7	~~2469.0~~435.	~~63.~~4.7 c	~~1014.0 ±~~
	SFI (mm·h^{-1})	~~7.2~~648.1	~~6.0~~421.5 b	~~2.4~~246.6 c	~~3.4~~153.2	~~4.8 ±~~ 367.3 ±
	SFI$_{10}$ (mm·h^{-1})	~~24.8~~1672.	~~24.5~~1582.8	~~8.8~~888.4 b	~~9.4~~384.7	~~16.9 ±~~
	FR (unitless)	77.1 a	91.4 a	129.1 b	101.6 ab	101.6 ± 10.4
	TLG (min)	84.9 a	46.5 b	56.1 b	31.5 b	54.8 ± 11.7
	~~TLE (min)~~	~~17.1~~	~~8.6~~	~~20.8~~	~~7.3~~	~~13.5 ± 17.2~~
	TLM (min)	64.3 a	93.4 a	235.8 b	88.4 a	120.5 ± 22.1
	TLE (min)	17.1 a	8.6 b	20.8 a	7.3 b	13.5 ± 17.2
	SFD (h)	1.2 a	3.4 a	8.3 b	0.7 a	3.4 ± 0.9

Note: Event A, Event B and Event C are events with the single, double and multiple rainfall intensity peaks, respectively~~, and~~; Others are the events that excluded from the categorization~~.~~; TLG and TLM are ~~the~~ time lags of stemflow generating and maximizing ~~to~~after rains begin ~~of rainfall~~, respectively~~.~~; TLE is ~~the~~ time lag of stemflow ending ~~to cease of rainfall.~~after rain ceases; SFD is ~~the~~ stemflow duration~~.~~; SFV is ~~the~~ stemflow volume~~.~~; SFI ~~is~~are the average stemflow intensities at incident rains, respectively; Different letters indicate significant differences of stemflow variables between event categories (p<0.05) (rows at the table).

Table 4. Comparisons of stemflow intensity~~. SFI$_{10}$ is~~ and funnelling ratio at different basal diameter categories.

Species and stemflow variables		BD categories (mm)					
		5–10	10–15	15–18	18–25	>25	AVG
C. korshinskii	FR	163.7±12.2a	136±10.9b	119.5±13.0b	97.7±9.2b	NA	131±8.2
	SFI	716.2±118.7a	552.5±90.3b	619±103.3b	333.8±45.8b	NA	553.9±82.1
S. psammophila	FR	212±17.4a	84±6.4b	NA	44.2±3.0b	54.9±4.2b	100.6±7.9
	SFI	738.7±160.9a	360.7±82.7a	NA	197.2±44.9b	209.9±44.5b	372.2±79.4

Note: SFI and FR are the ~~maximum~~average stemflow intensity ~~in 10 min.~~

and funnelling ratio at incident rains, respectively; BD is branch basal diameter (mm); NA means not applicable; Different letters indicate significant differences of stemflow variables between event categories (p<0.05) (rows at the table).

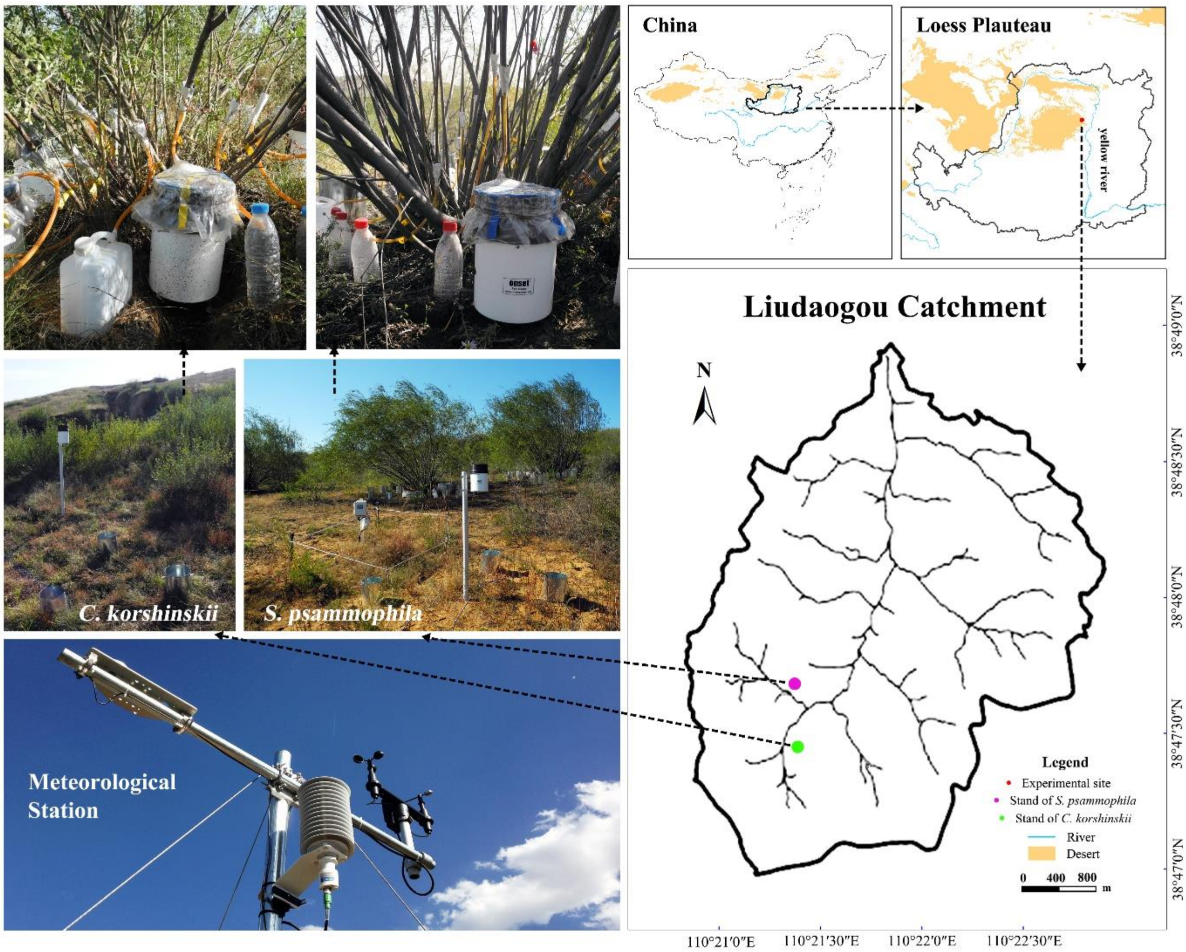

965

966 **Figure 1.** Locations and experimental settings in the plots of *C. korshinskii* and *S.*
967 *psammophila*.

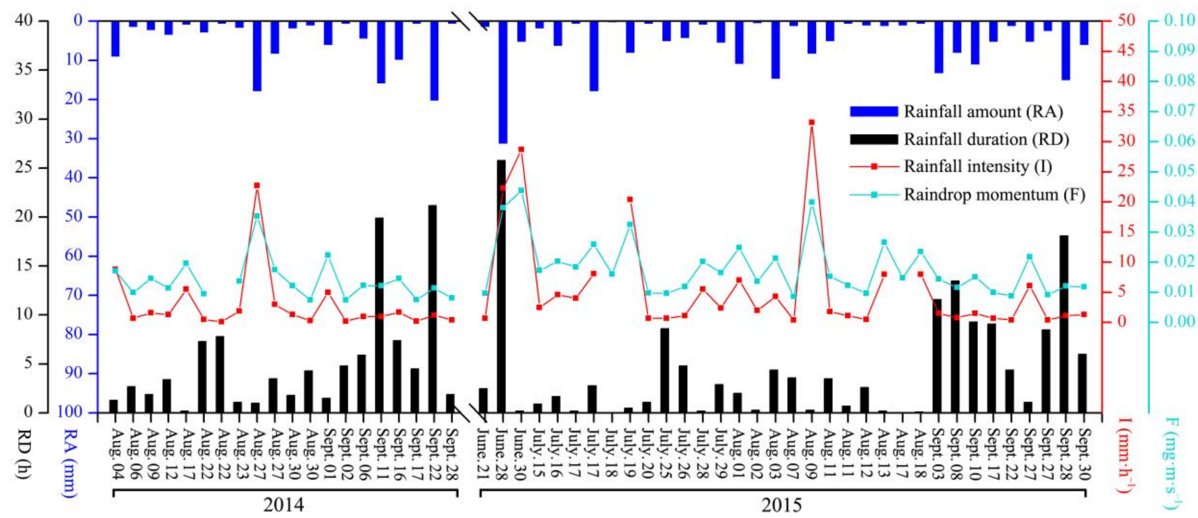

Figure 2. Inter-event variations in rainfall characteristics during the experimental period.

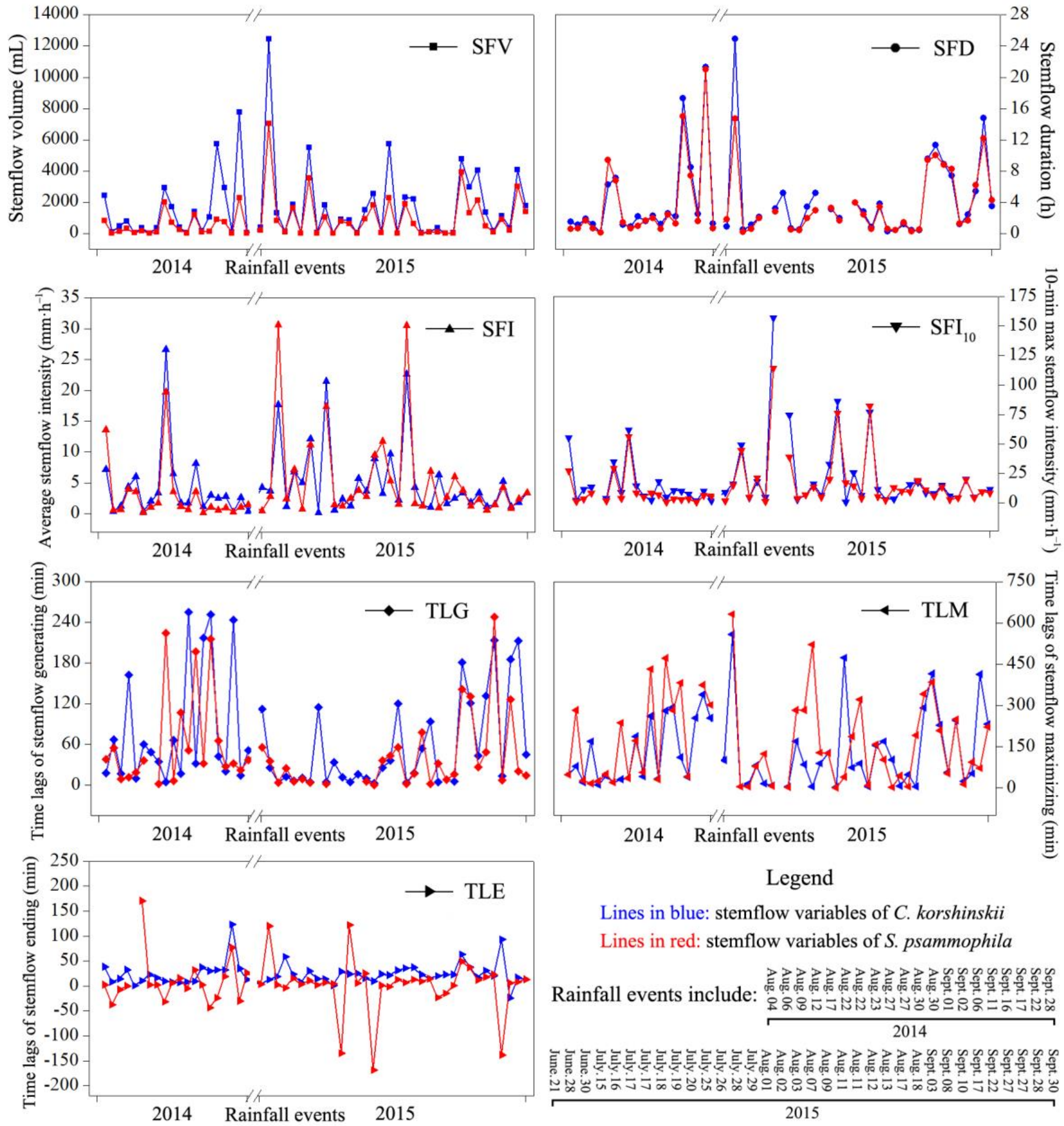
SFV
Stemflow volume (mL)
SFD
Stemflow duration (h)
SFI
Average stemflow intensity (mm·h⁻¹)
SFI10
10-min max stemflow intensity (mm·h⁻¹)
TLG
Time lags of stemflow generating (min)
TLM
Time lags of stemflow maximizing (min)
TLE
Time lags of stemflow ending (min)
2014
Rainfall events
2015
Legend
Lines in blue: stemflow variables of C. korshinskii
Lines in red: stemflow variables of S. psammophila
Rainfall events include:
Aug. 04 Aug. 06 Aug. 09 Aug. 12 Aug. 17 Aug. 22 Aug. 23 Aug. 27 Aug. 30 Sept. 01 Sept. 02 Sept. 06 Sept. 11 Sept. 16 Sept. 17 Sept. 22 Sept. 28
2014
June. 21 June. 28 June. 30 July. 15 July. 16 July. 17 July. 17 July. 18 July. 19 July. 20 July. 25 July. 26 July. 28 July. 29 Aug. 01 Aug. 02 Aug. 03 Aug. 07 Aug. 09 Aug. 11 Aug. 11 Aug. 12 Aug. 13 Aug. 17 Aug. 18 Sept. 03 Sept. 08 Sept. 10 Sept. 17 Sept. 22 Sept. 27 Sept. 28 Sept. 30
2015

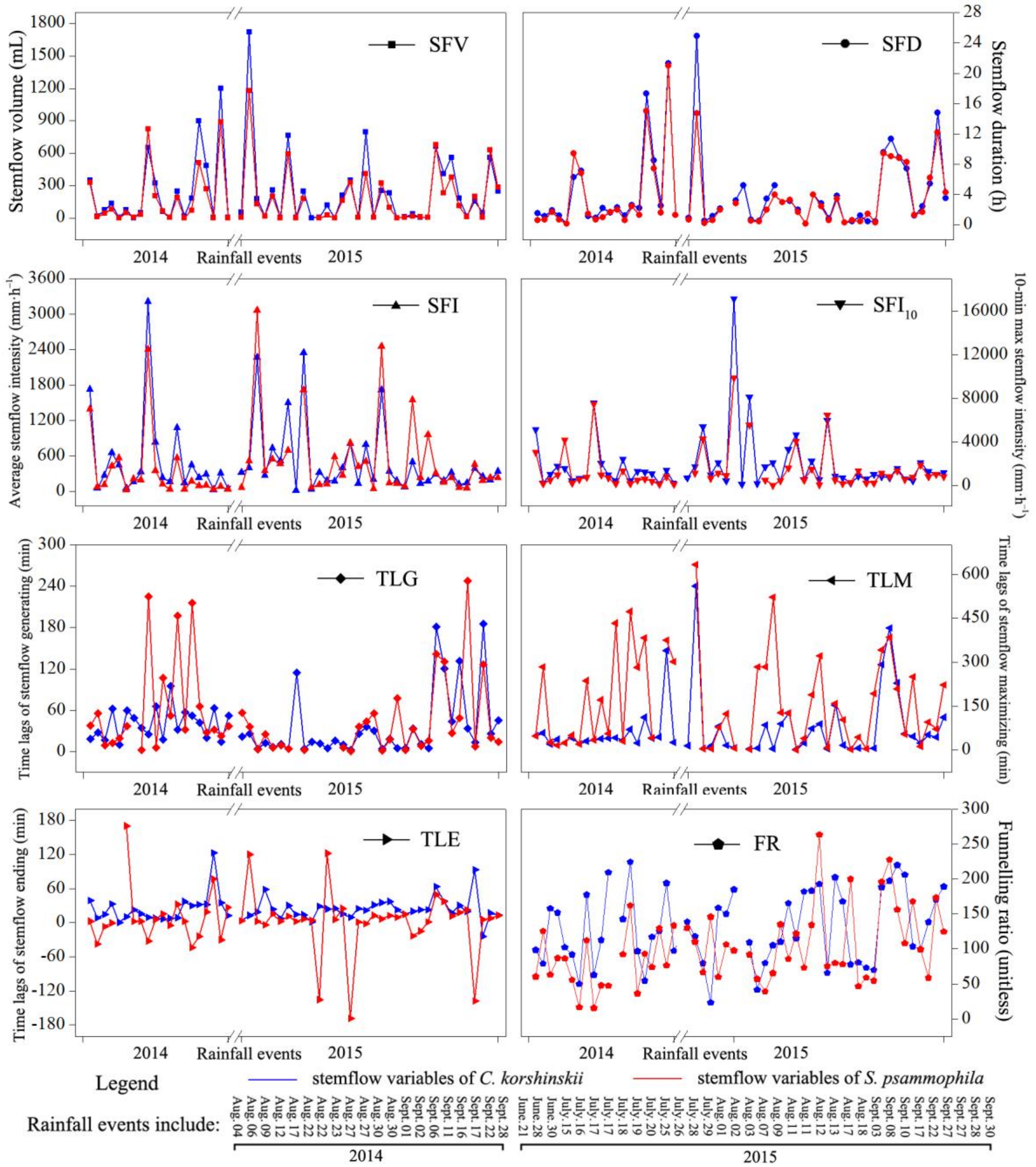

Figure 3. Inter-event variations in stemflow variables of *C. korshinskii* and *S. psammophila* during the experimental period.

974 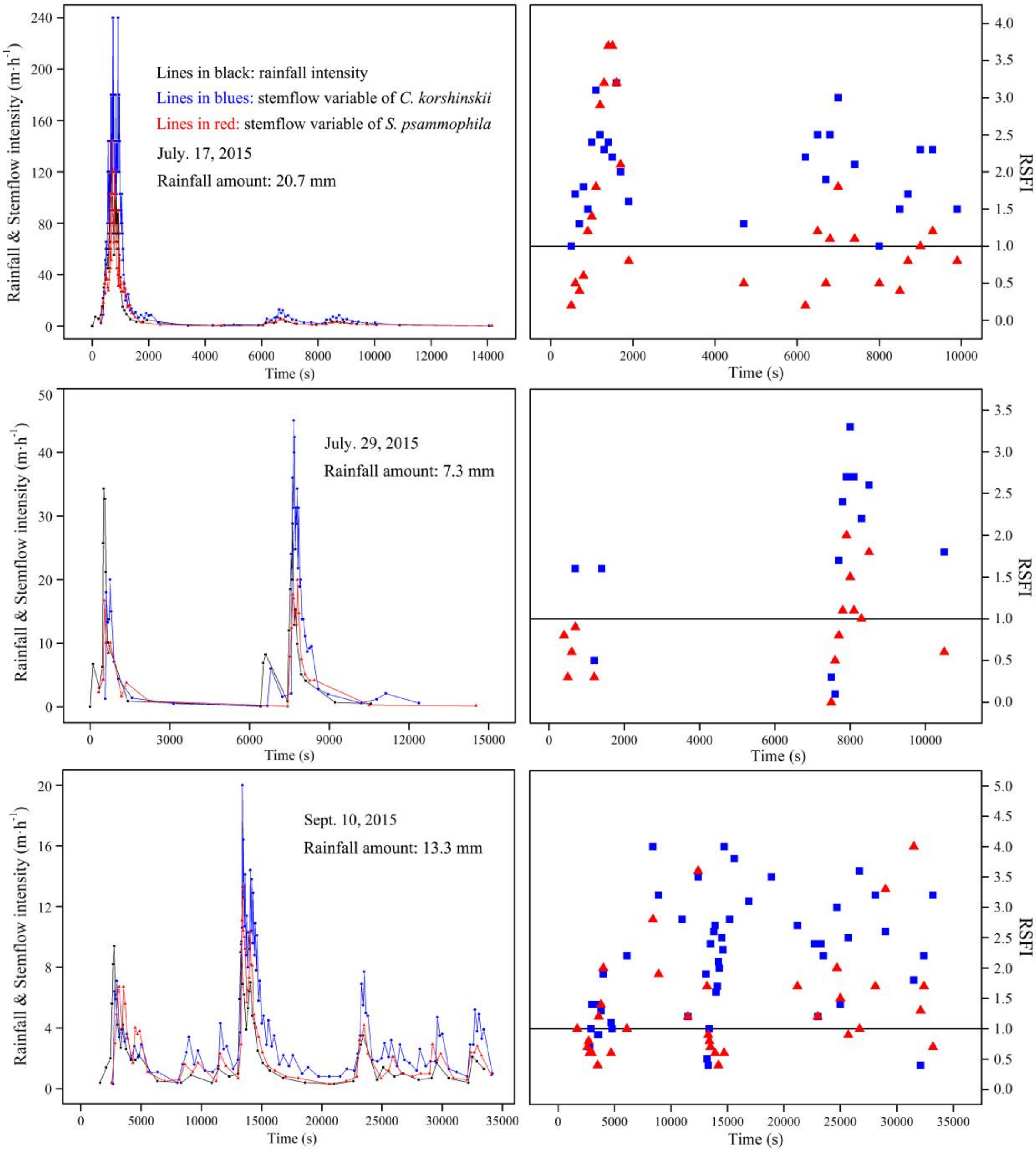
Lines in black: rainfall intensity
Lines in blues: stemflow variable of C. korshinskii
Lines in red: stemflow variable of S. psammophila
July. 17, 2015
Rainfall amount: 20.7 mm
July. 29, 2015
Rainfall amount: 7.3 mm
Sept. 10, 2015
Rainfall amount: 13.3 mm
Rainfall & Stemflow intensity (m·h-1)
Time (s)
RSFI

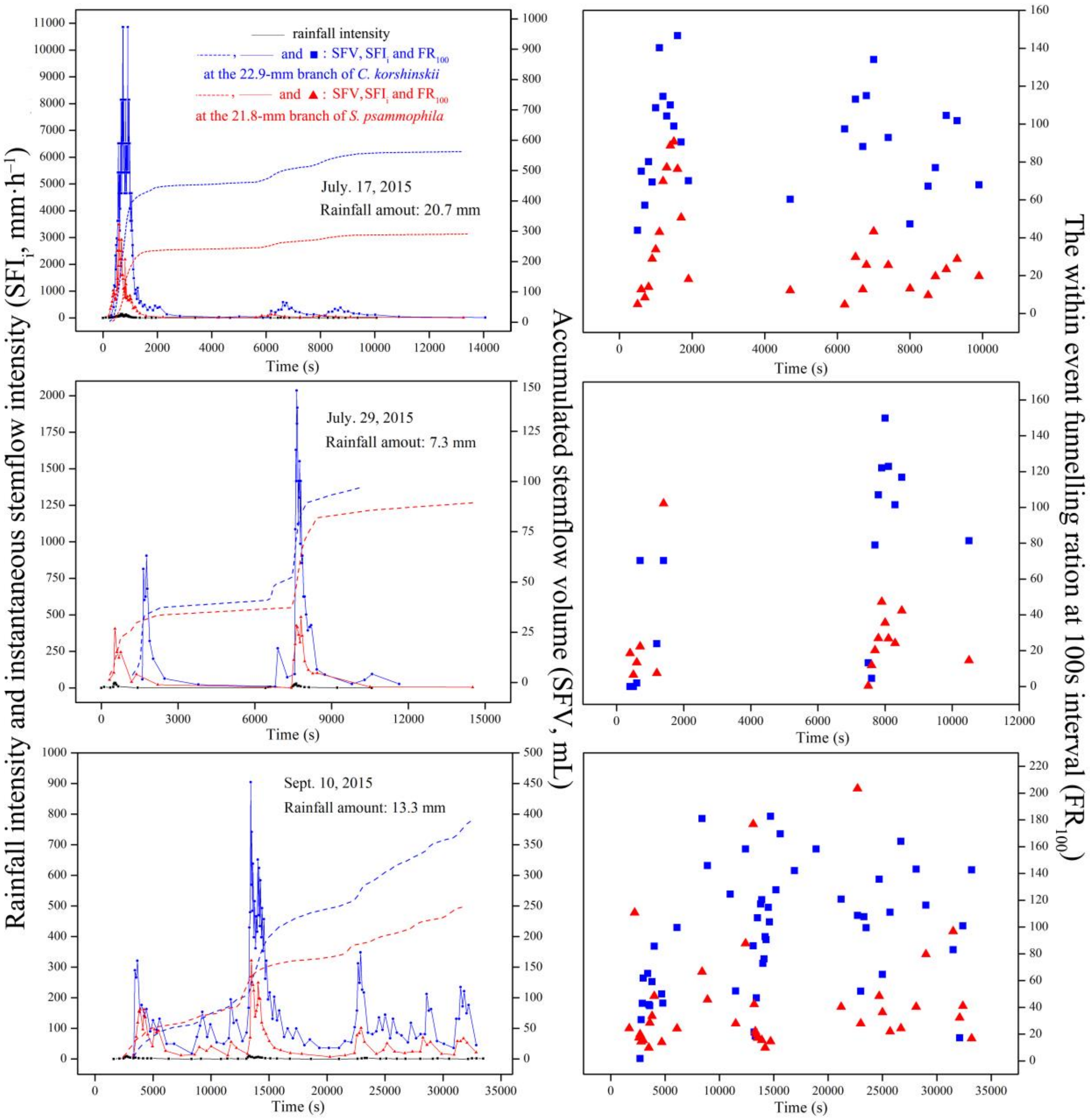

Figure 4. Stemflow synchronicity of *C. korshinskii* and *S. psammophila* to rains during representative events with different rainfall-intensity ~~peaks.~~ peak amounts.

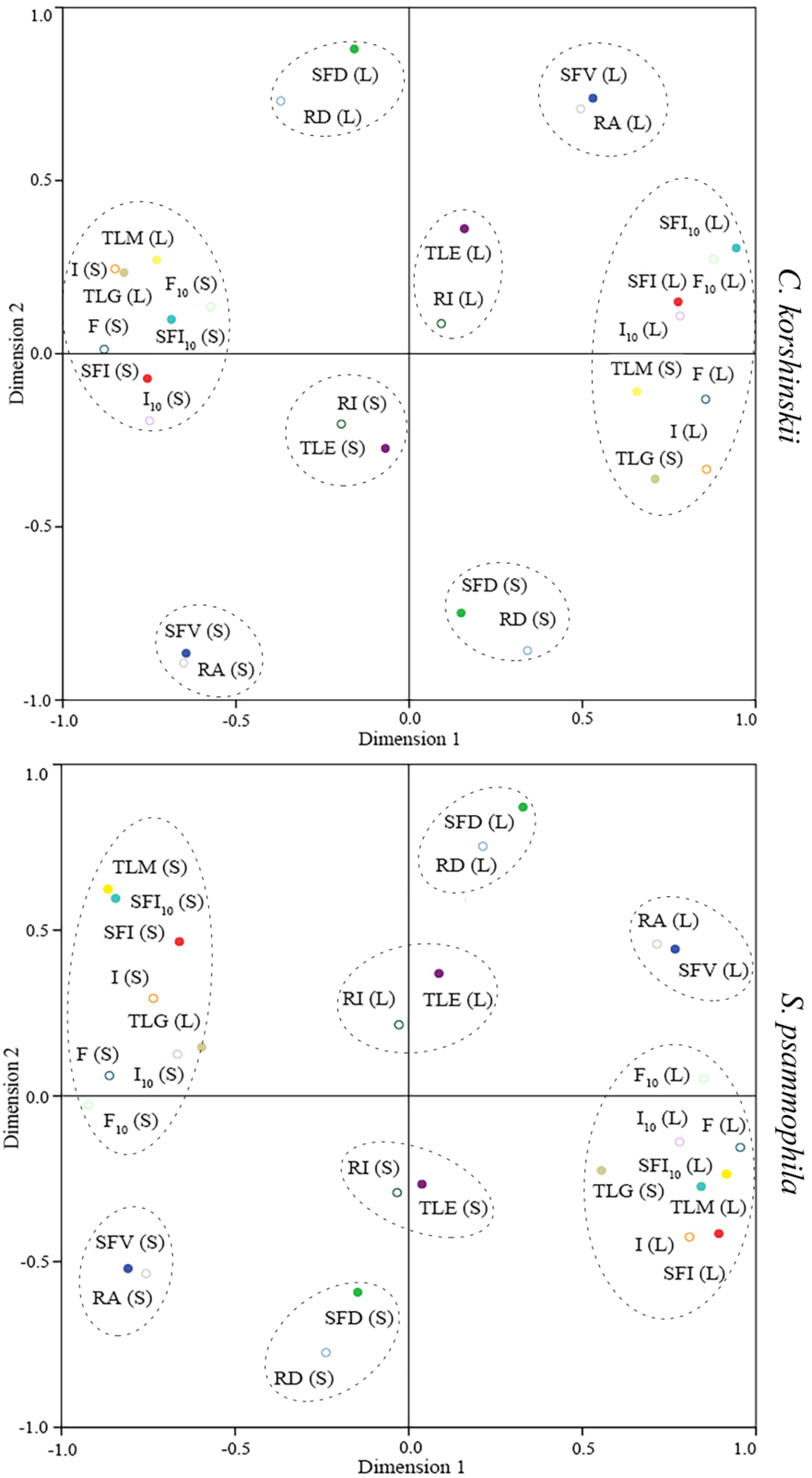
C. korshinskii
Dimension 1
Dimension 2
SFD (L)
RD (L)
SFV (L)
RA (L)
TLM (L)
I (S)
TLG (L)
F_{10} (S)
F (S)
SFI_{10} (S)
SFI (S)
I_{10} (S)
TLE (L)
RI (L)
SFI_{10} (L)
SFI (L)
F_{10} (L)
I_{10} (L)
TLM (S)
F (L)
I (L)
TLG (S)
RI (S)
TLE (S)
SFD (S)
RD (S)
SFV (S)
RA (S)
S. psammophila
TLM (S)
SFI_{10} (S)
SFI (S)
I (S)
TLG (L)
F (S)
I_{10} (S)
F_{10} (S)
RI (L)
TLE (L)
RA (L)
SFV (L)
F_{10} (L)
I_{10} (L)
F (L)
SFI_{10} (L)
TLG (S)
TLM (L)
I (L)
SFI (L)
RI (S)
TLE (S)
SFV (S)
RA (S)
SFD (S)
RD (S)

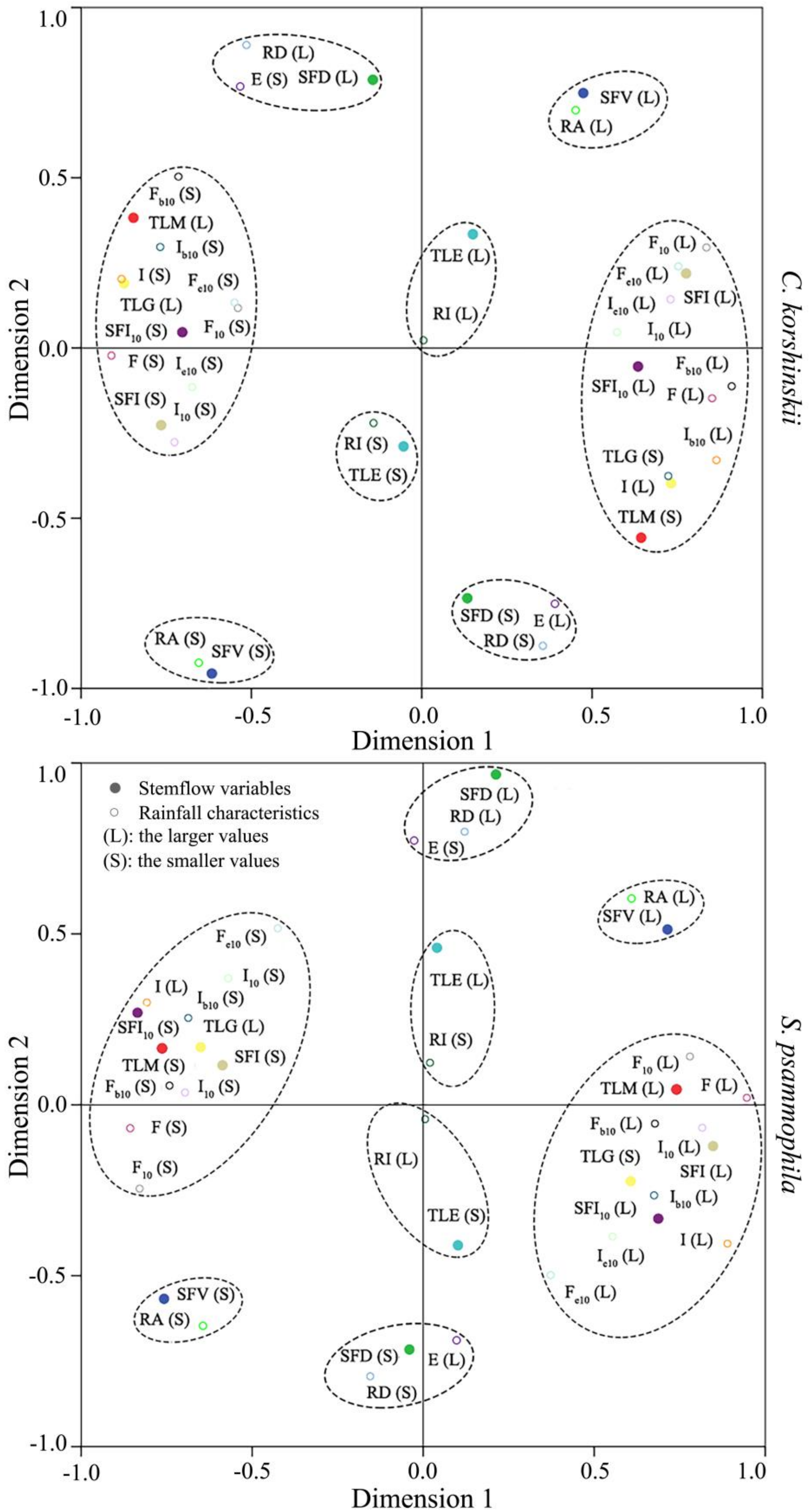

Figure 5. Correspondence ~~map~~maps of stemflow variables with rainfall characteristics for *C. korshinskii* and *S. psammophila*.

982

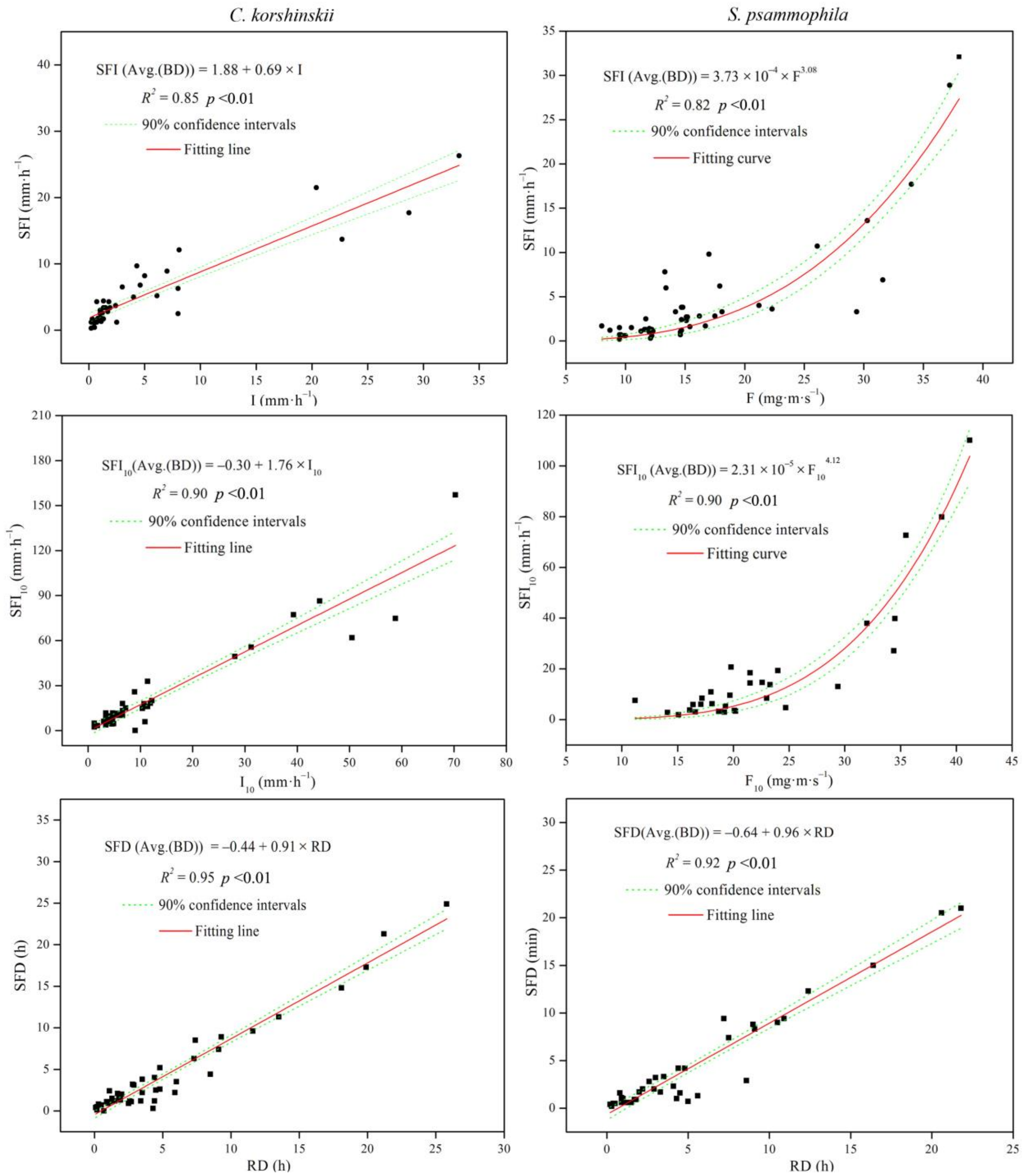
C. korshinskii
S. psammophila
SFI (Avg.(BD)) = 1.88 + 0.69 × I
R^2 = 0.85 p <0.01
90% confidence intervals
Fitting line
SFI (mm·h^{-1})
I (mm·h^{-1})
SFI (Avg.(BD)) = 3.73 × 10^{-4} × F$^{3.08}$
R^2 = 0.82 p <0.01
90% confidence intervals
Fitting curve
SFI (mm·h^{-1})
F (mg·m·s^{-1})
SFI$_{10}$(Avg.(BD)) = –0.30 + 1.76 × I$_{10}$
R^2 = 0.90 p <0.01
90% confidence intervals
Fitting line
SFI$_{10}$ (mm·h^{-1})
I$_{10}$ (mm·h^{-1})
SFI$_{10}$ (Avg.(BD)) = 2.31 × 10^{-5} × F$_{10}$$^{4.12}$
R^2 = 0.90 p <0.01
90% confidence intervals
Fitting curve
SFI$_{10}$ (mm·h^{-1})
F$_{10}$ (mg·m·s^{-1})
SFD (Avg.(BD)) = –0.44 + 0.91 × RD
R^2 = 0.95 p <0.01
90% confidence intervals
Fitting line
SFD (h)
RD (h)
SFD(Avg.(BD)) = –0.64 + 0.96 × RD
R^2 = 0.92 p <0.01
90% confidence intervals
Fitting line
SFD (min)
RD (h)

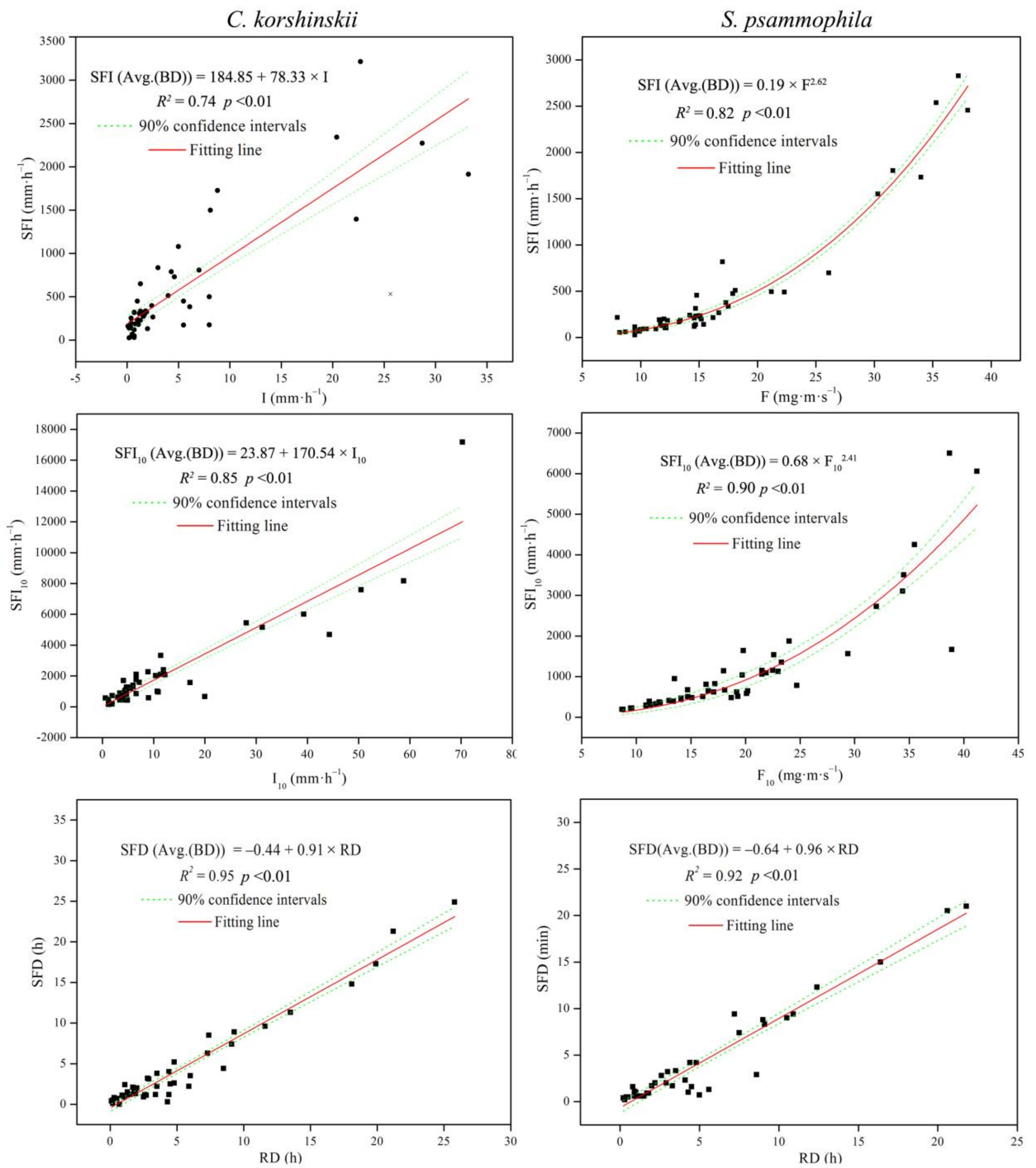

Figure 6. Relationships of stemflow intensity and duration with rainfall characteristics.

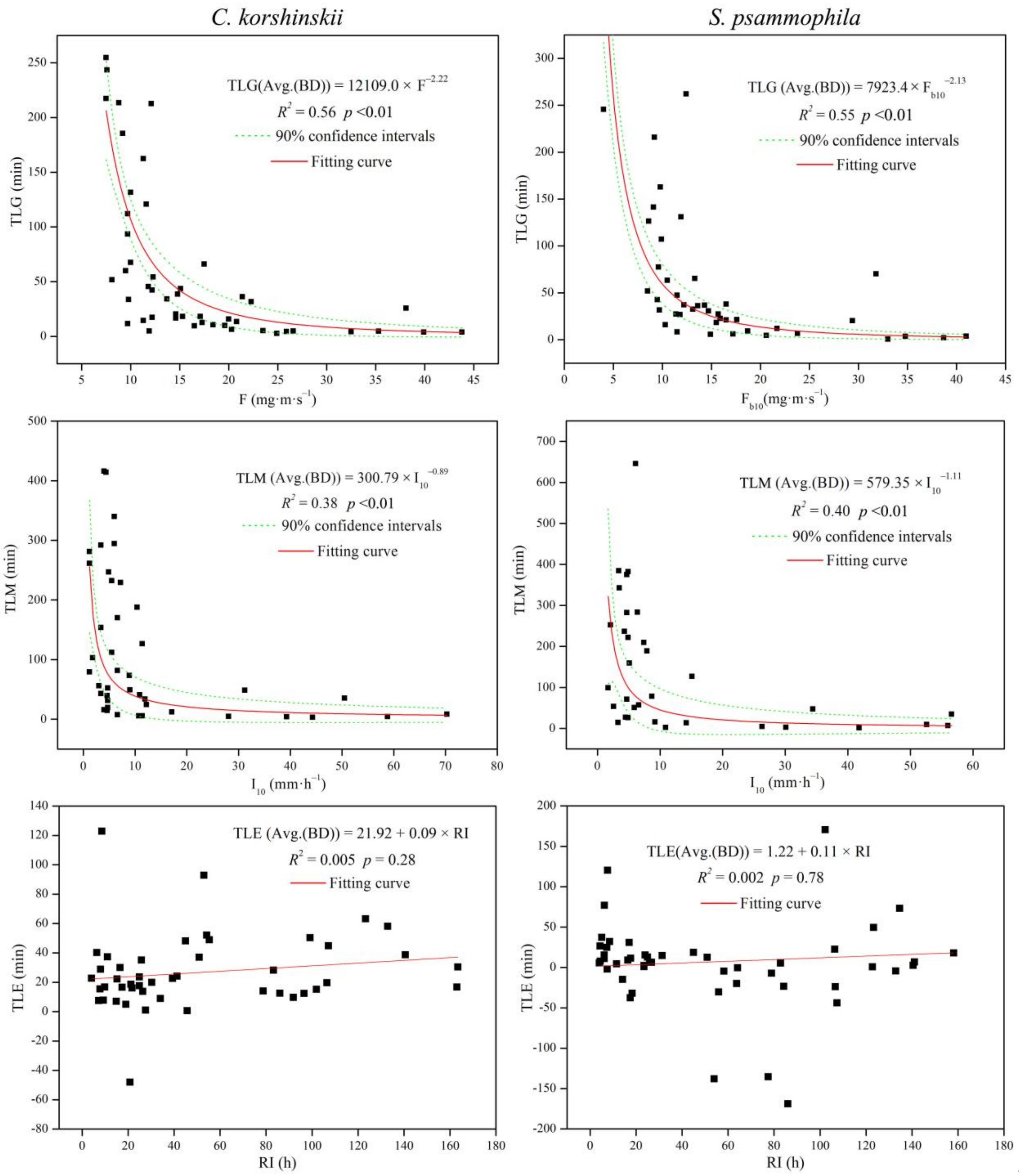
C. korshinskii
S. psammophila
TLG(Avg.(BD)) = 12109.0 × F^−2.22
R^2 = 0.56 p <0.01
90% confidence intervals
Fitting curve
TLG (min)
F (mg·m·s^−1)
TLG (Avg.(BD)) = 7923.4 × F_b10^−2.13
R^2 = 0.55 p <0.01
90% confidence intervals
Fitting curve
TLG (min)
F_b10(mg·m·s^−1)
TLM (Avg.(BD)) = 300.79 × I_10^−0.89
R^2 = 0.38 p <0.01
90% confidence intervals
Fitting curve
TLM (min)
I_10 (mm·h^−1)
TLM (Avg.(BD)) = 579.35 × I_10^−1.11
R^2 = 0.40 p <0.01
90% confidence intervals
Fitting curve
TLM (min)
I_10 (mm·h^−1)
TLE (Avg.(BD)) = 21.92 + 0.09 × RI
R^2 = 0.005 p = 0.28
Fitting curve
TLE (min)
RI (h)
TLE(Avg.(BD)) = 1.22 + 0.11 × RI
R^2 = 0.002 p = 0.78
Fitting curve
TLE (min)
RI (h)

986

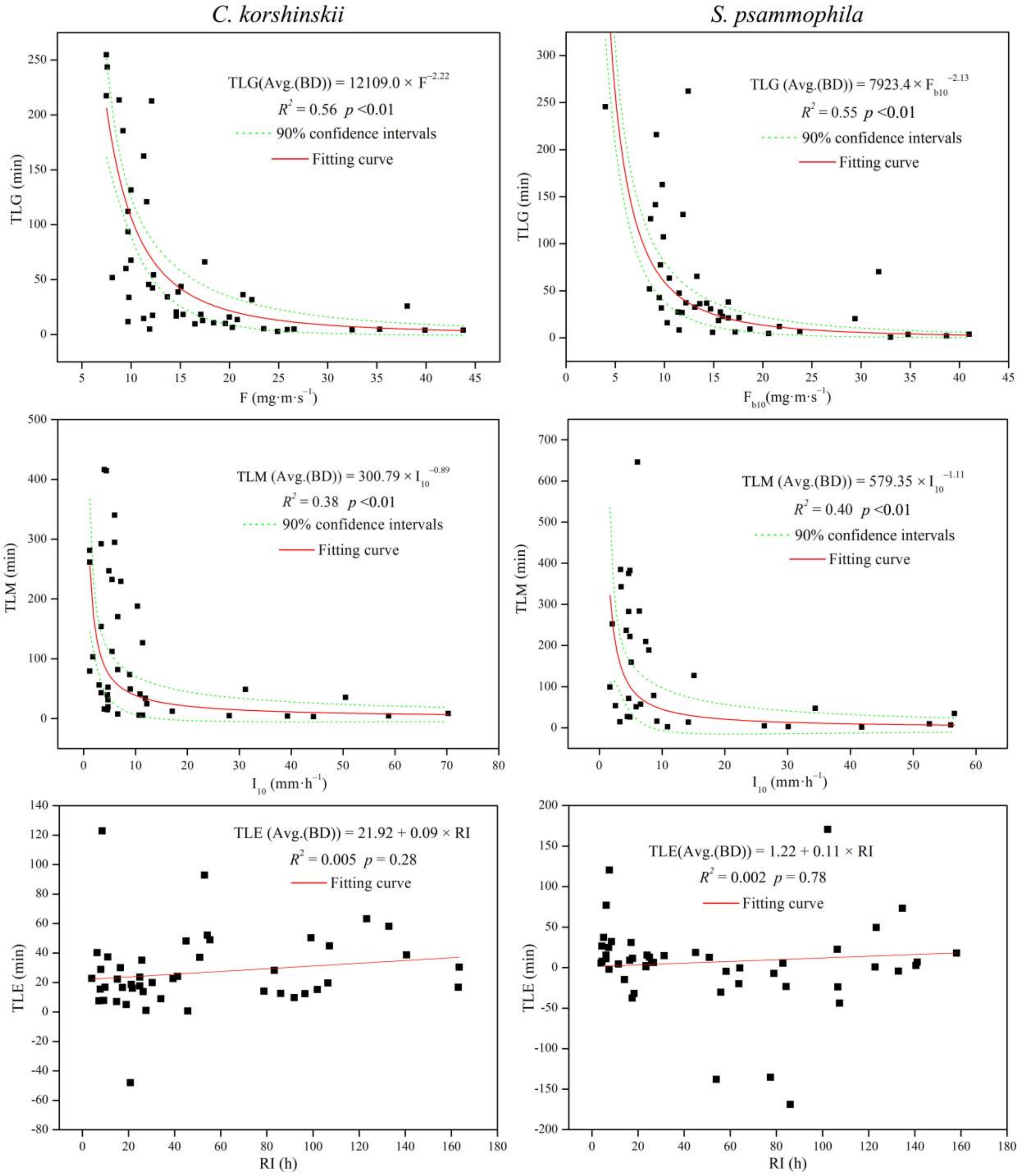

987 **Figure 7.** Relationships of stemflow time lags with rainfall characteristics.